Acta Acustica 2024, **8**, 41

https://doi.org/10.1051/aacus/2024019

Available online at:
https://acta-acustica.edpsciences.org

SCIENTIFIC ARTICLE OPEN ACCESS

Acoustic waves in gas-filled structured porous media: Asymptotic tortuosity/compliability and characteristic-lengths reevaluated to incorporate the influence of spatial dispersion

D. Lafarge*

Laboratoire d'Acoustique de l'Université du Mans, UMR 6613, 72085 Le Mans, France

Received 30 November 2023, Accepted 20 May 2024

Abstract – This study extends efforts to incorporate spatial dispersion into Biot-Allard's long-wavelength theory, with a focus on poroelastic media with intricate microgeometries where spatial dispersion effects play a significant role. While preserving Biot's small-scale quasi-"en-bloc" frame motion to keep the structure of the theory intact, the paper challenges Biot's quasi-incompressibility of fluid motion at that scale by introducing structurations in the form of Helmholtz's resonators. Consequently, Biot-Allard's theory undergoes a significant augmentation, marked by the arising of non-local dynamic tortuosity and compliability, which are associated with potentially resonant fluid behavior. Building on an acoustic-electromagnetic analogy, the study defines these non-local responses and suggests simplifying them into pseudo-local ones, now potentially resonant and reminiscent of Veselago-type phenomena. In the high-frequency limit of small boundary layers and as an extension of the classical Johnson-Allard's findings, simple field-averaged formulas are demonstrated for pseudo-local ideal-fluid tortuosity and compliability (real frequency-dependent) and viscous and thermal characteristic lengths (positive frequency-dependent). These formulations are grounded in the Umov-Heaviside-Poynting thermodynamic macroscopic acoustic stress concept, suggested by the analogy. Future theoretical and computational investigations, spanning various fundamental microgeometries, are planned to assess assumed pseudo-local simplifications, encompass low- and intermediate frequencies, and unveil potential behavioral outcomes resulting from the incorporation of spatial dispersion effects.

Keywords: Sound propagation, Helmholtz resonators, Spatial dispersion, Biot's theory, Porous media

1 General introduction – exploring the foundations of Biot-Allard's theory: unveiling the implicit constraints and path to non-local operators

As recently emphasized in a previous paper in this Journal [1], and rapidly mentioned in other previous works, e.g. [2, 3] and [4] (p. 271 footnote 48), Biot-Allard's long-wavelength theory [5, 6], widely used to describe sound propagation in various gas-saturated (ambient air in general) poroelastic materials for noise control, relies on two pivotal assumptions. These impose constraints on permissible microgeometries in such a way that, once lifted, materials with hitherto unforeseen properties become conceivable. Let us present formulations for these two previously overlooked hypotheses, thus elucidating their common nature. Firstly, the solid frame's motion exhibits a quasi-"en-bloc" nature at a small scale, precluding microstructures like mass-spring. Concurrently, the gas motion is characterized by quasi-incompressible fluid motion, excluding small-scale structures such as Helmholtz resonators. It should be clear that these features of the motion categorized under the labels "incompressibility hypothesis" or simply "incompressibility" in [1], do not result solely from the long wavelengths typically associated with macroscopic theories (the so-called scale-separation). Rather, these two characteristics arise from the confinement to particular microgeometries, leading to a significant narrowing of potential physics and behaviors. Essentially, they underscore the presence of implicit constraints on microgeometries, aiming to prevent the occurrence of the phenomenon known as *spatial dispersion*. As a result, classical Biot-Allard's theory only includes *temporal dispersion*. Here, the terms "spatial dispersion" and "temporal dispersion" bear the same significance as explained in the field of macroscopic electromagnetics [7], from which they originate. Their use, therefore, presuppose the existence of an acoustic-electromagnetic analogy. It is closely linked to the concept of non-local responses. For a detailed understanding of this analogy, we refer the reader to [4] and [8] where it is thoroughly explained in two steps (the fluid itself, and when it permeates a structure), and to [7] and [9] for background on non-local effects. Spatial

*Corresponding author: denis.lafarge@univ-lemans.fr

dispersion is inherently tied to the spatial variability of macroscopic fields, whereas temporal dispersion is inherently tied to the temporal variability of these fields (see below the relations of type (35) or (36)).

For a long time in electromagnetics, spatial dispersion has been regarded as a minor correction that becomes relevant when wavelengths decrease sufficiently. At the beginning of this century, it became clear that, despite what was previously thought in classical electromagnetic literature [7], appropriately structured media can exhibit significant spatial dispersion effects at long wavelengths [10]. These effects could smooth out at some macroscopic outer scale, allowing for a macroscopic but non-local description of the propagation. This immediately ties in with the above remarks: in Biot-Allard's theory, microgeometric constraints have been implicitly imposed, suppressing spatial dispersion, and once lifted, will allow the emergence of potentially huge new effects. Indeed, it is crucial to understand that the fundamental overarching dismissal of spatial dispersion within the framework of Biot-Allard's theory leads to a corresponding absence of full temporal dispersion. This phenomenon presents itself in a distinctly limited capacity. In particular, as detailed in [11] Appendix A and [12] Appendix C, due to the principle of incompressibility the response functions in Fourier space exhibit singularities – enumerable distribution of zeros and poles, within periodic microgeometries, see e.g. [13] – exclusively along the half (causal) frequency imaginary axis. This occurs rather than across the entirety of the half (causal) frequency complex plane. As a result, the actual Biot-Allard's responses are extraordinarily constrained and limited compared to those conceivable on the basis of causality alone.

To clarify the dual aspects of incompressibility, the quasi-"en-bloc" character of frame Biot motion shapes the entire framework, manifesting itself in the structure of macro-level operational relations. Such relations involve macroscopic Biot-Allard's densities and elastic measures – $\hat{\rho}_{11}, \hat{\rho}_{12}, \hat{\rho}_{22}, \hat{P}, \hat{Q}, \hat{R}$, and $\hat{N}$ – which are linked to the foundational tortuosity $\hat{\alpha}$ and compliability $\hat{\beta}$ operators, respectively. The quasi-divergence-free nature of the fluid motion, on the other hand, is instrumental in forcing the absence of spatial dispersion and restricted nature of the allowed temporal dispersion in the above operators. Once the latter hypothesis is lifted and the operators become fundamentally non-local, new dispersive behaviors can arise. To ensure clarity and aid in understanding, Appendix A details how Biot-Allard's theory can be derived from the incompressibility hypothesis and Lagrangian considerations, both with and without a dissipation function. This derivation is applicable particularly in the high-frequency or quasi-static regimes, often referred to as the frozen or relaxed states. Leaving aside Lagrangian considerations with the dissipation function which lose their meaning in general time variations, as is explained, e.g., in the theoretical physics course by Landau and Lifshitz [7, 14–16] and in Goldstein [17], we then also detail in this Appendix A how Biot-Allard's theory is extended to the arbitrary harmonic regime by again exploiting the incompressibility hypothesis.

The expressions can be formulated in relation to the compliability and tortuosity local-operators, $\hat{\beta}$ and $\hat{\alpha}$, as follows: the fluid effective bulk modulus operator $\hat{K}_f^{-1}$ which is an ingredient in the expressions of $\hat{P}, \hat{Q}$ and $\hat{R}$ derived from Biot-Willis classical *gedanken experiments* (see [6, 18, 19] and present Appendix A) is represented as $K_a^{-1}\hat{\beta}$, while the density coefficients are determined by the equations $\hat{\rho}_{11} = \rho_s(1-\phi) + \rho_0\phi(\hat{\alpha}-1)$, $\hat{\rho}_{12} = \phi\rho_0\hat{\alpha}$ and $\hat{\rho}_{22} = -\phi\rho_0(\hat{\alpha}-1)$. Here, $K_a = \chi_0^{-1}$ is the fluid adiabatic bulk modulus (γP_0 for ambient air), ρ_s is the density of the solid of which the material skeleton is made, ρ_0 is the fluid ambient density and ϕ is the porosity. Due to the quasi-"en-bloc" Biot motion of the solid, the tortuosity and compliability local-operators, or their associated dynamic frequency kernel-functions $\tilde{\alpha}(\omega)$ and $\tilde{\beta}(\omega)$, remain the same as those observed in a material with identical microgeometry but with a solid frame that remains acoustically motionless. This, because it is too heavy/rigid to be shaken at all by the acoustic wave propagation occurring in the saturating gas. In this case the Biot-Allard formalism reduces, enabling us to perceive our material as an equivalent fluid of equivalent density $\hat{\rho} = \rho_0\hat{\alpha}/\phi$ and equivalent compressibility $\hat{\chi} = K_a^{-1}\phi\hat{\beta}$.

Due to the constrained temporal dispersion that aligns with the fluid quasi-indivergent motion, there exists a relatively simple definition of principle of operator functions $\hat{\alpha}$ and $\hat{\beta}$ from microgeometry, see e.g. [1] or [8] Appendix. As a result, there are relatively straightforward full-frequency model functions (encompassing low, mid, and high frequencies) to characterize the quantities $\tilde{\alpha}(\omega)$ and $\tilde{\beta}(\omega)$. They consist of core relaxation functions [1] $\tilde{\chi}(\omega)$ and $\tilde{\chi}'(\omega)$ with non-resonant and monotonic behavior (in Laplace representation, where they are purely real, they decrease smoothly from 1 in the relaxed $\omega \to 0$ limit, to 0 in the frozen $\omega \to \infty$ limit as frequency increases), well described in terms of a short list of low- and high-frequency geometric parameters of the pore space [20]. Successive refinements of the models are possible by incorporating the effects of more and more low- and high-frequency parameters of the pore-space, for which we can have explicit identifications at low frequency in terms of simple field-averaged formulas, see [8] Appendix, and [21]. At high frequency a different expansion process applies for the identifications of parameters. Explicit known formulas (Johnson-Allard's [11, 22] and [8] Appendix) have been obtained for the two first leading terms, based on the premise that the pore-wall surface is smooth at the scale of viscous and thermal boundary layers. The distinction between low- and high-frequency (the relaxed and frozen regimes) is relative to whether the viscous and thermal skin depths $\delta = (2\eta/\rho_0\omega)^{1/2}$ and $\delta' = (2\kappa/\rho_0 c_P\omega)^{1/2}$ are large or small relative to the pore size.

In this paper, a limited but profound extension of the theory will be considered so that spatial dispersion can enter the scene, liberating also temporal dispersion. We will uphold the concept of solid quasi-incompressibility, thereby preserving the overall framework of Biot-Allard's theory. However, we will eliminate the assumption of fluid quasi-incompressibility, thereby permitting the consideration of

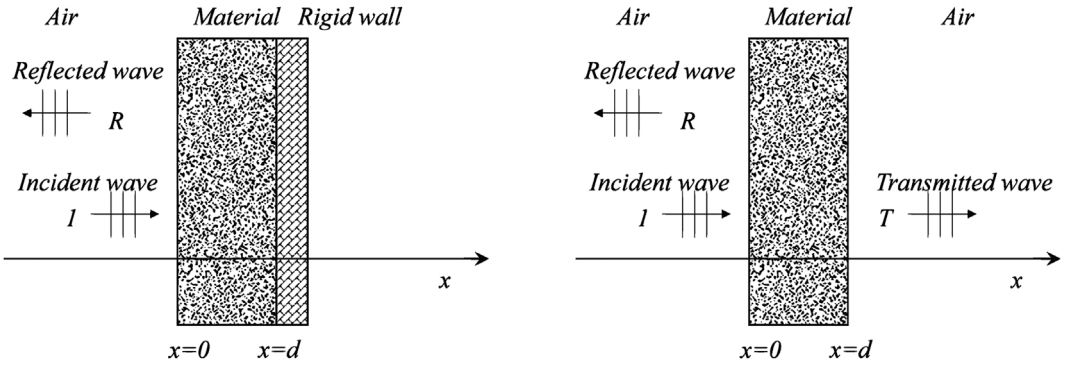

Figure 1. Reflection and reflection/transmission problems.

microgeometries that encompass structures such as Helmholtz resonators. In this situation, the tortuosity and compliability operators $\hat{\alpha}$ and $\hat{\beta}$, and then also the densities $\hat{\rho}_{ij}$ and elasticity $\hat{P}$, $\hat{Q}$ and $\hat{R}$ quantities, previously local-operators, will transform into *non-local operators*, incorporating spatial dispersion into their characteristics: Helmholtz resonance depends on spatial variations of fields due to mass conservation, thus implying a connection to spatial dispersion. We refer the reader again to Appendix A to make the connection between the extensive definitions of the non-local operators $\hat{\alpha}$ and $\hat{\beta}$ introduced in [8] and recalled in the present text, and the complex nuances of defining the corresponding newly extended "Biot-Allard" densities and elastic non-local quantities $\hat{\rho}_{ij}$ and $\hat{P}, \hat{Q}, \hat{R}$ – which are related to the new $\hat{\alpha}$ and $\hat{\beta}$ in the same way as they were in classical Biot-Allard theory. This involves substituting in the reasonings the Umov stress field notion to be mentioned below, in place of the conventional unquestioned (volume-averaged) notion of macroscopic excess pressure. Henceforth, for the sake of simplicity in our discourse, we will proceed in the following Sections without sacrificing more generality, assuming like in [1] and [8] the solid to be rigid and/or heavy enough to prevent any frame motion or deformation.

In this convenient case of a motionless solid frame, the present extended Biot-Allard's formalism reduces as before the classical Biot-Allard's one, allowing us to consider our material as a kind of equivalent-fluid [†] with equivalent density $\hat{\rho}$ and equivalent bulk modulus $\hat{\chi}^{-1}$ related as written before to the tortuosity $\hat{\alpha}$ and inverse compliability $\hat{\beta}^{-1}$ operators ([†] for this, in the application of normal-incidence we consider here, see Figure 1, axisymmetry will be assumed; specifically, the axis denoted as x, with the unit vector $\hat{\mathbf{x}}$, has a special property: a pressure drop along this axis induces a macroscopic motion oriented along $\hat{\mathbf{x}}$; in general a non-local equivalent-solid would be necessary to consider and we leave this for further work). However, the revised inclusion of spatial dispersion by permitting more diverse microgeometries, including Helmhotz-type structures, will profoundly alter the potential results. The equivalent fluid will now be, like $\hat{\alpha}$ and $\hat{\beta}^{-1}$, inherently non-local. When articulated in their simplified forms as novel pseudo-local functions, the tortuosity and compliability depart from their previous representations, no longer entailing straightforward non-resonant relaxation functions. This time the full half (causal) complex plane will be allowed for the location of the singularities of the pseudo-local response functions. As the solid quasi-incompressibility remains untouched, it should a priori be clear that the extended Biot-Allard's theory still implies significant narrowing of potential physics and behaviors. Yet, the formidable scenario of lifting both constraints simultaneously is well beyond the purview of the present study.

The introduction and detailed definition of the non-local operators $\hat{\alpha}$ and $\hat{\beta}$, as well as their repercussions, are extensively examined across two sequential book chapters [4, 8]. These chapters effectively use an acoustic-electromagnetic analogy to delve into the subject. Notably, these operators are introduced as the acoustic counterparts to the scaled electric and magnetic permittivities $\hat{\epsilon}$ and $\hat{\mu}$, highlighting a novel perspective in understanding acoustic phenomena through the lens of electromagnetism and vice-versa. An important observation made in [4, 8] is that the incorporation of spatial dispersion within the definitions of $\hat{\alpha}$ and $\hat{\beta}$ introduces a significant ambiguity. This issue parallels a recognized dilemma in electromagnetics, where spatial dispersion has led to the belief that searching for a single, definitive description of both electric and magnetic susceptibilities may be in vain. Taking a cue from the established practice in electromagnetic literature when dealing with spatial dispersion, as presented in [7, 9, 23], one could opt to encapsulate all effects of dispersion within $\hat{\alpha}$, effectively setting $\hat{\beta}$ to a default value of 1. This approach in acoustics mirrors the electromagnetic strategy of incorporating all dispersion influences into the electrical permittivity, thereby simplifying the magnetic permittivity to reflect the characteristics of free space. In the acoustic context, this strategy simplifies the effective fluid compressibility to directly equate to the adiabatic compressibility, offering a streamlined approach to understanding the impact of dispersion effects.

This strategy – inherently, just an expedient – diverges from the recommendations in [4, 8]. These references argue that the core issue in electromagnetics stems from a lack of available thermodynamic principles, leading to ambiguity. This gap in the theoretical framework makes it challenging

to accurately pinpoint the Maxwell field $\boldsymbol{H}$, especially amid spatial dispersion. Such ambiguity further complicates grasping the concepts and specifics of the Heaviside-Poynting energy flux density $\boldsymbol{E} \times \boldsymbol{H}$ in "electromagnetic form". However, in acoustics, leveraging current thermodynamic insights enables the introduction, made in [4] and [8], of a parallel energy flux density, designated in "acoustic form", thereby dispelling uncertainties by depicting the related Umov macroscopic stress field. This approach effectively establishes a clear and distinct acoustic counterpart to the electromagnetic macroscopic Maxwell $\boldsymbol{H}$ field, enriching our understanding and application of these concepts across both fields.

A specific action-response procedure ensued, allowing, in principle, the clear simultaneous definition and computation of both non-local operators $\hat{\alpha}$ and $\hat{\beta}$ based on microstructure [8]. Nevertheless, it appears challenging in general to unravel and condense the possible resulting behaviors in a straightforward manner. Dispersion in the operator functions $\hat{\alpha}$ and $\hat{\beta}$ arises from both the fluid's inherently inertial and compressible behavior within the complex geometry, as well as from viscous and thermal losses. Therefore, the dispersion characteristics are influenced not only by the relationship of frequency to the (more or less complete) development of viscous and thermal processes, but also by its relationship to potential resonances. Although we can still categorize the different regimes in frozen (viscous and thermal processes do not have time to develop on a period), relaxed (viscous and thermal processes have time to fully develop on a period), and intermediate (neither frozen nor relaxed) regimes, what was once easily described in the relaxed regime is now far from clear. Events in the intermediate regime may no longer be tightly coupled to the relaxed and frozen regimes due to the non-straightforward positioning of singularities. Finally, in the general non-local regime (whether relaxed intermediate or frozen), we do not currently have condensed field-averaged formulas for the real and imaginary parts of the kernel functions, unlike the ones that were easily obtained in the general local regime (see [8] Appendix, equations (7.185) and (7.186), where $\tilde{\alpha}'$ is related to $\tilde{\beta}$ by (7.174)).[1] The non-local frozen regime remains the only one that can be analyzed as straightforwardly as before, despite its potential complexity. It can still be approached with methods closely resembling those previously used. Incidentally, due to the significant dimensions required to generate audio-frequency Helmholtz resonances, boundary layer thicknesses are likely to be small in the geometries that motivate the non-local extension of classical theory. Thus we expect that the frozen regime, which is a perturbative modification of ideal-fluid behavior, will be especially pertinent in practical applications where Helmholtz resonances need to be taken into account. In this context, we focus on the high-frequency frozen regime and present the new condensed formulas obtained in this limit where the pore walls are smooth on the scale of boundary layer thicknesses.

In the considered frozen regime the fluid motion follows that of an ideal fluid, only perturbed by the presence of progressively diminishing viscous and thermal boundary layers at the pore walls. While the notion that the functions $\tilde{\alpha}$ and $\tilde{\beta}$ expand in power series of the viscous and thermal boundary layers δ and δ' respectively, cannot be maintained for all higher order terms (unlike in the local-theory approach), it remains valid for the first two leading terms, which persist as zero and first powers of $1/\omega^{1/2}$. Therefore the reasoning employed in [8] Appendix to derive Allard-Johnson's high-frequency (HF) results can be revisited to derive the corresponding new generalized results and their associated parameters. Remarkably, they resemble the known local forms as closely as possible, thanks to our application of the Umov method to resolve ambiguity. Additionally, this method is expected to be instrumental in justifying the non-local generalization of Biot-Willis *gedanken experiments* discussed in Appendix A, and the permanence of the operator relations, giving the $\hat{\rho}_{ij}$ from $\hat{\alpha}$, on one hand, and the $\hat{P}$, $\hat{Q}$ and $\hat{R}$ from $\hat{\beta}$, on the other hand, in same way as before. The pattern of these results lends weight to the general system of ideas introduced in the two book chapters [4, 8], with its central importance given to the Umov stress field. The derivation of more general condensed field-averaged formulas including the mid-frequency and relaxed low-frequency non-perturbative situations[2] remains open and warrants a clarification[3] which, we can expect, will re-emphasize the importance of the Umov stress field.

In this paper, for the sake of illustrating our concepts with a straightforward example, we will consider the need to solve a reflection or reflection/transmission problem. This involves determining the complex reflection/transmission coefficients R and T in the harmonic regime (as depicted in Fig. 1) for a layer of material positioned in ambient air, whether backed by a rigid wall or not. We note that the solution sketched here for simplicity in the case of a rigid frame can be straightforwardly reworked with frame vibrations, in line with well-known calculations for materials under the full Biot formalism. This is standard knowledge in Biot's theory (see e.g. [25] and [26] Chapter 10) and does not need to be repeated here. In the present non-local context, to maintain simplicity, we adhere to normal-incidence, assuming that the normal axis x aligns with a macroscopic symmetry axis of the material. Diverging from conventional theory, the introduction of oblique-incidence in the reflection-transmission problem requires a non-trivial generalization that extends beyond merely accounting for traditional isotropy/anisotropy. Generally,

[1] Added in proof: Non-local condensed field-averaged formulas can, in fact, be derived through a more involved but similar analysis. This will be addressed in a forthcoming paper that examines the question raised in the Conclusions of [8], specifically whether, and how, the operators $\hat{\rho}$ and $\hat{\chi}$ can be determined by supplying heat rather than work. The paper will also correct the alternative and slightly inaccurate definition of $\hat{\chi}$ given in [24], which was deliberately avoided in [4, 8], and the present paper.

[2] Note that in the present context it may not be realistic to look for a truly relaxed regime at the audio frequencies due to the large dimensions involved to generate Helmholtz resonances.

[3] This clarification – see footnote 1 – is to appear shortly.

the rigid-framed medium may not be accurately represented as a non-local fluid even in some microgeometries that may appear isotropic when analyzed through the traditional local-theory. This is because the concept of macroscopic pressure is now open to extension into the new Umov-Heaviside-Poynting macroscopic stress tensor, leading instead to a structure of equations of a non-local solid type. Note also that in the new non-local description, strictly speaking, there can be no macroscopically homogeneous finite layer of material. In the present simplified treatment we overlook the finite-dimension end-effects associated with this aspect and replace our operators by difference-kernel operators, see below (39). The exploration of both aspects (developing a new understanding of isotropy and anisotropy to address oblique incidence, as well as considering end-effects) is postponed to future studies. Note that in the solution to the reflection-transmission problem, it is once again clear that the Umov constraint plays a central role in extending the previous methods, since it is through it that we are allowed to state a simple continuity condition for the macroscopic pressure at the air-material boundaries.

The paper is organized as follows. First we recall in preliminary Section 2 the elements of traditional divergence-free local theory approach valid in simple (non-resonant) geometries. Its principle can be revisited in the recent paper [1], which was written in light of the insights provided by the current extension. Here, we recapitulate the outcomes of the classical approach, placing emphasis on the Johnson-Allard HF limit. Our objective is indeed to later derive the succinct results that incorporate the effects of spatial dispersion in HF limit. To this aim and before proceeding next, we broaden the perspective in this preliminary Section 2 by imagining the presence of Helmholtz-like structures, and, in this context, we revisit the general concept of "macroscopic variables", leading us to the Umov stress concept. In Section 3, we present the more general non-local Maxwell-Umov equation structure that is directly suggested by the acoustic-electromagnetic analogy. It is this new structure that is intended to cope, at long-wavelengths, with general microgeometries potentially including resonators. We precise from it the definition of principle, from microstructure, of the non-local operators. We argue that this description can be simplified into a superficially local medium representation of bulk properties within geometries that are "not too complicated". However, the task of determining which geometries can yield results accurately approximated by this pseudo-local simplification is far from straightforward. Such an endeavor would likely necessitate conducting explicit numerical solutions across a broad spectrum of geometries. This extensive effort would be aimed particularly at understanding the influence of couplings between resonant elements, size of the Representative Elementary Volume (REV) relative to inner structures, randomness, and so on. Such questions will have to be addressed in further studies. In Section 4, we shift our focus to a fully frozen, lossless, or ideal-fluid limit where the viscous and thermal skin depths δ and δ' are considered entirely negligible. In Section 5, we ultimately explore the novel non-local frozen perturbed HF limit, where both the viscous and thermal skin depths are small. In this frozen limit, incorporating the first two leading terms, we present straightforward field-averaged formulas for the non-local operators, their pseudo-local simplifications, and the new parameters that replace Johnson-Allard's classical local ones. Significantly, a new nontrivial pseudo-local frozen limit emerges for the previously unknown concept of "compliability". "Compliability" is a new word coined here by analogy with "tortuosity" for the new concept and quantities. In Section 6, we briefly outline the solutions to the reflection-transmission problems in the new HF pseudo-local limit, giving the expressions of R and T in terms of the new derived pseudo-local parameters. Finally we give conclusions in Section 7.

2 Preliminary considerations – understanding local theory, need for non-local theory, and macroscopic averages

Consider the normal-incidence transmission of long-wavelength small-amplitude sound waves as they pass through a macroscopically homogeneous porous layer structure permeated by ambient air. In addition to assuming without loss of generality for reasons explained above there is no motion in the frame, which leads to the vanishing of the fluid velocities at the pore walls, we simplify further by assuming the frame has substantial thermal inertia and thermal conductivity [12]. This allows it to function like a thermostat, keeping the surrounding temperature constant. As a result, are eliminated as well the excess temperatures at the pore walls. The acoustic wavefield in the saturating fluid is described by the equations (28)–(33) which state the general laws of conservation of mass, momentum and energy, the constitutive Stokes and Fourier laws, and the annulation boundary conditions. In the realm of local macroscopic theory, the structures under consideration typically feature pores with relatively well-defined and comparable sizes, denoted as ℓ. Given that the wavelengths are significantly larger than the physical dimensions L of a Representative Elementary Volume (REV) – mathematically expressed as $\lambda >> L >> \ell$ – this size disparity leads to the fluid motion being quasi divergence-free at the micro-scale, in the sense of $\nabla \bullet \boldsymbol{v} \sim v/\lambda <<< v/\ell$, where v represents a typical velocity magnitude. Furthermore, in addressing the dynamics of excess pressures within the porous medium, we adopt the formulation $p = p' + P$, wherein p' signifies the relatively minor in this context, fluctuating pore-scale component of excess pressure, and P represents the macroscopic excess pressure in the wavefield. The latter is defined by $P = \langle p \rangle_p$, where

$$\langle \cdot \rangle_p(\boldsymbol{x}) = \frac{1}{V_p} \int_{V_p} \cdot \, dV, \tag{1}$$

denotes the ("Lorentz") volume averaging operation performed over the pore space in the REV of central position $\boldsymbol{x}$ (e.g. an averaging sphere of radius R_h, see [1] and its Appendix A). By abuse of language, V_p will indifferently

denote, depending on the context, the REV pore space and/or its volume (the fluid volume), and sometimes even the entire pore space. Since the fluid domain deviates from a system of aligned straight channels, p' is obviously non-zero. However, in any non-trivial microgeometry where the currently used notion of a relatively well-defined size parameter ℓ can make sense, $\nabla p'$ and ∇P have similar magnitudes. That is, $P/\lambda \sim p'/\ell$, so in the present context we infer that $p' \sim \ell P/\lambda <<< P$. This relationship emphasizes that the overpressure field p is very close to its macroscopic mean P. This is not the case for its gradients $\nabla p(\boldsymbol{r})$, where the vector $\boldsymbol{r} = x\hat{\mathbf{x}} + y\hat{\mathbf{y}} + z\hat{\mathbf{z}}$ denotes positions in V_p, that are different from the macroscopic ∇P $(\boldsymbol{x})$ ($\boldsymbol{x}$ being the central value of $\boldsymbol{r}$ in the REV). However, it will be possible to consider them (in the harmonic regime) in fixed relation to the latter. Under these circumstances, the velocities in the different REVs appear with respect to the term $-\nabla p$ in (28) as if the fluid were incompressible and the macroscopic gradients $-\nabla P$ within each REV were uniform. This pure constancy introduced in the representation, instead of the actual slow variations, is a marker of the concomitant rejection of spatial dispersion. Simultaneously the excess temperatures τ (for all notations in this paper, unless otherwise noted, we refer to [4]) appear in relation to the $\beta_0 T_0 \dfrac{\partial p}{\partial t}$ term in (31), as if the latter were given by its macroscopic part $\beta_0 T_0 \dfrac{\partial P}{\partial t}$ only, of which the slow spatial variations (that occur on macroscopic distances) can be abstracted in totality. By macroscopic homogeneity these variations, which are linear inside a REV, can be forgotten because their effects cancel out by symmetry, producing no result on the averaged excess temperature $\langle\tau\rangle_p$. In short, to compute the excess temperature and velocity patterns

$$\tau(t,\boldsymbol{r}) = \tilde{\tau}(\omega,\boldsymbol{r})e^{-i\omega t},\ \boldsymbol{v}(t,\boldsymbol{r}) = \tilde{\boldsymbol{v}}(\omega,\boldsymbol{r})e^{-i\omega t}, \tag{2}$$

within a REV in harmonic regime – with these patterns representing the distributions of values inside this REV – we approach the problem by abtracting from the spatial variations of either macroscopic pressure (for τ) or its gradient (for $\boldsymbol{v}$). This significant simplification, which substitutes actual gradual variations with constancy, highlights our deliberate disregard for spatial dispersion. By treating these macroscopic factors as uniform across the REV, we acknowledge the impact of temporal variations of macroscopic pressure and its gradient on these patterns but abstract from the potential (and possibly huge) effects the slight differences in their amplitudes across various positions inside the REV could have. Thus, we effectively decouple the computation of microscopic excess-temperature and velocity patterns from the influences of spatially varying macroscopic pressure or gradient, a decoupling that intrinsically rejects spatial dispersion and is consistent with the vision of locally divergence-free fluid flow. In this way we content ourselves to solve, respectively, for the excess temperature pattern, and the velocity pattern in harmonic regime, the following microscopic problems, where C and C' stand for amplitude constants whose values do not change spatially or otherwise:

$$\rho_0 c_P \frac{\partial \tau}{\partial t} = \beta_0 T_0 \frac{\partial P}{\partial t} + \kappa \nabla^2 \tau,\ \beta_0 T_0 \frac{\partial P}{\partial t} = C' e^{-i\omega t}, \quad \text{in } V_p, \tag{3}$$

$$\tau = 0, \quad \text{on } S_p, \tag{4}$$

and

$$\rho_0 \frac{\partial \boldsymbol{v}}{\partial t} = -\nabla p' + \eta \Delta \boldsymbol{v} + \boldsymbol{f},$$

$$\boldsymbol{f} = -\nabla P = C e^{-i\omega t}\hat{\mathbf{x}}, \text{in } V_p, \tag{5}$$

$$\nabla \cdot \boldsymbol{v} = 0, \quad \text{in } V_p, \tag{6}$$

$$p' : \text{spatially stationary random field/periodic field}, \quad \text{in } V_p, \tag{7}$$

$$\boldsymbol{v} = \boldsymbol{0}, \quad \text{on } S_p, \tag{8}$$

with V_p and S_p the pore-space and pore-wall surface in the selected REV (see [1] where the arrival at these problems and their solution is also discussed in more details). In (5) the bulk body force $\boldsymbol{f}$ either comes from the presence of a macroscopic pressure drop accross the REV, or an external bulk body force due to a gravitational field. The p' represents a fluctuating response pressure, inherent in the need for circulation within the complex geometry. Like $\boldsymbol{v}$ it is characterized as a microgeometric response to $\boldsymbol{f}$, determined by the indivergent equations. Its value, given by the problem equations up to a spatial constant only, can be completely fixed by the condition $\langle p'\rangle_p = 0$, which is required if P is the macroscopic pressure and $p'+P$ represents pressure p. The REV is often conveniently assumed to be a period in a periodic medium. The seeked response fields $\boldsymbol{v}$ and p' and τ then are subject to periodic boundary conditions. Their patterns will depend on the time variations, the angular frequency ω in harmonic regime. The periodic or stationary random patterns, $\tilde{\boldsymbol{v}}(\omega,\boldsymbol{r})$ and $\tilde{\tau}(\omega,\boldsymbol{r})$, obtained for the fields $\boldsymbol{v} = \tilde{\boldsymbol{v}}(\omega,\boldsymbol{r})e^{-i\omega t}$ and $\tau = \tilde{\tau}(\omega,\boldsymbol{r})e^{-i\omega t}$ solutions to (5)–(8) and (3), (4), are complex-valued patterns; only in the relaxed and frozen limits $\omega\to 0$ and $\omega\to\infty$ they become real-valued, meaning no phase shift between velocities/excess temperatures at different positions in the REV. These two limiting (frozen and relaxed) real patterns will be markedly different.

This is illustrated in the two-dimensional plot of relaxed (left panel) and frozen (right panel) velocity patterns of Figure 2, adapted with permission from the computational work of N. Martys and E. J. Garboczi at the National Institute of Standards and Technology (NIST).[4] These correspond to the above different divergence-free velocity patterns observed in the limits of LF $\omega\to 0$ purely viscous diffusive regime and HF $\omega\to\infty$ inviscid purely propagative

[4] See their paper [27] and the electronic monograph https://concrete.nist.gov/monograph, Part III, General Random Porous Materials, Length Scales Relating Fluid Permeability and electrical conductivity in random two-dimensional porous media, alinea: Comparison between electrical and fluid flow problems.

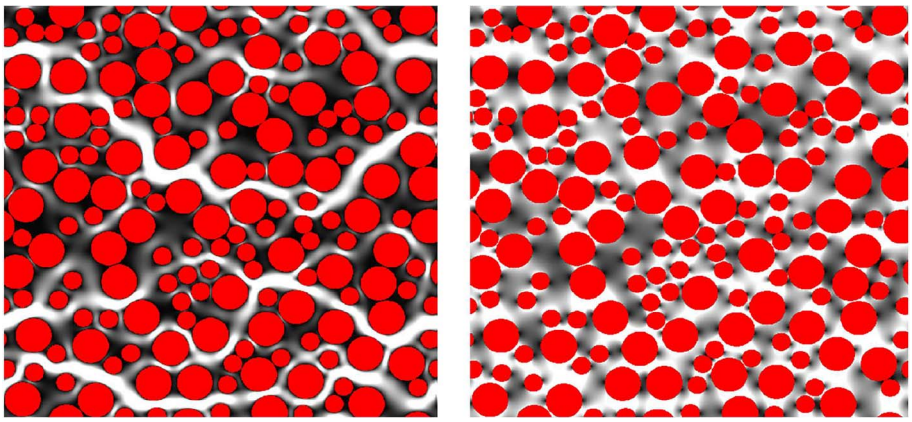

Figure 2. REV and relaxed (left) and frozen (right) divergence-free velocity patterns.

regime, respectively, understood in the sense of either large or small viscous skin depth $\delta = (2\eta/\rho_0\omega)^{1/2}$ compared to the characteristic dimensions (say ℓ as above) involved in defining the pore geometry. The left/right panels give qualitative representations of the magnitude of the divergence-free relaxed and frozen states velocities $\boldsymbol{v}$ (Stokes flow solution, on the left, when the inertial term $\rho_0 \dfrac{\partial \boldsymbol{v}}{\partial t}$ is suppressed, and Laplace flow solution, on the right, when the viscous term $\eta \Delta \boldsymbol{v}$ is suppressed), where light/grey colors in the fluid indicate regions of high/low $|\boldsymbol{v}|$.

On closer inspection, the reader can see that the 2D REV considered by Martys and Garboczi actually represents one irreducible period of dimension $L \times L$ in a periodic medium. For the case commonly called "stationary random" in [1, 8], and to mimic the corresponding absence of periodicity, we can approach this type of geometry by taking much larger dimensions L of the period before repetition of the structure. In this case, the corresponding periodic fields of artificial period $L \to \infty$ will give us mental ideal of what is called "stationary random". The physical REV, as defined by Lorentz's volume-averaging concept – see Lorentz's theory of electrons [28], beginning of Chap. IV pp. 133-134 §§113-114 – and further refined by Russakoff's signal theory approach [29], is independent of this artificial period dimension. It will be significantly smaller while still maintaining a reasonable size, and correspond to the homogenization radius R_h discussed later that will be much smaller than the artificial L. With such simplifications (5)–(8) and (3), (4) and mental representations on their meaning, it is common knowledge (that is recalled in [1] and [8] Appendix), how for the acoustic wave propagation in harmonic regime $e^{-i\omega t}$ one ends up at the macroscopic level with equations having the form:

$$\rho_0 \tilde{\alpha}(\omega) \frac{\partial \langle \boldsymbol{v} \rangle_p}{\partial t} = -\nabla \langle p \rangle_p, \quad \frac{1}{K_a} \tilde{\beta}(\omega) \frac{\partial \langle p \rangle_p}{\partial t} = -\nabla \cdot \langle \boldsymbol{v} \rangle_p, \quad (9)$$

where obviously, the so-called dynamic tortuosity $\tilde{\alpha}(\omega)$ is given as follows from the solution to (5)–(8):

$$\tilde{\alpha}(\omega) = \frac{C}{-\rho_0 i\omega \langle \tilde{\boldsymbol{v}} \rangle_p \cdot \hat{\mathbf{x}}}, \quad (10)$$

and $\tilde{\beta}(\omega)$ for which we introduce the wording "dynamic compliability", is easily shown to be given as follows from the solution to (3) and (4):

$$\tilde{\alpha}'(\omega) = \frac{C'}{-\rho_0 c_P i\omega \langle \tilde{\tau} \rangle_p}, \quad \tilde{\beta}(\omega) = \gamma - (\gamma - 1)/\tilde{\alpha}'(\omega), \quad (11)$$

where $\gamma = c_P/c_V$ is the heat coefficient ratio. For simplicity equations (9) are written here without forcing; however, if an external bulk body force $\boldsymbol{f} = \tilde{\boldsymbol{f}}_0 e^{-i\omega t + ikx}$ is present with long-wavelength variations, i.e. arbitrary $k = 2\pi/\lambda$ with $\lambda/4 \gg R_h$, it can just be added in right-hand side equations (9a) ("a" meaning here the left equations (9)). The equation (11a) is a definition, while the equation (11b) is obtained by using the equations (29)–(31), making averages $\langle \bullet \rangle_p$, and using the identity

$$\langle \nabla \cdot \boldsymbol{v} \rangle_p = \nabla \cdot \langle \boldsymbol{v} \rangle_p, \quad (12)$$

demonstrated using spatial averaging theorem (84) and pore-wall b.c. The reasoning is as follows. Introduce a thermal counterpart $\tilde{\alpha}'(\omega)$ of $\tilde{\alpha}(\omega)$ by setting in the harmonic regime the macroscopic definition $\rho_0 c_P \tilde{\alpha}'(\omega) \dfrac{\partial \langle \tau \rangle_p}{\partial t} = \beta_0 T_0 \dfrac{\partial \langle p \rangle_p}{\partial t}$ written in analogy to the definition (9a) and the affinity between the microscopic equations (5) and (3). Then average the equation of state (30) and take its time derivative to obtain $\gamma \chi_0 \dfrac{\partial \langle p \rangle_p}{\partial t} = \dfrac{\partial \langle b \rangle_p}{\partial t} + \beta_0 \dfrac{\partial \langle \tau \rangle_p}{\partial t}$. Insert the $\tilde{\alpha}'(\omega)$ definition to obtain, after using the general thermodynamic identity (59), the result $\chi_0 \left[\gamma - \dfrac{\gamma - 1}{\tilde{\alpha}'(\omega)} \right] \dfrac{\partial \langle p \rangle_p}{\partial t} = \dfrac{\partial \langle b \rangle_p}{\partial t}$. Finally, average (29) and introduce the identity (12) to rewrite the latter result as $\chi_0 \left[\gamma - \dfrac{\gamma - 1}{\tilde{\alpha}'(\omega)} \right] \dfrac{\partial \langle p \rangle_p}{\partial t} = -\nabla \cdot \langle \boldsymbol{v} \rangle_p$. By comparison with equation (9b), the result as given in (11) is then obtained. Equations and results equivalent to (9), (10) and (11) were originally derived in [30] by using the two-scale asymptotic theory of homogenization. A derivation using same technique but with a presentation closer to our present notations and definitions can be found in

[12]. Indeed, employing this technique subtly incorporates the incompressibility hypothesis. It emerges naturally from the assumed existence of a small parameter $\epsilon = \ell/\lambda$ and the use this technique makes, of it. The Biot theory itself is known to be derived by this technique which makes also emerge the "en-bloc" motion of the solid as the counterpart of the fluid "incompressible" motion (see [31] equations (8g) or (11) and equations (8c) or (13)). In our more recent work [1] or [8] to avoid confusion, we have chosen not to use it to derive the description (1)–(11) because we now see the process as fundamentally flawed. Its principle correctly provides the desired local description as a "leading order" approximation in the macroscopic description, but at the same time it introduces "higher order" terms obtained in sequence, which would account for effects of the type of spatial dispersion that appear only when wavelengths are sufficiently reduced. Not only does this not incorporate the recent understanding of long-wavelength spatial dispersion in electromagnetics, recalled in the previous Section 1, but certainly the actual short-wavelength spatial dispersion effects predicted would eventually differ from the existing ones. The technique is fundamentally flawed for our purposes, and we leave it aside. Our assertion of an inherent flaw in the two-scale asymptotic homogenization approach, which is not present in the non-local general approach we will propose, will require further work beyond the scope of this paper to be properly substantiated; however, the result is undoubted.

The well-known time-harmonic description (1)–(11), which expresses in arbitrary time variations through related spatially-local operators $\hat{\alpha}$ and $\hat{\beta}$, allows us to deduce the effective macroscopic properties of the material in the form of a frequency-dependent equivalent-fluid density of the material $\tilde{\rho}(\omega) = \frac{\rho_0}{\phi}\tilde{\alpha}(\omega)$ or local-operator $\hat{\rho} = \frac{\rho_0}{\phi}\hat{\alpha}$, and equivalent-fluid compressibility or inverse bulk modulus $\tilde{\chi}(\omega) = \tilde{K}^{-1}(\omega) = K_a^{-1}\phi\tilde{\beta}(\omega) = \chi_0\phi\tilde{\beta}(\omega) = \frac{\phi}{\rho_0 c_0^2}\tilde{\beta}(\omega)$ or local-operator $\hat{\chi} = \chi_0\phi\hat{\beta}$. Here, ρ_0 is ambient air density, $K_a = \gamma P_0$ air adiabatic bulk modulus, $\chi_0 = 1/K_a$ air adiabatic compressibility, ϕ porosity, c_0 soundspeed in air, with $\rho_0\chi_0 c_0^2 \equiv 1$. The appearance of factors of ϕ in these definitions is intentional. It allows us to highlight and consider $\phi\langle \boldsymbol{v}\rangle_p = \langle \boldsymbol{v}\rangle$ as the useful macroscopic velocity, a quantity conserved at interfaces. This formulation employs the total-volume averaging operation $\langle\cdot\rangle$, which is defined as in (1) but with a key modification: it normalizes by the total volume V instead of the fluid volume only $V_p = \phi V$, which is obviously preferable when treating the material as a whole. Alternatively, the effective macroscopic properties can be represented in terms of the two quantities, effective propagation constant (wavenumber) $\tilde{q}(\omega) = \omega/\tilde{c}(\omega) = \sqrt{\tilde{\alpha}(\omega)\tilde{\beta}(\omega)}\omega/c_0$, with definition $\tilde{\rho}(\omega)\tilde{\chi}(\omega)\tilde{c}^2(\omega) \equiv 1$, and characteristic impedance $\tilde{Z}_c(\omega) = \tilde{\rho}(\omega)\tilde{c}(\omega) = \frac{\rho_0 c_0}{\phi}\sqrt{\tilde{\alpha}(\omega)/\tilde{\beta}(\omega)}$, with again, expression adapted for the whole volume. These representations facilitate a straightforward and conventional approach to solving problems in the harmonic regime, including reflection issues or reflection/transmission problems at normal incidence, see Figure 1. The explicit determination of the functions $\tilde{\alpha}(\omega)$ and $\tilde{\beta}(\omega)$ and then local-operators $\hat{\alpha}$ and $\hat{\beta}$ (of which they are the Fourier kernels), can be made by solving, resp., the viscous-inertial and thermal pore-scale simplified problems (5)–(8) and (3), (4) at each ω, and making the macroscopic averages. Because of the simplistic nature of temporal dispersion involved (sum of purely damped components in Fourier space, recall the discussion in Section 1 and see [13, 32] and [33]) and relatively simple nature of geometries encountered, fairly good approximations of the full frequency functions exist in terms of a few (relaxed/frozen) geometrical parameters associated with the pore-space, and that correspond to the two extreme d.c. and HF simpler problems at $\omega = 0$ and $\omega\to\infty$, (see [8] Appendix, and [1] for details). Usually, in noise control applications, efficient absorbing materials are obtained when their pores dimensions ℓ are on the order of 10^{-4} m, see e.g. [6]. The dimensions match the order of magnitude of the viscous and thermal skin depths, δ and δ', at audio frequencies. This match means the penetration depths of vortical motions are neither too large to cause direct reflection of the acoustic perturbation – since the wave is prevented from significantly entering the material due to viscous locking, making it a hard surface – nor too small to hinder absorption. In this case, although transmission is efficient, it lacks sufficient internal damping to facilitate absorption. There is an intermediate optimum to be found that will depend on the configuration but will remain in the intermediate region $(\delta, \delta') \sim \ell$ (as the Prandtl number is 0.7 in air and $\delta/\delta' = \mathrm{Pr}^{1/2}$ the two skin depths are comparable). In these circumstances, it is evident that the materials used likely exhibit significant intrinsic damping and overall absorption. This is due to their large fluid-solid contact area per unit volume – on the order of $\ell^{-1}\sim 10^4$ m^{-1} – where dissipation is triggered by the annulation boundary conditions. Note also that, given that wavelengths at audio frequencies fall within the range of tens of centimeters, the parameter $\epsilon = \ell/\lambda$ is consequently very small. This underscores the feasibility of employing two-scale asymptotic homogenization theory. In the high frequency limit $\omega\to\infty$ that will specifically concern us in this paper, the wavelength is still large but the skin depths are small compared to the pore sizes. While not optimal, the absorption can still be significant and needs to be considered due to the relatively large area of contact. This is determined by the product $(\delta, \delta')/\ell$ of the area $\sim 1/\ell$ with the skin depths, which become small, although not excessively so. The effective properties then are efficiently described in terms of Johnson's ideal-fluid tortuosity α_∞, Johnson's viscous characteristic length Λ_∞, and Allard's thermal characteristic length $\Lambda\prime_\infty$, precised below. In this HF limit the successive terms are expected to appear in polynomial expansion in powers of the respective complex skin depths $\tilde{\delta} = \left(\frac{\nu}{-i\omega}\right)^{1/2}$ and $\tilde{\delta}' = \left(\frac{\nu'}{-i\omega}\right)^{1/2}$ (where $\nu = \frac{\eta}{\rho_0}$, $\nu' = \frac{\kappa}{\rho_0 c_P} = \nu/\mathrm{Pr}$). This is because we assume that the pore-wall surface is smooth

and we know the role played by these quantities for the way vortical and entropic components of the field decrease above flat and gently curved surfaces. We have the following expansions:

$$\alpha(\omega) = \alpha_\infty \left[1 + \left(\frac{v}{-i\omega} \right)^{1/2} \frac{2}{\Lambda_\infty} + \dots \right], \tag{13}$$

and

$$\beta(\omega) = 1 + (\gamma - 1) \left(\frac{v\prime}{-i\omega} \right)^{1/2} \frac{2}{\Lambda\prime_\infty} + \dots . \tag{14}$$

The two first terms in these expansions were obtained by Johnson and Allard, see [11, 22] and [8] Appendix. The two Johnson's quantities α_∞ and Λ_∞ are determined as follows by the incompressible ideal-fluid velocity pattern $\boldsymbol{v}_\infty(\boldsymbol{r})$ – frozen field velocity pattern defined below, see equations (17)–(20). No tilde is indicated in the expressions as this velocity pattern can be taken real independent of frequency by choice $\mathsf{C} \propto -i\omega$ of the forcing amplitude constant in (17):

$$\alpha_\infty = \frac{\langle \boldsymbol{v}_\infty^2(\boldsymbol{r}) \rangle_p}{\langle \boldsymbol{v}_\infty(\boldsymbol{r}) \rangle_p^2}, \frac{2}{\Lambda_\infty} = \frac{\int_{S_p} \boldsymbol{v}_\infty^2(\boldsymbol{r}) dS}{\int_{V_p} \boldsymbol{v}_\infty^2(\boldsymbol{r}) dV}. \tag{15}$$

Allard's $\Lambda\prime_\infty$, is just:

$$\frac{2}{\Lambda\prime_\infty} = \frac{\int_{S_p} dS}{\int_{V_p} dV}, \tag{16}$$

because it is constructed like Johnson's but with the frozen excess temperature field $\tau_\infty(\boldsymbol{r})$ which is a pure spatial constant τ_∞; as such it cancels in the expression. The above ideal-fluid incompressible velocity field $\boldsymbol{v}_\infty(\boldsymbol{r})$ in $\boldsymbol{v}_\infty = \boldsymbol{v}_\infty(\boldsymbol{r}) e^{-i\omega t}$ is defined through the solution to:

$$\rho_0 \frac{\partial \boldsymbol{v}_\infty}{\partial t} = -\nabla p\prime_\infty + \boldsymbol{f}, \quad \boldsymbol{f} = -\nabla P = \mathsf{C}\, e^{-i\omega t} \hat{\mathbf{x}}, \quad \text{in } V_p, \tag{17}$$

$$\nabla \cdot \boldsymbol{v}_\infty = 0, \quad \text{in } V_p, \tag{18}$$

$$p'_\infty : \text{ spatially stationary random field/periodic field}, \quad \text{in } V_p, \tag{19}$$

$$\boldsymbol{v}_\infty \cdot \hat{\boldsymbol{n}} = 0, \quad \text{on } S_p, \tag{20}$$

where $\hat{\boldsymbol{n}}$ is the local unit normal to S_p. The ideal-fluid being inviscid the Laplacian viscous term in (5) is removed and the b.c. (8) is replaced by no penetration condition. The pattern $\boldsymbol{v}_\infty(\boldsymbol{r})$ also coincides with an electric field pattern $\boldsymbol{E}(\boldsymbol{r})$ or current density pattern $\boldsymbol{j}(\boldsymbol{r}) = \sigma_f \boldsymbol{E}(\boldsymbol{r})$ appearing when the pore-space is filled with a fluid of conductivity σ_f and the solid is insulating (giving the no penetration b.c. at S_p) [34]. Obviously, for a unit macroscopic electric field imposed $\boldsymbol{e} = \frac{V}{L}\hat{\mathbf{x}}$ with unit value for the potential drop V along distance L, the electric field $\boldsymbol{E}$ in the pores is the solution to

$$\boldsymbol{E} = -\nabla\varphi + \boldsymbol{e}, \ \boldsymbol{e} = 1\hat{\mathbf{x}}, \quad \text{in } V_p, \tag{21}$$

$$\nabla \cdot \boldsymbol{E} = 0, \quad \text{in } V_p, \tag{22}$$

$$\varphi : \text{ spatially stationary random field/periodic field, in } V_p, \tag{23}$$

$$\boldsymbol{E} \cdot \hat{\boldsymbol{n}} = 0, \quad \text{on } S_p. \tag{24}$$

Simple comparison shows the proportionnality relations, $-\rho_0 i\omega \boldsymbol{v}_\infty(\boldsymbol{r}) = \mathsf{C}\boldsymbol{E}$, and $p'_\infty(\boldsymbol{r}) = \mathsf{C}\varphi$ (when chosen with zero mean), justifying the assertion. With these definitions of α_∞, Λ_∞ and Λ'_∞ the proof of (13) and (14) can be found in [8] Appendix.

Suppose we keep the shape of the microgeometry unchanged, but significantly and uniformly increase all dimensions. With the same pattern of microgeometry but pore dimensions now significantly larger than 10^{-4} m, the expanded homothetic material will not be very interesting acoustically. Only the effect of α_∞ (of unchanged dimensionless value) on the characteristic impedance and refractive index will remain and be the same. The important noise-controlling loss corrections resulting from the characteristic lengths Λ_∞ and Λ'_∞ (now large compared to the respective skin depths δ, δ') will be small and have little effect on the acoustics. Conversely, because of the very important viscous friction, the significantly shrunken homothetic material would have very high intrinsic attenuation (not well described by (13) and (14), because more terms would have to be considered in it, or even more, the expansion over the powers of the skin depths themselves would have ceased to be). But it would not be very interesting acoustically either, since it would show almost total reflection at its front side, provoked by the too small pore sizes (viscous locking), and its possible interest in preventing transmission would be quickly mitigated by the well-known mass law. In fact, the assumption of a motionless solid, as in the present context, would quickly become irrealistic. The vibrations of the Biot solid would have to be taken into account and would lead to a transmission that is basically given by the law of mass.

Now, given the expanded homothetic material, suppose we start hollowing out some inclusions, as depicted in Figure 3, to produce the structure in the form of a Helmholtz resonator involving, ultimately, widely different pore sizes: neck apertures dimensions smaller than cavities dimensions, by one order of magnitude or more. Then, Helmholtz resonances may appear within a range of frequencies corresponding to wavelengths long enough to ensure that a macroscopic description of the propagation exists. When this happens, and the flow in and out of the cavities is not prevented by viscous friction, (the viscous skin depth being assumed sufficiently small including in the narrow necks), it is no longer meaningful to model the velocity pattern as divergence-free. In particular, local

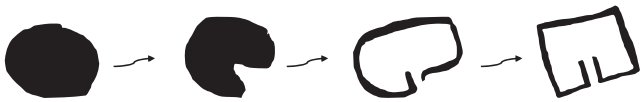

Figure 3. Helmholtz resonators.

imbalances in the condensation field or the excess pressure field will appear, that were not present in the non resonant material.

In this scenario, the material is not homogenizable in the conventional sense, as the concept of a relatively well-defined unique ℓ and associated small parameter $\epsilon = \ell/\lambda$ loses its validity. Consequently, we will need to reassess the classical models to derive a more comprehensive and precise prediction of the reflection and transmission properties of a material layer. This evaluation will involve the Umov condition, which will establish a new general definition of macroscopic pressure. In the conventional divergence-free approach, the two different methods of performing the pressure average, the previous $P = \langle p \rangle_p$ one, and the Umov one, yield identical results. This has been established in [1]. However, this equivalence may not hold true in this broader context.

Therefore, we will now briefly discuss the notion of macroscopic averaging. While the notion of a macroscopic ensemble average would present advantages if it could be properly introduced for the materials under study (recalling the advantages of Gibbs' averaging conceptions in statistical physics, see Marle's penetrating remarks [35]), here, to fix our ideas and get closer to an ordinary reflection or transmission experiment performed on a single sample instead of an ensemble of realizations of the sample, we will continue to think in terms of volume averages performed in a REV. A discussion of this notion of macroscopic volume averaging can be found in Lorentz's classic monograph [28] in the pages previously cited. Emerging from his "Theory of Electrons" program of understanding Maxwell's macroscopic equations by starting at the microscopic level, the concept is clearly stated. Essentially, with Lorentz averaging we have in mind performing coarse-grained averaging in averaging spheres with a "homogenization radius" R_h chosen not too large to obliterate the variations than can effectively be measured and not too small to be affected by fluctuations before convergence; such a R_h will be used in what follows when it is necessary to specify the previous REV size parameter "L". Note that the sole use of Lorentz's macroscopic averaging volumes will remain sufficient for our purposes of analyzing material properties while abstracting from potential macroscopic end effects at its boundaries. However, when addressing these end effects, introducing averages conceived as surface – not volume – averages could be beneficial. We leave this consideration for further work as we do not address these effects here.

Consider $V(\boldsymbol{x})$ to be an averaging sphere of radius R_h, which can be centered at various positions $\boldsymbol{x}$ within the material. Due to homogeneity, R_h does not depend on $\boldsymbol{x}$. Similarly, let $V_p(\boldsymbol{x})$ represent the pore-space associated with $V(\boldsymbol{x})$. Its microscopic configuration depends on $\boldsymbol{x}$, though its macroscopic characteristics do not. We use $\boldsymbol{r}$ to denote the microscopic position vector spanning all microscopic positions within $V_p(\boldsymbol{x})$ or $V(\boldsymbol{x})$. The volumes within $V(\boldsymbol{x})$ and $V_p(\boldsymbol{x})$ are denoted by the same symbols V and Vp, respectively, and they do not depend on $\boldsymbol{x}$, with the relationship $V_p = \phi V$ indicating their proportionality. The pore-wall domain surface within V is denoted as S_p, which can be considered, like the spatial domains $V(\boldsymbol{x})$ or $V_p(\boldsymbol{x})$, a function of $\boldsymbol{x}$, $S_p(\boldsymbol{x})$. Later, we will introduce $\boldsymbol{r}_w$ (w for "pore walls") as the microscopic position vector spanning all possible microscopic positions in the domain $S_p(\boldsymbol{x})$.

Let us now start with a discussion of the notion of macroscopic fluid velocity, as defined by the following averages:

$$\langle \boldsymbol{v} \rangle(\boldsymbol{x}) = \frac{1}{V} \int_{V_p} \boldsymbol{v}(\boldsymbol{r}) dV, \; \langle \boldsymbol{v} \rangle_p(\boldsymbol{x}) = \frac{1}{V_p} \int_{V_p} \boldsymbol{v}(\boldsymbol{r}) dV. \quad (25)$$

The integrations are over volume elements $d^3\boldsymbol{r}$ where $\boldsymbol{r}$ spans all positions in $V_p(\boldsymbol{x})$. As we have seen there are reasons to prefer the former, normalized with total volume. The second may be preferable if one is willing to have averaged values that are representative of the values in the fluid phase only. But that is not the point that interest us here. Following Marle's remarks [35], let us raise the following objection to the definition of macroscopic velocities based on such direct volume averaging. Velocity is not an additive quantity: its integral over a volume lacks a specific physical meaning. Consequently, its macroscopic average, $\langle\ \rangle$ or $\langle\ \rangle_p$, should also lack a well-defined physical meaning. However, our context here is a *small amplitude linear theory*. Within this framework, the definitions of macroscopic velocities $\langle \boldsymbol{v} \rangle$ and $\langle \boldsymbol{v} \rangle_p$ gain physical significance as follows. Mass and momentum densities, ρ and $\rho \boldsymbol{v}$, are additive variables. Their integrals within V_p correspond to the mass and momentum of the fluid within the volume V_p or V. Following Marle's advocacy [35], there are no objections to generally defining the macroscopic mean velocity in the fluid, as, $\langle \boldsymbol{v} \rangle_p = \int_{V_p} \rho \boldsymbol{v} dV / \int_{V_p} \rho dV$, by definition of a suitable average operation $\langle\ \rangle_p$. With linearization where $\rho = \rho_0 + \rho'$, and by retaining only the leading terms, we discard the terms based on ρ'. This approach yields the definition:

$$\langle \boldsymbol{v} \rangle_p = \frac{1}{V_p} \int_{V_p} \boldsymbol{v} dV_p. \quad (26)$$

This argument shows that, within linearization, the definition (25) is justified and provides fully meaningful macroscopic magnitudes. What is important is that this holds true even in the presence of local imbalances that result in distributed excess density variations on a small scale. Such variations may be induced by Helmholtz structures.

We present another enlightening general argument leading to the same conclusion, also based on small-amplitude linearization. This argument begins by revisiting the electromagnetic-acoustic analogy of Ref. [4], which is described in detail in its Appendix on pages 259–271, is applied to a rigid-frame fluid-saturated material in the next chapter Ref. [8], and is presented again in the present paper.

In fact, as mentioned p. 270, this analogy is intended for future application to structured materials. For the structured materials derived, say, by combining Figures 2 and 3, the postulated non-local structure of the macroscopic equations, originally partially defective in the fluid itself (see general considerations in [4] and in particular Section 6.12.3), is expected to evolve into a completely well-formed structure due to the fluid-solid interactions. In this context, this analogy would involve replacing the – known to be *covariant* vector – macroscopic electromagnetic potential field A_i by the macroscopic mean fluid displacement field $\langle a^i \rangle$ (see the observation on p. 266 before equation (6.191), here we have to add the averaging symbol since we are not in the free fluid but in the material), in which we raise the index i since it will turn out to be contravariant. The time derivative of this field, $V^i = \partial \langle a^i \rangle / \partial t$, corresponds to our mean velocity vector. Since in electromagnetics we have the possibility of writing the electric field as $E_i = \partial A_i / \partial t$, (see [4] footnote 37 p. 245 for the rationale for this, which involves the notion that the macroscopic media provide the necessary reference frame in which to invoke Weyl's gauge), this mean velocity is proposed as an acoustic analog of the macroscopic electric field E_i. An immediate objection would be that an acoustic finite mean displacement $\langle a^i \rangle$ cannot possess tensorial properties. Similarly, the microscopic displacement a^i itself cannot have tensorial nature either. This is clearly seen when using Gauss' general coordinates: such quantities which connect two points located at two different space positions cannot transform, under general changes of Gauss coordinates, like a physical vector, (which attaches to only one spatial point – or spatio-temporal point in a relativistic context).[5] However, we intend here to work in linearized limit. Because of this we can consider (as mentioned in [4] p. 266) that the associated mean displacement fields $\langle a^i \rangle$ (whose indexes i in spite of their seemingly contravariant notation are devoid of tensorial significance) are actually infinitesimals that behave as coordinates differentials dx^i i.e. true contravariant vectors. Taking their average does not change this fact. It merely results in the construction of a new contravariant macroscopic vector field, whose elements are anchored at the central positions of the averaging volumes. Thus, we see that linearization effectively addresses the above objection, allowing (26) to serve as an appropriate acoustic variable – a contravariant counterpart to the macroscopic covariant electric field E_i. This opens up the possibility of pursuing the analogy further, which will be done in the next section for heuristic reasons only. There will be no difficulty in justifying a posteriori the relations we are led to state in this way.

Likewise, because it is an additive excess density variable ρ' divided by a constant, the linearized condensation $b = \rho'/\rho_0$ can also be meaningfully macroscopically averaged with operations $\langle\ \rangle$ or $\langle\ \rangle_p$. Alternatively, the subtly different interpretation of b by means of the equation (29) below, just interpreted as a direct definition of this letter b, also shows that its direct average has physical meaning. This equation (29) keeps its form when averaged, because of the identity (12). With indice p canceled this identity remains true even in an inhomogeneous material presenting spatial variation of ϕ. By the way, this second interpretation of b is actually how we see this variable in the electromagnetic analogy: see e.g. [4] equation (6.98). It is inspiring that, in reality, the magnetic field is an antisymmetric tensor, and, the condensation conceived in this second way naturally generalizes as an opposite macroscopic strain tensor, giving an acoustic symmetric counterpart of the magnetic field (see [4]). Obviously, it is this tensor symmetric strain field which would have to be introduced and used in the circumstances mentioned for oblique incidence, where appear a Umov symmetric stress field defined by $\langle p \boldsymbol{v}_i \rangle = -H_{ij} \langle \boldsymbol{v}_j \rangle$.

In this connection, it is noteworthy that the averaging of the excess pressure thermodynamic variable p presents itself differently than the preceding direct volume averages. The excess temperature τ field is obviously not an additive field. From the relation (30) below, that expresses the fluid thermodynamic equation of state, p cannot be additive. Therefore, we cannot expect the general significance of the direct, volume averages, $\langle p \rangle_p$ or $\langle p \rangle = \phi \langle p \rangle_p$, in the presence of resonance that produce important small scale distribution of the excess pressure. What we will consider as the macroscopic pressure – or the opposite effective macroscopic stress field H in the fluid – is determined in a unique manner after identifying a suitable additive variable. The so-called current density of energy transported in acoustic form [4], represented by $p\boldsymbol{v}$, is recognized as an additive quantity in a specific surface-oriented sense. Its dot product and integral over a surface element $S\hat{\mathbf{x}}$ of sufficient size to be representative and whose normal is that of macroscopic motion's direction (x axis, refer to Fig. 1), namely $\int p\boldsymbol{v} \cdot \hat{\mathbf{x}} dS$, is endowed with a general physical significance. It represents the rate of disturbance energy crossing this surface in a usable acoustic form, contrasting with energy lost in viscous or thermal irreversible transfer processes. To illustrate, situating the representative surface S at a specific position x, the surface mean value $S^{-1} \int p\boldsymbol{v} \cdot \hat{\mathbf{x}} dS$ captures solely the "acoustic part" of the total macroscopic energy current density at that position, with the complement which we deem lost and do not need to quantify further. All of it has no acoustic effect at all. It comes either out of the thermostat or goes integrally to it without any capability for acoustic action. Shifting the surface across a total distance L to form a representative volume $V = SL$ centered at x, and recognizing that surface integral values in this volume, only change linearly along x at long wavelengths, we observe that the averaged line integral $L^{-1}S^{-1} \int p\boldsymbol{v} \cdot \hat{\mathbf{x}} dS dl$, equivalent to the averaged volume integral $V^{-1} \int p\boldsymbol{v} \cdot \hat{\mathbf{x}} dV = \langle p\boldsymbol{v} \rangle \cdot \hat{\mathbf{x}}$, aligns by symmetry of the variations along x with the initial surface mean value at x, $S^{-1} \int p\boldsymbol{v} \cdot \hat{\mathbf{x}} dS$. This quantity, as mentioned, holds

[5] For this understanding of what are tensors, we refer to Weinberg [36] or Brillouin [37] or Fournet [38].

meaningful significance. Consequently, we deduce that a macroscopic pressure P, as defined by the following indirect averaging procedure:

$$\langle p\boldsymbol{v}\rangle = P\langle \boldsymbol{v}\rangle, \tag{27}$$

will exhibit favorable general characteristics. This is none other than "Umov" definition suggested by our electromagnetic analogy, as we presented it in detail in [4] and [8]. Again, it is inspiring that the electromagnetic H field is a rank-two tensor, antisymmetric, and the above definition naturally extends in general, $\langle p\boldsymbol{v}_i\rangle = -H_{ij}\langle \boldsymbol{v}_j\rangle$, so as to yield again a rank-two tensor H, but this time, symmetric. Here, the alignment between $\langle p\boldsymbol{v}\rangle$ and $\langle \boldsymbol{v}\rangle$ is specifically due to our focus on propagation along the symmetry axis x. This topic of the tensor nature of acoustic H was previously mentioned in [4] (see its Appendix A and footnotes 10 and 48) as well as in [1, 8], and present Section 1. Without the symmetry assumption along x, the ensuing considerations in present paper would require significant generalization, a task we reserve for future work. In short, in the present context where the frame is motionless, the macroscopic vector of components $S_i = \langle pv_i\rangle$ represents a density of energy current associated with the fluid motion, and carried out in acoustic form. It presents itself as the product of two macroscopic fields, Umov H_{ij} field and macroscopic velocity field V_i. It reminds of the Poynting-Heaviside vector of components S_i, which also is the product of two fields, Maxwell H_{ij} antisymmetric field and macroscopic electric field E_j. (See more precisely [4], p. 265 equation (6.185), p. 270 equation (6.204), where covariant-contravariant notations are introduced for a precise formulation of this). The analogy emphasizes that the Poynting-Heaviside vector is a density of energy flow "in electromagnetic form", but the lack of thermodynamic embedding of macroscopic electromagnetics has so far prevented clearly understanding what it means and constructing this quantity from the underlying, also macroscopic, level of electronic flow within the solid lattice of nuclei, which is closer to its quantum origin than is the fluid motion of gas particles. This question remains unsettled today.

To finish, it is important to note that the definition (27) corresponds with the average pressure concept discussed in Pierce's insightful book [39], specifically in the "Lumped-Parameter Model" section. Re-examining Pierce's discussion on lumped-parameter models, our proposed general non-local Maxwell-Umov macroscopic framework (34)–(38) can be seen as representing a lumped-parameter model in the broadest sense. Within this model, the "aggregate variables" include the Lorentz and Maxwell fields – V, B, D, H – as will be further explored in Section 3, while the "lumped parameters" are the effective density and bulk modulus operators, $\hat{\rho}$ and $\hat{\chi}^{-1}$. The crucial roles played by the Heaviside-Poynting or Umov products, as well as the distinction to be made between Lorentz fields (direct averages) and Maxwell fields (indirect thermodynamic averages), were introduced in [24, 40], though with a misleading proposed definition of $\hat{\chi}$ (see the remark in the Conclusions of [8], p. 316). This issue was merely circumvented in [4, 8], rather than being duly clarified and corrected.[6] We will now delve into the non-local description, repeating in a more digestible form than in [4, 8] how it resolves the question of the insertion of spatial dispersion through the concrete implementation of the electromagnetic-acoustic analogy. It will become clear that although the analogy serves as a heuristic guide, the theoretical constructs it inspires can be justified independently, as we have just sketched above for the Umov definition of macroscopic pressure (for full details on the purely near-equilibrium thermodynamic reasons for this construct, see the foundational study [4]).

3 Non-local generalization: Maxwell structure of the equations, Umov condition, and definition of non-local and pseudo-local operators

Now, let us focus our attention on the propagation of long-wavelength small-amplitude sound waves when the ambient air is permeating a porous layer whose microgeometry we imagine, say, to be drawn by combining Figure 2 with Figure 3 for some inclusions, then opening the possibility of resonant behaviors. At the "microscopic" scale, (which is already considered a thermodynamic, thus macroscopic, level), for small amplitude linear movements, the governing equations in the pore volume V_p completely filled with air will be those of the linearized, near-equilibrium, Navier-Stokes-Fourier model:

$$\rho_0 \frac{\partial \boldsymbol{v}}{\partial t} = -\nabla p + \eta \Delta \boldsymbol{v} + \left(\frac{\eta}{3} + \zeta\right)\nabla(\nabla \cdot \boldsymbol{v}) + [\boldsymbol{f}], \quad \text{in } V_p, \tag{28}$$

$$\nabla \cdot \boldsymbol{v} + \frac{\partial b}{\partial t} = 0, \quad \text{in } V_p, \tag{29}$$

$$\gamma \chi_0 p = b + \beta_0 \tau, \quad \text{in } V_p, \tag{30}$$

$$\rho_0 c_P \frac{\partial \tau}{\partial t} = \beta_0 T_0 \frac{\partial p}{\partial t} + \kappa \Delta \tau, \quad \text{in } V_p, \tag{31}$$

with boundary conditions at the pore-wall surface S_p,

$$\boldsymbol{v} = \boldsymbol{0}, \quad \text{on } S_p, \tag{32}$$

$$\tau = 0, \quad \text{on } S_p. \tag{33}$$

We refer to [4, 8] for the notations and derivation of these equations from principle and empiricism. In (28), to facilitate the subsequent definition of non-local operators, we introduce a source term $[\boldsymbol{f}]$ that envisages the air being subject to an external bulk body force $\boldsymbol{f}$ per unit air volume, capable of varying arbitrarily in time and space. The bracket notation indicates our consideration of both scenarios: where this external source term is either present

[6] Added in proof: A full correction of the flawed definition is to appear shortly – see footnotes 1 and 3.

or absent. We conceptualize it as a conservative force field $\boldsymbol{f} = -\hat{\mathbf{x}}\nabla_x \mathcal{P}(t,x)$ per unit air volume, originating from a potential $\mathcal{P}$ that varies arbitrarily but is composed solely of long-wavelength Fourier components, $\tilde{\mathcal{P}} e^{-i\omega t + ikx} + c.c.$, where $k = 2\pi/\lambda$ and $\lambda/4 \gg R_h$. This condition serves as a prerequisite because our present work employs the concept of Lorentz average.[7] As noted in Sections 1 and 2, to circumvent significant complications associated with the potential tensor nature of the forthcoming H field, macroscopic symmetry along the axis x is presumed, implying that $\langle p\boldsymbol{v}\rangle$ and $\langle \boldsymbol{v}\rangle$ are colinear, directed along x. We maintain this symmetry assumption regardless of whether resonances occur or not, or whether the overpressure p constitutes a contrasting field at the REV scale (thus requiring the generalization to be introduced) or not (thus falling within the local approach discussed earlier).

For the actual situation of small amplitude motion along a symmetry axis x, it has been argued in [4, 8], based on the developed electromagnetic analogy, that at the outer macroscopic scale, we should encounter acoustic equations with a non-local Maxwell-Umov-type structure. This structure makes appear suitably defined and related coarse-grained variables, and the long-wavelength arbitrary source term $+[-\nabla_x \mathcal{P}]$, which plays a similar role to the applied macroscopic current density $[\boldsymbol{J}]$ in electromagnetics. Note that the transformation of characteristic antisymmetry in the electromagnetic case, into characteristic symmetry in the acoustic case, see [4] Appendix, prevents giving meaning to the signs in the transformation. This concerns not only the force/current and acoustic-displacement/EM-potential parallel but also all other correspondences. This source term in the macroscopic Maxwell description can act in the medium, or not, without any effect on the intrinsic susceptibilities:

$$\frac{\partial B}{\partial t} + \nabla_x V = 0, \; \frac{\partial D}{\partial t} = \nabla_x H + [-\nabla_x \mathcal{P}], \tag{34}$$

$$D(t,x) = \hat{\rho} V(t,x) = \int \rho(t-t',x,x') V(t',x') dt' dx', \tag{35}$$

$$H(t,x) = -\hat{\chi}^{-1} B(t,x) = -\int \chi^{-1}(t-t\prime,x,x\prime) B(t\prime,x\prime) dt\prime dx\prime. \tag{36}$$

This framework incorporates both temporal and spatial dispersion through the $\int \mathrm{d}t'$ and $\int \mathrm{d}x'$ integrations [7, 9]. It utilizes two directly averaged coarse-grained ("Lorentz") variables, $V(t, x)$ and $B(t, x)$, velocity and condensation, assuming the roles of macroscopic electric and magnetic fields, respectively. These are derived from the underlying microscopic 3-vector $\boldsymbol{a}$ – acoustic displacement, not EM potential[8] – and represent direct volume averages of the same underlying kinematic fields:

$$B(t,x) = \langle b\rangle(t,x), \; V(t,x) = \langle \boldsymbol{v}_x\rangle(t,x),$$
$$b = -\nabla \cdot \boldsymbol{a}, \; \boldsymbol{v} = \partial \boldsymbol{a}/\partial t. \tag{37}$$

Furthermore, an indirectly averaged ("Maxwell") density variable, $H(t, x)$, serves the role of the macroscopic electromagnetic $\boldsymbol{H}$ field, established by the "Umov" condition:

$$H(t,x)\langle v_x\rangle(t,x) \equiv -\langle p v_x\rangle(t,x). \tag{38}$$

This condition posits that the macroscopic current density of energy, transported in a usable acoustic form and denoted by $S = \langle p v_x\rangle$, in contrast to a degraded, lost form, must be derived from the direct product of the Maxwell field H and Lorentz field V – remarkably, in a non-local context, both quantified at the same spatio-temporal location. This unique stipulation underscores a profound aspect of how the usable disturbance energy is conveyed across space and time in such contexts. Regrettably, while it is clear that the similar direct product of H and E fields should represent the "energy current-density transported in electromagnetic form" [4, 42] no counterpart condition in electromagnetics has been identified due to the absence of the required thermodynamic framework for describing macroscopic electronic motions, which hinders the understanding of this notion. Lastly, a "Maxwell" density variable, $D(t, x)$, plays the role of the Maxwell induction field $\boldsymbol{D}$, completing the structure.

This structure emerges under the assumption that the material can be "homogenized," in the sense of "lumped," enabling a macroscopic description of motion through aggregated variables. Importantly, this framework can be established as such, independently of the heuristic electromagnetic analogy initially employed to conceptualize it in [4, 8]. The derivation of the first macroscopic equation (34) alongside definitions (37) naturally follows from the volume averaging of the microscopic equation (29). Subsequent equations, namely the second macroscopic equation (34), (35) and (36), followed by the significant addition of (38), are effectively definitions. Following a rationale akin to that presented in Landau and Lifshitz [7], the incorporation of a non-local response term based on field B in (35) is deemed superfluous due to the interrelation between fields B and V as specified in (34a), implying that the impact of such a term is implicitly accounted for within the response term on V, as it is non-local. This argument extends to negate the necessity of a response term predicated on V within (36), given the structure's internal non-local relationships. In essence, the definitive and unique interpretation of all quantities arises from a compatibility analysis between macroscopic and microscopic equations, diverging from a mere direct averaging of all microscopic equations. While the first field equation (34a) results from averaging equation (29), the subsequent equation (34b) is not derived by averaging (28), even though the term $-\nabla_x \mathcal{P}$ is effectively the mean $\langle\,\rangle_p$ of $[\boldsymbol{f}_x]$ in (28). Consequently, the second macroscopic equation primarily facilitates the definition of

[7] This prerequisite could be omitted in favor of an ensemble-average approach, as discussed around Gibbs average in [8] and exemplified in [41].

[8] See [4] for an explanation of how here in the analogy the EM potential can be put in the form of a 3-vector, playing the role of 3-vector acoustic displacement, through working in the Weyl jauge in the rest frame of the electromagnetic material medium.

the D field, once the H field has been defined via condition (38).

We anticipate that the field H will exhibit continuity at the air/material boundaries, specifically, $H = -p$ at such boundaries, where p represents the excess pressure in the air immediately outside, and H denotes the macroscopic stress in the saturating air immediately inside. This continuity is derived from the presumption of continuous normal acoustic energy flow across the boundary surface element $\int \hat{\mathbf{x}} dS$: thus, $\int p\boldsymbol{v} \cdot \hat{\mathbf{x}} dS = \int (P = -H)\, \boldsymbol{V} \cdot \hat{\mathbf{x}} dS$, indicating that there should be no loss of normal acoustic energy flow at the boundary, unless surface dissipation or specific mechanisms such as Wood's anomaly are explicitly present. Importantly, the continuity of normal volume flow is required, $\int \boldsymbol{v} \cdot \hat{\mathbf{x}} dS = \int \boldsymbol{V} \cdot \hat{\mathbf{x}} dS$, which establishes the air/material b.c. $H = -p$, (a special case of general continuity of stresses[9]). Regarding the macroscopic "Maxwell" field $D(t,x)$, it is conceptualized as representing "momentum in acoustic form" per unit of representative fluid volume, a thermodynamic concept introduced and discussed in Refs. [4, 24]. It appears as a reversible part, given not by the total momentum, but by that from which we have removed the contributions of all irreversible exchanges. Despite the absence of a straightforward thermodynamic definition, its characteristics are indirectly yet definitively specified by the Umov equation (38). Ultimately, the structure of the Maxwell-Umov equations guarantees that all elements, particularly the non-local operators, are delineated through the compatibility between the systems of "microscopic" and "macroscopic" equations, with the Umov condition (38) playing a pivotal role in the micro-macro integration.

Let us proceed. In addressing spatial non-locality, we acknowledge that boundaries inherently disrupt translational invariance, making a finite slab of material never truly homogeneous. This complexity typically necessitates separate kernel arguments x and x' as illustrated in equations (35) and (36). Nevertheless, our analysis proceeds with a simplification: we approximate the material as homogeneous by sidestepping edge effects. This approximation leads us to consider kernels dependent only on the difference $x - x'$, effectively reducing them to their difference-kernel forms:

$$\rho(t-t',x,x') \approx \rho(t-t',x-x'),\ \chi^{-1}(t-t',x,x') \approx \chi^{-1}(t-t',x-x'). \tag{39}$$

Thus, we represent our material using the following simplified macroscopic scenario[10]:

$$D(t,x) = \hat{\rho} V(t,x) = \int \rho(t-t',x-x') V(t',x') dt' dx', \tag{40}$$

$$H(t,x) = -\hat{\chi}^{-1} B(t,x) = -\int \chi^{-1}(t-t',x-x') B(t',x') dt' dx', \tag{41}$$

Equations for the kernels, incorporating this simplification, are given by:

$$\begin{aligned} \rho(t-t',x-x') &= \int \frac{d\omega}{2\pi}\frac{dk}{2\pi} \tilde{\rho}(\omega,k) e^{-i\omega(t-t')+ik(x-x')}, \\ \chi^{-1}(t-t',x-x') &= \int \frac{d\omega}{2\pi}\frac{dk}{2\pi} \tilde{\chi}^{-1}(\omega,k) e^{-i\omega(t-t')+ik(x-x')}. \end{aligned} \tag{42}$$

This approach allows us to momentarily disregard edge effects, deferring their thorough examination to future work, while focusing on a homogeneous approximation for our current analysis.

Let us now show how the micro-macro compatibility Umov condition (38) determines the theoretical framework for calculating the Fourier constitutive amplitudes, $\tilde{\rho}(\omega,k)$ and $\tilde{\chi}^{-1}(\omega,k)$, from the microstructure. This process effectively "homogenizes" the material.

Initially, at the *microscopic level*, we examine equations (29)–(33) concerning the real fields and isolate a *unique complex Fourier component* in the Fourier representation of the arbitrary real forcing $\boldsymbol{f}$, denoted by ($\tilde{\mathcal{P}}$ as a complex constant, k as a real wavenumber chosen independently of ω):

$$f_x = -\nabla_x \mathcal{P} = -ik\tilde{\mathcal{P}} e^{-i\omega t+ikx},\ f_y = f_z = 0. \tag{43}$$

There exists a unique abstract solution for forced fields to equations (29)–(33) with the specified expression of $\boldsymbol{f}$. This solution can be expressed as, $\boldsymbol{v} = \tilde{\boldsymbol{v}}(\omega,k,\boldsymbol{r}) e^{-i\omega t+ikx}$, $b = \tilde{b}(\omega,k,\boldsymbol{r}) e^{-i\omega t+ikx}$, $p = \tilde{p}(\omega,k,\boldsymbol{r}) e^{-i\omega t+ikx}$, $\tau = \tilde{\tau}(\omega,k,\boldsymbol{r}) e^{-i\omega t+ikx}$, where the tilde amplitudes are determined as unique complex quantities. These amplitudes are interpreted as either stationary random fields (in stationary random geometries) or periodic fields (in periodic geometries). Regarding existence and unicity, there are important remarks of principle to be made. The existence and unicity are deemed automatic in the stationary random case, not in the periodic case. In this case, there is ambiguity in the choice of the spatial period. Tilde fields can be taken periodic over the smallest, irreducible period, or over two-times multiple one, and so on. Here, however, we wish to work with Lorentz averages, so that we have the prerequisite of long-wavelength Fourier components. In that case, in a limit, the ambiguity disappears as the tilde solutions are the same irrespective of the chosen period. Numerically,

[9] In the general case where the macroscopic stress in the saturating fluid becomes the symmetric tensor H_{ij} due to non-localities, this would translate to $H_{ij} = p\delta_{ij}$ at air/material boundaries.

[10] Note that when using Gauss coordinates, the non-difference kernel form with separate spatial arguments x, x', is always mandatory even for the inherently homogeneous, thus unbounded, materials, see [4] Appendix. This is the general, non-simplifiable form of equations. It can be seen as an example of the convergence of simplicity and generality in physics – think, for example, of the electromagnetic equations of fields generated by charges and currents in empty space, written, as in the time of Maxwell's treatise, as a very large number of component noncovariant equations, versus, their drastic reduction in a few covariant statements.

choosing the shortest period is most efficient. In what follows, in spite of our focus on long wavelengths, it will be convenient to consider also the "unphysical" solutions when k does not respect the scale separation with the REV. In this case, uniqueness in periodic geometries is lost, and in order to fix future developments, it will be quite possible, as we will later explain, to assume that the periodicity conditions are imposed on the irreducible period. With this in mind, let us come back to our abstract fields solutions that are unique and defined in principle whatever wavelengths.

The real or imaginary parts, $\boldsymbol{v}^{\mathfrak{R}}$ or $\boldsymbol{v}^{\mathfrak{I}}$, of the abstract fields, $\boldsymbol{v} = \tilde{\boldsymbol{v}}(\omega, k, \boldsymbol{r})e^{-i\omega t+ikx}$, and similarly for other fields, correspond to the physical fields generated by a real force, which can be derived from either the real or imaginary part, $\boldsymbol{f}^{\mathfrak{R}}$ or $\boldsymbol{f}^{\mathfrak{I}}$, of the abstract force given in (43). These two sets $\mathfrak{R}$ and $\mathfrak{J}$ of physical fields contain redundant information: the two forces are identical but shifted in time by a quarter of the period. For clarity, consider $-ik\tilde{\mathcal{P}} = \tilde{f}$ to be real, achievable by an appropriate choice of the time or space origin. The abstract force is expressed as $f_x^{\mathfrak{R}} + if_x^{\mathfrak{I}} = \tilde{f}[\cos(kx - \omega t) + i\sin(kx - \omega t)]$. The force $f_x^{\mathfrak{I}}$ at time t corresponds to the force $f_x^{\mathfrak{R}}$ at time $t+\pi/2\omega$, indicating that the response fields at time t for $f_x^{\mathfrak{I}}$ are essentially the response fields for $f_x^{\mathfrak{R}}$ at time $t+\pi/2\omega$. Introducing scaled real amplitudes $'$ and $''$ to denote, $\tilde{\boldsymbol{v}}(\omega, k, \boldsymbol{r}) = [\tilde{\boldsymbol{v}}'(\omega, k, \boldsymbol{r}) + i\tilde{\boldsymbol{v}}''(\omega, k, \boldsymbol{r})]\tilde{f}$, etc., the $\mathfrak{R}$ fields in response to $f_x^{\mathfrak{R}} = \tilde{f}\cos(kx - \omega t)$ are:

$$\boldsymbol{v}^{\mathfrak{R}} = [\tilde{\boldsymbol{v}}'(\omega, k, \boldsymbol{r})\cos(kx - \omega t) - \tilde{\boldsymbol{v}}''(\omega, k, \boldsymbol{r})\sin(kx - \omega t)]\tilde{f},$$

etc., and the $\mathfrak{J}$ fields in response to $f_x^{\mathfrak{I}} = \tilde{f}\sin(kx - \omega t)$ are given by substituting $\cos(kx - \omega t)$ with $\sin(kx - \omega t)$ and $-\sin(kx - \omega t)$ with $\cos(kx - \omega t)$, etc.

Let us now turn to the *macroscopic level* equations (34)–(38) concerning the real fields, and identify the same unique complex Fourier component within the forcing mechanism. This component acts as an analogous external macroscopic current in electromagnetics. Under complex excitation (43) substituted in (34)–(38) the *abstract forced field solution* is represented as $V = \tilde{V}e^{-i\omega t+ikx}$, $B = \tilde{B}e^{-i\omega t+ikx}$, $H = \tilde{H}e^{-i\omega t+ikx}$, and $D = \tilde{D}e^{-i\omega t+ikx}$. Here, the tilde amplitudes, $\tilde{V}$, $\tilde{B}$, $\tilde{H}$, and $\tilde{D}$, are complex constants that depend on ω and k. This leads to the system of equations as follows:

$$-i\omega B = -ikV, \quad -i\omega D = ikH - ik\mathcal{P}, \tag{44}$$

$$D = \tilde{\rho}(\omega, k)V, \quad H = -\tilde{\chi}^{-1}(\omega, k)B, \tag{45}$$

$$B = \langle b \rangle, \quad V = \langle v_x \rangle, \tag{46}$$

$$H\langle v_x \rangle = -\langle p v_x \rangle. \tag{47}$$

The only equation that involves perhaps unusual algebra is (47), due to the rare instance of managing unconjugated products of fields in a complex representation. For completeness and in light of previous considerations, a detailed derivation is provided in Appendix B.

It is important to note that the extraction of single or double exponentials e^{ikx} or e^{2ikx} from under the averaging symbols in (46) and (47) can be done with the Gibbs ensemble averaging concept. This concept involves averaging microscopic fields or products of such fields, at a given position $\boldsymbol{x}$, without any spatial integration but in the sense of an ensemble of realizations. Thus with Gibbs averaging, after extraction of exponentials and cancellation, we can rewrite the same equations (44)–(47) with tildes on all micro and macro fields. As per the Lorentz volume averaging method we use here, the same can be done only in the long wavelength limit (e.g., $kR_h \ll 2\pi/4$), see [4, 8]. For shorter wavelengths, it is by a petition of principle that we consider applying the equations (44)–(47) again to the tilde fields. This definition is allowed as a way to definitively fix the forthcoming Lorentz kernels, because the influence this choice will have on their detailed spatial variations will not be seen in the only region we are interested in with Lorentz averages, namely the physical long wavelength region that allows us to meaningfully homogenize the material. This is also our justification for not worrying about the aforementioned ambiguity of the solutions at short wavelengths. In short, with Lorentz averages and by a definition that we are free to make, we assume that all the above equations (44)–(47) hold directly with tildes placed on the micro and macro fields, regardless of the values of ω and k, and further consider that the tildes are those defined on the irreducible period.

The micro-macro compatibility of our system of equations and definitions should now be fully ensured, and the consequences of this should be as follows. Given the forced solution $\boldsymbol{v} = \tilde{\boldsymbol{v}}(\omega, k, \boldsymbol{r})e^{-i\omega t+ikx}$, etc., for the microscopic equations (29)–(33) with excitation (43), we derive the three macroscopic variables V, B, H by direct and indirect averaging as described in (46) and (47). The requirement that these are the macroscopic variables involved in solving the macroscopic equations (44)–(47) with the same excitation is a compatibility condition that fixes the kernels. It requires that the operator kernels $\tilde{\rho}(\omega, k)$ and $\tilde{\chi}^{-1}(\omega, k)$ be identified as:

$$\begin{aligned} \tilde{\rho}(\omega, k) &= \frac{ik(H - \mathcal{P})}{-i\omega V} = \frac{D}{V}, \\ \tilde{\chi}^{-1}(\omega, k) &= -\frac{H}{B} = \frac{\omega D/k - \mathcal{P}}{B}, \end{aligned} \tag{48}$$

where we can also put tildes on the variables V, H, B, D, and $\mathcal{P}$, and where we are not forced to restrict our formal calculations to the long wavelengths. If k were short wavelength, a microscopic solution automatically exists, as disambiguated by our choice of irreducible period, and with the above sketched imposition of exponential extraction it allows defining values of the kernels, not intended to be physical but thought convenient to fix the mathematics.

These identifications and definitions therefore give a definite recipe to compute *in principle* the macroscopic non-local kernels, from the microstructure. Since V and B are not independent but directly related by equation (44a), and similarly H and D are related by equation (44b), the acoustic kernels $\tilde{\rho}(\omega, k)$ and $\tilde{\chi}^{-1}(\omega, k)$ are completely determined by ω, k and two macroscopic variables: a "Lorentz" variable resulting from direct averaging

(V or B), and a "Maxwell" variable resulting from indirect averaging (H or D). We conjecture that due to the fluid-solid interactions and the application of Navier-Stokes-Fourier thermodynamics, the Fourier kernels, when integrated as described in equation (42), lead to real-space kernels that are well defined and existent. This situation stands in contrast to that in the free fluid, where the convergence of Fourier transforms enables the determination of $\hat{\chi}^{-1}$, $\hat{\chi}$, and $\hat{\rho}^{-1}$ from the corresponding Fourier kernels $(\omega,\ k)$. However, the lack of convergence for $\hat{\rho}$ prevents its determination and highlights the limitations of near-equilibrium thermodynamics as described in the Navier-Stokes-Fourier framework (see [4], section 6.12.3). The corresponding shortcomings of the thermodynamic framework are deemed irrelevant as soon as fluid-solid interactions are introduced, relegating their effects to the background. This is an illustration of a well-known fact in electromagnetism, according to which the non-local characteristics of a macroscopic medium have in some ways more to do with the structuring of the medium than with the intrinsic properties of its constituents.

In what follows, by expressing the above kernels in the form:

$$\tilde{\rho}(\omega,k)=\rho_0\frac{\tilde{\alpha}(\omega,k)}{\phi},\qquad \tilde{\chi}^{-1}(\omega,k)=\chi_0^{-1}\phi^{-1}\tilde{\beta}^{-1}(\omega,k), \tag{49}$$

we introduce the postulated well-defined non-local tortuosity $\tilde{\alpha}(\omega,k)$ and, for lack of a better term, non-local inverse *compliability* $\tilde{\beta}^{-1}(\omega,k)$ kernels. These dimensionless quantities are normalized to give an apparent density $\rho_0\tilde{\alpha}$ and apparent compressibility $\chi_0\tilde{\beta}$ of the air phase. The inclusion of porosity ϕ in (49) follows naturally from equations (44)–(47) which incorporate the definitions $V=\phi\langle v_x\rangle_p$, and $B=\phi\langle b\rangle_p$. The continued use of "tortuosity" to refer indiscriminately to the operator $\hat{\alpha}$, the function $\alpha(t,x)$, the Fourier kernel $\tilde{\alpha}(\omega,k)$, or the (forthcoming in Section 4) principal or pseudo-local function $\tilde{\alpha}(\omega)$ and its high-frequency (HF) limit $\tilde{\alpha}_\infty(\omega)$, despite significant conceptual evolution from its traditional understanding, is a matter of convenience. Similarly, "compliability" is suggested for the operator $\hat{\beta}$, the function $\beta(t,x)$, the Fourier kernel $\tilde{\beta}(\omega,k)$, or the principal or pseudo-local function $\tilde{\beta}(\omega)$ and its HF limit $\tilde{\beta}_\infty(\omega)$.[11] The scalar kernels as functions of ω and k satisfy characteristic symmetry relations of the type [7], $\tilde{f}(-\omega,-k)=\tilde{f}^*(\omega,k)$, where * denotes the complex conjugate, indicating the reality of the original-space response kernels (42). For thermodynamic reasons, the operators $\hat{\rho}$ and $\hat{\chi}^{-1}$ and their inverses fall within the class of generalized susceptibilities [7, 14], necessitating the symmetry $\tilde{f}(\omega,k)=f(\omega,-k)$, which, for scalars here, embodies the symmetric nature inherent to kinetic coefficients in thermodynamics (Onsager-Casimir principle, see equations (103.6) and (103.10) in [7]). In the absence of forcing ($\mathcal{P}=0$), the system (44) and (45) leads to the dispersion equation:

$$\tilde{\rho}(\omega,k)\tilde{\chi}(\omega,k)\omega^2=\rho_0\chi_0\tilde{\alpha}(\omega,k)\tilde{\beta}(\omega,k)\omega^2=k^2, \tag{50}$$

determining, for any given real ω, the potential frequency-dependent wavenumbers $\tilde{k}(\omega)$ of propagating/attenuating waves within the medium, always complex with simultaneously non-zero real and imaginary part due to the losses.

Given that the kernels are *even functions of* k due to the general thermodynamic property of symmetry in kinetic coefficients, we ascertain that for a specified real ω, if $\tilde{k}(\omega)$ (complex) solves (50), then $-\tilde{k}(\omega)$ must also be a solution. This condition illustrates what is known as the property of reciprocity: allowing changing the sign of $\tilde{k}$ results in the propagation of waves of same phase speeds and attenuations along x and $-x$ directions. Recall, in the context of wave propagation and due to inherent losses, a wave identified as propagating in the $+x$ direction must exhibit attenuation in this same direction. This requirement automatically selects one of the two possible signs of $\Im(\widetilde{k})=\Im(\omega/\widetilde{c})=\omega\Im\left[1/\sqrt{\tilde{\rho}(\omega,\widetilde{k})\tilde{\chi}(\omega,\widetilde{k})}\right]$, determining a choice for the square root determination, that depends on whether the wave along $+x$ will be written with $e^{i\widetilde{k}x}$ or $e^{-i\widetilde{k}x}$. At variance the sign of $\Re(\widetilde{k})$ for a wave propagating in $+x$ direction is not imposed a priori by chosing the form $e^{i\widetilde{k}x}$ or $e^{-i\widetilde{k}x}$. It is dictated only by the specific dynamic solution in the wave, which for the real phase velocity $c_\varphi=\Re(\widetilde{c})=\Re\left[1/\sqrt{\tilde{\rho}(\omega,\widetilde{k})\tilde{\chi}(\omega,\widetilde{k})}\right]$ can have either positive or negative sign, as determined by the above imposed square root determination, i.e. pointing either in the direction of propagation (direction of attenuation) or in the opposite direction. With representation $e^{\mp i\omega t+i\widetilde{k}x}$, the criterion for a wave propagating along $+x$, is, $\Im(\widetilde{k})>0$; the sign of $\Re(\widetilde{k})$ depends on the wave dynamics. In this study, given our assumption of finite REVs underpinning our volume-averaging operations – typically characterized by periodic boundary conditions and not overly complex structures – we consider the potential solutions $\widetilde{k}(\omega)$ to (50) to be distinctly discrete and enumerable. This includes solutions such as $\pm\widetilde{k}_1(\omega)$, $\pm\widetilde{k}_2(\omega)$, and so forth, which do not form a continuum and are nondegenerate. Furthermore, our interest centers on scenarios where wavelengths substantially exceed the dimensions of the REV. In such contexts, particularly within materials featuring relatively simple internal geometries, we anticipate that primarily the leading or principal mode solution – the one exhibiting minimal attenuation – assumes physical significance, residing within the long-wavelength domain. Other solutions, barring proximity to resonances, are typically deemed non-physical as they generally do not align with long-wavelength criteria and exhibit very large attenuation. As pointed out by Landau and Lifshitz in continuum electrodynamics [7], resonance conditions can induce significant shifts in a

[11] Note that, in same manner as the term "tortuosity" is adapted to different contexts with qualifiers such as ideal-fluid tortuosity, static tortuosity, dynamic tortuosity, operator tortuosity, similarly, the term "compliability" will be further specified depending on the context with analogous terms.

nonphysical solution, moving it into the physically relevant long-wavelength region while relegating the former primary solution to the nonphysical domain. We will assume that solutions can first be ordered by increasing attenuation i.e. ascending values of $\Im\left(\widetilde{k}_n\right) > 0$ in the vicinity of $\omega = 0$, and then continue to be continuously identifiable and traceable as ω increases. The question of degeneracies, or exceptional points where two different solutions might merge to create a different physics, would require a specific study beyond the scope of this paper. Commonly, the solution with the least attenuation at $\omega = 0$, designated as number 1, remains so at elevated frequencies. However, this does not preclude the scenario where a solution of a higher initial order could become the foremost in terms of minimal attenuation as ω ascends. In reflection/transmission experiments depicted in Figure 1, the field inside the material consists of sums of both right-propagating and left-propagating modes. Should a particular mode solution emerge as dominant – due to negligible corrections brought by alternative overly damped modes – it becomes relevant to approximate the field as primarily composed of this least-attenuated, right-going and left-going, mode, with wavenumbers $\pm\widetilde{k}_1(\omega)$ (or possibly another index in scenarios where a initially higher-order mode becomes the one predominant at the considered frequency). Moving forward, we will proceed under the assumption that such a single-mode representation of the field suffices. Note that in these circumstances the permissible frequency range for our macroscopic description, which leverages volume-averaged variables and necessitates a clear scale separation between macroscopic wavelengths and the characteristic size R_h of averaging volumes, will be confined to frequencies low enough to maintain the condition that the wavelengths $\lambda' = 2\pi/|\Re[\widetilde{k}_1(\omega)]|$ and $\lambda'' = 2\pi/\Im[\widetilde{k}_1(\omega)]$ qualify as long wavelengths, specifically, $\lambda'/4$, $\lambda''/4 \gg R_h$.

Finally, when the microgeometry within the REV is sufficiently simple to ensure that only the principal waves merit consideration (a definition of what precisely means, "sufficiently simple", is not evident and will have to be clarified in further studies through detailed simulations in various geometries), the dynamic behavior of the medium within the specified range will be effectively captured by principal, spatially pseudo-local, macroscopic equations:

$$\frac{\partial B}{\partial t} + \nabla_x V = 0, \quad \frac{\partial D}{\partial t} = \nabla_x H - \nabla_x \mathcal{P}, \tag{51}$$

$$D(t,x) = \hat{\rho} V(t,x) = \int \rho(t-t') V(t',x) dt', \tag{52}$$

$$H(t,x) = -\hat{\chi}^{-1} B(t,x) = -\int \chi^{-1}(t-t') B(t',x) dt', \tag{53}$$

where the principal or pseudo-local operators, $\hat{\rho}$ and $\hat{\chi}^{-1}$, are such that the Fourier-space kernels, $\widetilde{\rho}(\omega)$ and $\widetilde{\chi}(\omega)$, are the quantities, $\widetilde{\rho}\left[\omega, \widetilde{k}_1(\omega)\right]$ and $\widetilde{\chi}\left[\omega, \widetilde{k}_1(\omega)\right]$, with $\widetilde{k}_1(\omega)$ the principal least-attenuated solution to (50). The term "pseudo-local" is employed to signify that, despite utilizing a description reminiscent of local behavior, the properties described are fundamentally due to the influence of non-local responses. Also writing these operators, $\rho_0\widetilde{\alpha}(\omega)/\phi$ and $\chi_0\phi\widetilde{\beta}(\omega)$, give a generalized new, principal, pseudo-local theory definition for the ancients (conventional divergence-free approach) $\widetilde{\alpha}(\omega)$ and $\widetilde{\beta}(\omega)$. These new, pseudo-local $\widetilde{\alpha}(\omega)$ and $\widetilde{\beta}(\omega)$ are now capable to account for possible resonant effects in more general microgeometries. When the frequencies can be made sufficiently high while maintaining long-wavelengths, resulting in skin depths that are small compared to all pore sizes, the pseudo-local kernels $\widetilde{\alpha}(\omega)$ and $\widetilde{\beta}(\omega)$ exhibit only minor but acoustically important perturbations from the new principal ideal-fluid, pseudo-local kernels $\widetilde{\alpha}_\infty(\omega)$ and $\widetilde{\beta}_\infty(\omega)$. Unlike their truly local predecessors $\widetilde{\alpha}_\infty = \text{constant} > 1$ and $\widetilde{\beta}_\infty \equiv 1$, which are purely geometrical, these new ideal-fluid kernels are now functions of frequency whose frequency dependencies arise from a resonant interplay between inertial effects, associated with the fluid density ρ_0, and elastic effects, associated with the compressibility χ_0. The definitions of these latter kernels $\widetilde{\alpha}_\infty(\omega)$ and $\widetilde{\beta}_\infty(\omega)$ and the derivation of their visco-thermal perturbations $\widetilde{\alpha}(\omega)$ and $\widetilde{\beta}(\omega)$ are next considered. First, we introduce the new ideal-fluid pseudo-local kernels in Section 4, and then in Section 5, we present their explicit expressions and those of their perturbations, in terms of appropriate condensed-field averages of the ideal-fluid field patterns.

4 Frozen limit

The paper now shifts its focus to the main topic: a new pseudo-local description of the very important in practice high-frequency limit, $\omega \to \infty$, or frozen asymptotics, where the fluid's viscous and thermal properties cause small perturbations on propagation properties that are acoustically important. This situation arises when the thicknesses of the viscous and thermal boundary layers become much smaller than all relevant sizes in the pore dimensions, such as necks-apertures of Helmholtz cavities, while the wavelengths remain long. This regime, characterized by vanishing boundary layer thicknesses, is referred to as the "frozen asymptotics" and is investigated in Section 5. The limit itself, denoted the "frozen limit", is introduced in this section. In this limit, the fluid is seen as ideal fluid. The viscous and thermal relaxational processes are said to be frozen because they do not have enough time to develop. Compared to the situation analyzed in [8] Appendix and recalled in Section 2 where small-scale motion was assumed to be divergence-free, the one considered now is considerably generalized in that it allows resonance imbalances to appear in small-scale fields. In the frozen asymptotics, small perturbations induced by viscous and thermal effects modify the primary ideal lossless fluid behavior of the "frozen limit". The "frozen limit" is precisely defined by artificially making the viscosity and thermal conduction coefficients tend to zero. However, this presents challenges due to the resulting infinitely rapid variations in velocity and excess

temperature near the pore walls. In the process of definition of the limit, the specific method of reducing the parameters to zero is not critical. To facilitate mathematical consistency, we use a classical regularization expedient. We introduce a parameter $i\epsilon \to i.0$ into the equations to represent effects related to the vanishing viscosity. A similar parameter $i\epsilon' \to i.0$ could also be incorporated to represent effects related to diminishing heat conduction. However, these parameters primarily serve to prevent mathematical anomalies and their explicit inclusion for heat conduction does not provide additional substantive insights. The $i\epsilon'$ will be mentioned in some relations in next Section, for physical completeness, only. For convenience, by "frozen behavior" and "frozen fields" below, we will refer specifically to the ideal-fluid behavior and corresponding ideal-fluid fields determined in the above sketched simplified process of regularization.

Specifically, to unambiguously define this primary "frozen behavior", destined to be, in next Section 5, slightly but in an essential manner perturbed by the viscous and thermal processes arising in the frozen asymptotics, we suppress all viscous and thermal conduction terms in the equations (29)–(31) and we accordingly revise the boundary conditions (32) and (33) while however simultaneously keeping, for mathematical regularization, an artificial arbitrarily small $\hat{\epsilon}$ dissipative term-operator factor applicable to the constant ρ_0 in the inertial dynamic term of momentum equation, (see below equation (55)). We set the operator $\hat{\epsilon}$ to produce by definition an infinitesimal friction term factor $\pm i\epsilon$ when applied to an acceleration vector complex field induced by a forcing in representation $e^{\pm(-i\omega t+ikx)}$. The purely imaginary nature of it and the ϵ constancy are because we are not concerned with the true, actual, frequency or wavenumber, and pore-locations, dependencies, of the losses. For example, a pure, bulk, friction-type contribution would have the form $\pm i\epsilon = b/(\mp i\omega\rho_0)$, with b a friction coefficient. The only effect of our introduction of the $\hat{\epsilon}$, giving $\pm i\epsilon$ on $e^{\mp i\omega t}$ and its subsequent reduction to zero, will be to remove indeterminations that would appear at resonances if it were exactly set to zero, reestablishing physical continuity. Thus we write as the definition of the "frozen" ideal-fluid variable fields:

$$\nabla \cdot \boldsymbol{v}_\infty + \frac{\partial b_\infty}{\partial t} = 0, \text{in } V_p, \tag{54}$$

$$\rho_0(1+\hat{\epsilon})\frac{\partial \boldsymbol{v}_\infty}{\partial t} = -\nabla p_\infty + [\boldsymbol{f}], \quad \text{in } V_p, \tag{55}$$

$$\gamma\chi_0 p_\infty = b_\infty + \beta_0\tau_\infty, \quad \text{in } V_p, \tag{56}$$

$$\rho_0 c_P \frac{\partial \tau_\infty}{\partial t} = \beta_0 T_0 \frac{\partial p_\infty}{\partial t}, \quad \text{in } V_p, \tag{57}$$

with boundary conditions at the pore-wall surface S_p, (as the fluid viscosity has been removed, the fluid has no penetration b.c. at the pore walls),

$$\boldsymbol{v}_\infty \cdot \hat{\boldsymbol{n}} = 0, \quad \text{on } S_p. \tag{58}$$

If used, the similar addition of a thermal-conduction ϵ' loss term, would correspond to the insertion of a similar $(1+\hat{\epsilon}')$ operator after the constant $\rho_0 c_P$ in (57). Extracting as before with (43) a unique complex Fourier component in $e^{-i\omega t+ikx}$ in the Fourier representation of the arbitrary real forcing in (55), there is a unique abstract forced fields solution to equations (54)–(58) with $\hat{\epsilon}$ replaced by $i\epsilon$. Indeed, due to this regularization, the existence and uniqueness of the solution are maintained, consistent with the discussion in the preceding Section 3. It has the form, $\boldsymbol{v}_\infty = \widetilde{\boldsymbol{v}}_\infty(\omega,k,\boldsymbol{r})e^{-i\omega t+ikx}$, $b_\infty = \widetilde{b}_\infty(\omega,k,\boldsymbol{r})e^{-i\omega t+ikx}$, $p_\infty = \widetilde{p}_\infty(\omega,k,\boldsymbol{r})e^{-i\omega t+ikx}$, $\tau_\infty = \widetilde{\tau}_\infty(\omega,k,\boldsymbol{r})e^{-i\omega t+ikx}$, with tilde amplitudes presenting rapid complex variations at pore scale in the presence of resonances.

Note that the above frozen condensation and excess temperature and pressure are in adiabatic relation, which expresses e.g. as $b_\infty = \chi_0 p_\infty$ and $\tau_\infty = \dfrac{\gamma-1}{\beta_0}\chi_0 p_\infty$, obtained after straightforward calculation by using (56) and (57) and the known general thermodynamic identity [4]:

$$\gamma - 1 = \frac{T_0\beta_0^2 c_0^2}{c_P}. \tag{59}$$

As for the velocity and excess pressure patterns, therefore, they are the solution to the smaller system:

$$\rho_0(1+i\epsilon)\frac{\partial \boldsymbol{v}_\infty}{\partial t} = -\nabla p_\infty + [\boldsymbol{f}], \quad \text{in } V_p, \tag{60}$$

$$\chi_0 \frac{\partial p_\infty}{\partial t} = -\nabla \cdot \boldsymbol{v}_\infty, \quad \text{in } V_p, \tag{61}$$

$$\boldsymbol{v}_\infty \cdot \hat{\boldsymbol{n}} = 0, \quad \text{on } S_p, \tag{62}$$

from which can also be obtained, by the adiabatic relations, the condensation and excess temperature. To be complete, note that, with a $(1+\hat{\epsilon}')$ applied to $\rho_0 c_P$ in (57) as a trace of the thermal exchanges, quasi-adiabatic relations $b_\infty = \chi_0\left[\gamma - (\gamma-1)(1+\hat{\epsilon}')^{-1}\right]p_\infty$ and $\tau_\infty = \frac{\gamma-1}{\beta_0}\chi_0(1+\hat{\epsilon}')^{-1}p_\infty$ would follow by the same straightforward calculations, giving here in particular, $b_\infty = \chi_0[1+(\gamma-1)i\epsilon']p_\infty$, and, thus also, the equation (61) rewritten with the constant χ_0 replaced by $\chi_0[1+(\gamma-1)i\epsilon']$.

For the corresponding macroscopic description of "frozen" compressive motions along the x axis of symmetry, we will have according to the general analysis made before in Section 3 the following non-local macroscopic equations, which include both temporal and spatial dispersion and in which we perform the previous simplification of ignoring macroscopic inhomogeneity of the material properties due to non-local edge effects:

$$\frac{\partial B_\infty}{\partial t} + \nabla_x V_\infty = 0, \quad \frac{\partial D_\infty}{\partial t} = \nabla_x H_\infty - \nabla_x \mathcal{P}, \tag{63}$$

$$\begin{aligned} D_\infty(t,x) &= \hat{\rho}_\infty V_\infty(t,x) \\ &= \int \rho_\infty(t-t',x-x')V_\infty(t',x')dt'dx', \end{aligned} \tag{64}$$

$$\begin{aligned} H_\infty(t,x) &= -\hat{\chi}_\infty^{-1} B_\infty(t,x) \\ &= -\int \chi_\infty^{-1}(t-t',x-x')B_\infty(t',x')dt'dx', \end{aligned} \tag{65}$$

where we have introduced two directly averaged coarse grained ("Lorentz") "frozen" variables $B_\infty(t,\,x)$ and $V_\infty(t,\,x)$, such that:

$$B_\infty(t,x) = \langle b_\infty\rangle(t,x), \quad V_\infty(t,x) = \langle \boldsymbol{v}_{\infty x}\rangle(t,x), \tag{66}$$

and an indirect averaged ("Maxwell") "frozen" variable, $H_\infty(t,\,x)$, such that,

$$H_\infty(t,x)\langle v_{\infty x}\rangle(t,x) \equiv -\langle p_\infty v_{\infty x}\rangle(t,x). \tag{67}$$

With again the same unique long wavelength complex Fourier component (43) for the external force $f_x = -\nabla_x \mathcal{P}$, the macroscopic equations (63)–(67) will write as follows for the complex abstract fields, (including the exponentials):

$$-i\omega B_\infty = -ikV_\infty, \quad -i\omega D_\infty = ikH_\infty - ik\mathcal{P}, \tag{68}$$

$$D_\infty = \widetilde{\rho}_\infty(\omega,k)V_\infty, \quad H_\infty = -\widetilde{\chi}_\infty^{-1}(\omega,k)B_\infty, \tag{69}$$

$$B_\infty = \langle b_\infty\rangle, \quad V_\infty = \langle v_{\infty x}\rangle, \tag{70}$$

$$H_\infty\langle v_{\infty x}\rangle = -\langle p_\infty v_{\infty x}\rangle, \tag{71}$$

and for the same reasons as in previous section it will be considered that these equations also write in exactly same manner for the tilde amplitudes (not including the exponentials).

As in the previous section, we define the operator "frozen" kernels $\widetilde{\rho}_\infty(\omega,k)$ and $\widetilde{\chi}_\infty^{-1}(\omega,k)$ using the following identifications, where tildes may also be applied to the fields:

$$\widetilde{\rho}_\infty(\omega,k) = \frac{ik(H_\infty - \mathcal{P})}{-i\omega V_\infty}, \quad \widetilde{\chi}_\infty^{-1}(\omega,k) = -\frac{H_\infty}{B_\infty}. \tag{72}$$

These identifications provide a specific method to calculate them, in principle, from the microstructure, based on the solution to the forced microscopic field equations (54)–(58) or more simply (60)–(62). As V_∞ and B_∞ are directly related by (44a), the acoustic "frozen" kernels $\widetilde{\rho}_\infty(\omega,k)$ and $\widetilde{\chi}_\infty^{-1}(\omega,k)$ are entirely determined by ω, k, and two macroscopic "frozen" variables, one direct-averaged "Lorentz" variable, (V_∞ or B_∞), and one indirect-averaged "Maxwell" variable, (H_∞ or D_∞).

By writing in what follows the "frozen" kernels as:

$$\widetilde{\rho}_\infty(\omega,k) = \rho_0\frac{\widetilde{\alpha}_\infty(\omega,k)}{\phi}, \quad \widetilde{\chi}_\infty^{-1}(\omega,k) = \chi_0^{-1}\phi^{-1}\widetilde{\beta}_\infty^{-1}(\omega,k), \tag{73}$$

we introduce well-defined "frozen" tortuosity and inverse compliability, $\widetilde{\alpha}_\infty(\omega,k)$, $\widetilde{\beta}_\infty^{-1}(\omega,k)$. They are dimensionless and normalized to give an apparent density $\rho_0\widetilde{\alpha}_\infty$ and apparent compressibility $\chi_0\widetilde{\beta}_\infty$ of the ideal-fluid phase. In absence of forcing, ($\mathcal{P}=0$), the system (68) and (69) yields the following dispersion equation:

$$\widetilde{\rho}_\infty(\omega,k)\widetilde{\chi}_\infty(\omega,k)\omega^2 = \rho_0\chi_0\widetilde{\alpha}_\infty(\omega,k)\widetilde{\beta}_\infty(\omega,k)\omega^2 = k^2. \tag{74}$$

Again, for general reasons related to reciprocity, the "frozen" kernels should be even functions of k, (see[12]). As before, we assume that at a given real value of ω, the solutions $\widetilde{k}_\infty$, $-\widetilde{k}_\infty$, to (74), appear as a set of enumerable distinct nondegenerate values $\widetilde{k}_{\infty,n}$, $-\widetilde{k}_{\infty,n}$, $n = 1,2,....$ It can be ordered as before in ascending values of $\Im\left(\widetilde{k}_{\infty,n}\right)$, where simultaneously nonzero real and imaginary parts always exist because of the $+i\epsilon$. In straight ducts (where regularization is not necessary due to the absence of resonances), the multiplicity of solutions includes: first, the well-known plane-wave mode propagating at the speed of sound in free space; second, a finite number of other propagating modes that occur only at frequencies above their cutoff frequency; and third, an infinite number of purely evanescent modes whose cutoff frequency exceeds the frequency of interest. These evanescent modes typically do not need consideration, except perhaps for the initial few, due to their geometrically damped nature. Also, higher order propagating modes appear only when the wavelengths become comparable to the duct cross-section size. In our case, assuming long wavelengths, we expect to remain in a regime without higher-order "propagating" modes. There will be a fundamental "frozen" mode, usually of wavenumber $\widetilde{k}_{\infty,1}$, which has the simplest field pattern of all modes, the largest phase velocity, and practically zero attenuation, except for infinitesimal, which comes from the regularization. Higher order "frozen" "propagating" modes with successively more complex field patterns appear only when the wavelengths are short enough to be comparable to the typical small-scale lengths. As such, they lie in the unphysical (in the present context of volume-averaged macroscopic theory) frequency regime of too-short wavelengths. Beyond the fundamental propagating mode, there will a priori be evanescent "frozen" modes, with $\Im\left(\widetilde{k}_{\infty,n}\right) > 0$ increasing with n and $\Re\left(\widetilde{k}_{\infty,n}\right)$ practically zero, but not exactly, due to the regularization. A priori, only in the vicinity of resonances, some initial higher-order modes may experience a rapid decrease in their damping and phase velocity (while the initial principal evolves rapidly at the same time), which would bring them into the physical long-wavelength solution domain, possibly even assuming the role of a new fundamental. Finally and as before, when the microgeometry within the REV is sufficiently simple to ensure that only the principal waves merit consideration (again this will have to be clarified in further studies through detailed simulations in various geometries), the dynamic behavior of the frozen field within the specified range, $\lambda'/4 >> R_h$, with $\lambda' = 2\pi/|\Re[\widetilde{k}_{\infty,1}(\omega)]|$, will be effectively captured by principal, pseudo-local, macroscopic equations:

$$\frac{\partial B_\infty}{\partial t} + \nabla_x V_\infty = 0, \frac{\partial D_\infty}{\partial t} = \nabla_x H_\infty - \nabla_x \mathcal{P}, \tag{75}$$

$$D_\infty(t,x) = \hat{\rho}_\infty V_\infty(t,x) = \int \rho_\infty(t-t')V_\infty(t',x)dt', \tag{76}$$

[12] Note that the reciprocity property is thermodynamic in origin. Here, in the frozen fields or kernels we have not tried to maintain a realistic physical trace of the physical losses. But a sort of mathematical trace of the thermodynamics subsists in the introduced presence of the $\pm i\epsilon$.

$$H_\infty(t,x) = -\hat{\chi}_\infty^{-1} B_\infty(t,x) = -\int \chi_\infty^{-1}(t-t') B_\infty(t',x) dt', \tag{77}$$

where the "frozen" effective, principal, local-operators kernels in Fourier space, $\widetilde{\rho}_\infty(\omega)$ and $\widetilde{\chi}_\infty(\omega)$, are the quantities, $\widetilde{\rho}_\infty\left[\omega, \widetilde{k}_{\infty,1}(\omega)\right]$ and $\widetilde{\chi}_\infty\left[\omega, \widetilde{k}_{\infty,1}(\omega)\right]$, with $\widetilde{k}_{\infty,1}(\omega)$ the principal solution to equation (74). These will be written more simply, $\rho_0\widetilde{\alpha}_\infty(\omega)/\phi$ and $\chi_0\phi\widetilde{\beta}_\infty(\omega)$, in *definition* of the principal new pseudo-local version of ancients (conventional divergence-free approach) α_∞ and $\beta_\infty \equiv 1$. The peudo-local kernels are capable to account for resonant effects. The wavenumber $\widetilde{k}_{\infty,1}(\omega)$ is real (except for infinitesimal regularization) as it corresponds to the principal mode in an undamped, $\epsilon \to 0$, medium. As we have long wavelengths we do not consider the case of a band gap. Suppressing the useless index 1 we expect that the above equations describe in free field ($\mathcal{P} = 0$) the propagation of harmonic waves with a wavenumber $\widetilde{k}_\infty(\omega) = \omega/\widetilde{c}_\infty(\omega)$ having real celerity $\widetilde{c}_\infty(\omega) = c_0/\sqrt{\widetilde{\alpha}_\infty(\omega)\widetilde{\beta}_\infty(\omega)}$ and characteristic impedance $\widetilde{Z}_{c\infty}(\omega) = -H_\infty/V_\infty = \frac{\rho_0 c_0}{\phi}\sqrt{\widetilde{\alpha}_\infty(\omega)/\widetilde{\beta}_\infty(\omega)}$, while the functions $\widetilde{\alpha}_\infty(\omega)$ and $\widetilde{\beta}_\infty(\omega)$ are, a priori, complex with possibly negative real parts opening Veselago-type [43] of behavior. Thus, the characteristic impedance is, a priori, also complex. However, by applying the Umov definition of the macroscopic stress field, we will demonstrate that the a priori complex nature of the ideal-fluid functions $\widetilde{\alpha}_\infty(\omega)$ and $\widetilde{\beta}_\infty(\omega)$ does not actually occur. These functions necessarily reduce to real values, aside from their infinitesimal imaginary parts which arise from regularization and are disregarded. Future work will need to determine whether this reduction implies that both frozen susceptibility functions are always strictly positive real, in which case we would consistently have $\widetilde{\alpha}_\infty(\omega) > \widetilde{\beta}_\infty(\omega) > 1$ (see below), or whether, in certain special cases, simultaneous negative "Veselago-type" values might be possible. The reasoning presented below does not provide a definite answer to this question.[13]

5 Frozen asymptotics: generalization of Johnson-Allard's HF results

In a recent work [44] carried out within the classical local divergence-free approach it has been numerically demonstrated, in 2D, that the presence of edges at the pore walls is susceptible to profoundly alter the HF asymptotics of the dynamic tortuosity $\widetilde{\alpha}(\omega)$, tending to substitute to the characteristic asymptotics in inverse square-root-of-frequency convergence to the limit α_∞, a completely different, logarithmic one. In a forthcoming work, this finding will be justified by purely analytical considerations in line with those of Ref. [45]. For now, to avoid these difficulties, we will stick to Johnson and Allard's simplification that the pore wall surface appears locally flat everywhere on the scale of the small viscous and thermal boundary layers of thicknesses $\delta = (2\nu/\omega)^{1/2}$ and $\delta' = (2\nu'/\omega)^{1/2}$.

Given this simplification, we aim to determine the new pseudo-local description (51)–(53) that is applicable in the HF long-wavelength limit which is named above the "frozen asymptotics" and is consistent with the underlying non-local nature of the medium. Based on the conventional Johnson-Allard HF results mentioned in Section 2 and the previous analyses in Sections 3 and 4, it is easy to anticipate that the desired pseudo-local description should have kernels with the following form in this HF frozen asymptotics:

$$\widetilde{\rho}(\omega) = \rho_0\phi^{-1}\widetilde{\alpha}(\omega) = \rho_0\phi^{-1}\widetilde{\alpha}_\infty(\omega)\left[1 + \left(\frac{\nu}{-i\omega}\right)^{1/2}\frac{2}{\widetilde{\Lambda}_\infty(\omega)} + \ldots\right], \tag{78}$$

and

$$\widetilde{\chi}^{-1}(\omega) = \chi_0^{-1}\phi^{-1}\widetilde{\beta}^{-1}(\omega) = \chi_0^{-1}\phi^{-1}\widetilde{\beta}_\infty^{-1}(\omega)\left[1 + (\gamma-1)\left(\frac{\nu\prime}{-i\omega}\right)^{1/2}\frac{2}{\widetilde{\Lambda}\prime_\infty(\omega)} + \ldots\right] \tag{79}$$

where the calculation process of the $\widetilde{\alpha}_\infty(\omega)$ and $\widetilde{\beta}_\infty^{-1}(\omega)$ has been detailed in Section 4, and the calculation process of the $\widetilde{\alpha}(\omega)$ and $\widetilde{\beta}^{-1}(\omega)$ has been detailed in Section 3.

In this section, we will derive explicit expressions for the quantities $\widetilde{\alpha}_\infty(\omega)$, $\widetilde{\beta}_\infty^{-1}(\omega)$, $\widetilde{\Lambda}_\infty(\omega)$, and $\widetilde{\Lambda}\prime_\infty(\omega)$ in terms of averages over the frozen fields. These expressions extend the classical Johnson-Allard formulations for α_∞, $\beta_\infty^{-1} \equiv 1$, Λ_∞, and $\Lambda\prime_\infty$.

To identify the new lossless limit values $\widetilde{\alpha}_\infty(\omega)$ and $\widetilde{\beta}_\infty(\omega)$, that will differ from the conventional α_∞ and β_∞=1 when the frequency is not sufficiently high to be far from the resonances, and demonstrate that they are real, it suffices to fully express the cornerstone Umov condition (67). We can state it directly on the real fields associated with the propagation of one principal wave along $+x$. By omitting the (t, x) or $(t, \boldsymbol{r})$ arguments, we introduce a convenient notation for two abstract direct, and conjugated, complex parts in the fields. Macroscopic fields are noted in the form, $V_\infty(t,x) = V_\infty + V_\infty^* = \widetilde{V}_\infty e^{-i\omega t + i\widetilde{k}_{\infty,1}x} + \widetilde{V}_\infty^* e^{i\omega t - i\widetilde{k}^*_{\infty,1}x}$ etc. Microscopic fields are noted in the form, $\boldsymbol{v}_\infty(t,\boldsymbol{r}) = \boldsymbol{v}_\infty + \boldsymbol{v}_\infty^* = \widetilde{\boldsymbol{v}}_\infty(\omega,\boldsymbol{r})e^{-i\omega t + i\widetilde{k}_{\infty,1}x} + \widetilde{\boldsymbol{v}}_\infty^*(\omega,\boldsymbol{r})e^{i\omega t - i\widetilde{k}^*_{\infty,1}x}$, etc. The tilde amplitudes are eigen amplitudes associated with the right-going propagation with wavenumber $\widetilde{k}_{\infty,1}(\omega)$. The Umov condition (67) then links the macro and micro levels through the two following statements, expressed on the abstract two conjugated complex parts denoted here without arguments (t, x) or $(t, \boldsymbol{r})$, not to confuse them with the original real fields:

$$-H_\infty V_\infty \equiv \langle p_\infty v_{\infty x}\rangle, \tag{80}$$

and

$$-H_\infty V_\infty^* - H_\infty^* V_\infty \equiv \langle p_\infty v_{\infty x}^* + p_\infty^* v_{\infty x}\rangle, \tag{81}$$

The principle of forthcoming derivation is to express in two different ways, from macro equations and micro-equations, the following two quantities:

[13] To be addressed in the forthcoming paper mentioned in footnote 1.

$$\nabla_x(-H_\infty V_\infty) \equiv \nabla_x\langle p_\infty v_{\infty x}\rangle = \langle\nabla\cdot(p_\infty \boldsymbol{v}_\infty)\rangle, \tag{82}$$

$$\begin{aligned}\nabla_x\left(-H_\infty V^*_\infty - H^*_\infty V_\infty\right) &\equiv \nabla_x\left\langle p_\infty v^*_{\infty x} + p^*_\infty v_{\infty x}\right\rangle \\ &= \left\langle\nabla\cdot\left(p_\infty \boldsymbol{v}^*_{\infty x} + p^*_\infty \boldsymbol{v}_\infty\right)\right\rangle.\end{aligned} \tag{83}$$

In the above identifications the equivalences are expression of the very definition (Umov definition) of H macroscopic stress field. The replacement of $v_{\infty x}$ by $\boldsymbol{v}_\infty$ and ∇_x by ∇ is because of the assumed macroscopic symmetry along x which makes $\langle p_\infty \boldsymbol{v}_\infty\rangle$ to be aligned to $\hat{\mathbf{x}}$, and similarly with the complex conjugations. The last equalities come immediately from the spatial averaging theorem, stating that, (see e.g. [8] with $\hat{\boldsymbol{n}}$ the outward normal at S_p from the fluid region):

$$\nabla\left[\frac{1}{V}\int_{V_p} a dV\right] = \nabla\langle a\rangle = \langle\nabla a\rangle + \frac{1}{V}\int_{S_p} a\hat{\boldsymbol{n}} dS, \tag{84}$$

where a is an arbitrarily variable microscopic field. Indeed, expressing $\langle\nabla\cdot(p_\infty \boldsymbol{v}_\infty)\rangle$ with this theorem, the surface integral term cancels because of $\boldsymbol{v}_\infty\cdot\hat{\boldsymbol{n}} = 0$ at S_p, and similarly with the complex conjugations.

Expressing the first, (82), will give us the wanted new condensed field-averaged expressions for $\widetilde{\alpha}_\infty(\omega)$ and $\widetilde{\beta}_\infty(\omega)$, and expressing the second, (83), will establish the reality (except for the infinitesimal imaginary regularization parts) of the result functions. We begin by expressing the quantity in (82) at the macroscopic level. To do so, we first note the following general identity for the original real fields,

$$\nabla_x(-H_\infty V_\infty) = \frac{\partial D_\infty}{\partial t}V_\infty + H_\infty\frac{\partial B_\infty}{\partial t} - V_\infty\nabla_x\mathcal{P}. \tag{85}$$

It is immediately derived from the two equations (75). For its application here, we suppress the external force and consider a single (principal) wave propagating in direction $+x$. In this case the use of the abstract parts: $V_\infty = \widetilde{V}_\infty e^{-i\omega t + ik_{\infty,1}x}$, etc., is allowed in equations (75) without source, thus also in abstract manner in (85). The equation (85) gives, when using such fields:

$$\nabla_x(-H_\infty V_\infty) = i\omega(D_\infty V_\infty - H_\infty B_\infty). \tag{86}$$

Moreover in (76) and (77) this use is also allowed and it gives, since the convolution integrals transform in multiplications: $D_\infty = \rho_0\phi^{-1}\widetilde{\alpha}_\infty(\omega)V_\infty$, and $H_\infty = -\chi_0^{-1}\phi^{-1}\widetilde{\beta}^{-1}_\infty(\omega)B_\infty$. Then, (86) also reads:

$$\begin{aligned}\nabla_x(-H_\infty V_\infty) &= i\omega\left[\rho_0\phi^{-1}\widetilde{\alpha}_\infty(\omega)V^2_\infty + \chi_0\phi\widetilde{\beta}_\infty(\omega)H^2_\infty\right], \\ &= i\omega\left[\rho_0\phi^{-1}\widetilde{\alpha}_\infty(\omega)V^2_\infty + \chi_0^{-1}\phi^{-1}\widetilde{\beta}^{-1}_\infty(\omega)B^2_\infty\right].\end{aligned} \tag{87}$$

Likewise, the direct macroscopic expression of (83) is written as:

$$\begin{aligned}\nabla_x\left(-H_\infty V^*_\infty - H^*_\infty V_\infty\right) &= -\frac{\partial D_\infty}{\partial t}V^*_\infty \\ &+ H_\infty\frac{\partial B^*_\infty}{\partial t} - \frac{\partial D^*_\infty}{\partial t}V_\infty + H^*_\infty\frac{\partial B_\infty}{\partial t}, \\ &= i\omega\left[\rho_0\phi^{-1}\left(\widetilde{\alpha}_\infty - \widetilde{\alpha}^*_\infty\right)V_\infty V^*_\infty - \chi_0^{-1}\phi^{-1}\left(\widetilde{\beta}^{-1}_\infty - \widetilde{\beta}^{*-1}_\infty\right)B_\infty B^*_\infty\right].\end{aligned} \tag{88}$$

Next, for the expression of the same two quantities, this time starting at the microscopic level, we recall, according to the discussion made before, the following regarding the $\hat{\epsilon}$ and $\hat{\epsilon}'$ operators:

$$\begin{aligned}\rho_0(1+\hat{\epsilon})\frac{\partial \boldsymbol{v}_\infty}{\partial t} &= -i\omega\rho_0(1+i\epsilon)\boldsymbol{v}_\infty = -\nabla p_\infty, \\ \rho_0(1+\hat{\epsilon})\frac{\partial \boldsymbol{v}^*_\infty}{\partial t} &= i\omega\rho_0(1-i\epsilon)\boldsymbol{v}^*_\infty = -\nabla p^*_\infty, \\ \chi_0\left[1+(\gamma-1)\hat{\epsilon}'\right]\frac{\partial p_\infty}{\partial t} &= -i\omega\chi_0\left[1+(\gamma-1)i\epsilon'\right]p_\infty = -\nabla\cdot\boldsymbol{v}_\infty, \\ \chi_0\left[1+(\gamma-1)\hat{\epsilon}'\right]\frac{\partial p^*_\infty}{\partial t} &= i\omega\chi_0\left[1-(\gamma-1)i\epsilon'\right]p^*_\infty = -\nabla\cdot\boldsymbol{v}^*_\infty.\end{aligned} \tag{89}$$

Therefore, from (54)–(57) without source term, and the first and third equations (89), and the previously mentioned quasi-adiabatic relation $b_\infty = \chi_0[1+(\gamma-1)i\epsilon']p_\infty$, we have, up to the first infinitesimal corrections:

$$\begin{aligned}\nabla\cdot\left(p_\infty\boldsymbol{v}_\infty\right) &= \nabla p_\infty\cdot\boldsymbol{v}_\infty + p_\infty\nabla\cdot\boldsymbol{v}_\infty, \\ &= i\omega[\rho_0(1+i\epsilon)\boldsymbol{v}^2_\infty + \chi_0[1+(\gamma-1)i\epsilon']p^2_\infty], \\ &= i\omega[\rho_0(1+i\epsilon)\boldsymbol{v}^2_\infty + \chi_0^{-1}[1-(\gamma-1)i\epsilon']b^2_\infty].\end{aligned} \tag{90}$$

Hence, taking the spatial average we get the following alternative expression of (82):

$$\begin{aligned}\nabla_x(-H_\infty V_\infty) &= i\omega[\rho_0(1+i\epsilon)\langle\boldsymbol{v}^2_\infty\rangle + \chi_0\left[1+(\gamma-1)i\epsilon'\right]\langle p^2_\infty\rangle], \\ &= i\omega[\rho_0(1+i\epsilon)\langle\boldsymbol{v}^2_\infty\rangle + \chi_0^{-1}\left[1-(\gamma-1)i\epsilon'\right]\langle b^2_\infty\rangle].\end{aligned} \tag{91}$$

The ϵ and ϵ' can be skipped as tending to zero. Comparison of the two results (87) and (91) and separate identification of the kinetic and potential energy terms lead us to the following interpretation and expression of the new "frozen" tortuosity and inverse compliability functions $\widetilde{\alpha}_\infty(\omega)$ and $\widetilde{\beta}^{-1}_\infty(\omega)$:

$$\begin{aligned}\widetilde{\alpha}_\infty(\omega) &= \frac{\phi\langle\widetilde{\boldsymbol{v}}^2_\infty\rangle}{\langle\widetilde{\boldsymbol{v}}_\infty\rangle^2} = \frac{\langle\widetilde{\boldsymbol{v}}^2_\infty\rangle_p}{\langle\widetilde{\boldsymbol{v}}_\infty\rangle^2_p},\ \widetilde{\beta}^{-1}_\infty(\omega) = \frac{\widetilde{H}^2_\infty}{\langle\widetilde{p}^2_\infty\rangle_p} \\ &= \frac{\langle\widetilde{b}^2_\infty\rangle_p}{\langle\widetilde{b}_\infty\rangle^2_p}.\end{aligned} \tag{92}$$

Importantly, the reason for the possible identification of the term on V^2_∞ in (87), namely the term $i\omega D_\infty V_\infty$ in (86), as the (opposite) rate of change of kinetic energy, is the previously mentioned (Section 3) interpretation of D_∞ as momentum "in acoustic form". In the present lossless context, there is no momentum other than acoustic, so $-i\omega D_\infty V_\infty$ is currently the rate of change of kinetic energy. Therefore this identification, which leads to the simple

formulas (92) reminiscent of those found in the conventional local description, is directly conditioned by the choice of the H_∞ field, as fixed by the Umov condition. This, once again, highlights the fundamental importance of this condition. Finally, the last expression of the frozen inverse compliability shows that the latter inverse interprets as a kind of tortuosity factor constructed from the condensation field b_∞ (or excess pressure or temperature field p_∞, τ_∞, as they are all adiabatically proportional) instead of the velocity field $\boldsymbol{v}_\infty$. While the frozen tortuosity $\widetilde{\alpha}_\infty(\omega)$ is a measure of disorder in the ideal-fluid velocity field, the frozen inverse compliability turns out to be the same type of measure of disorder, tansposed this time for the ideal-fluid condensation field (or excess pressure or temperature). Previously, in conventional local theory assuming divergence-free small-scale motion, the same thing occurred, but was masked by the cancellation up and down, giving $\beta_\infty^{-1} \equiv 1$, since the frozen condensation or excess temperature and pressure were not distributed. It was evident that $\alpha_\infty \geq \beta_\infty^{-1} = 1$ and such a statement must be reconsidered.

Due to the absence of complex conjugations, one might initially think that the expressions in (92) yield complex results. Indeed, in the above expressions, which must be taken in the $\epsilon \to 0$ limit, a significant difference from the usual divergence-free situation is that the new fields $\widetilde{\boldsymbol{v}}(\omega, \boldsymbol{r})$ and $\widetilde{b}(\omega, \boldsymbol{r})$ can now be distributed, very significantly, on a small scale. At arbitrary frequencies it is clear that the small-scale point-to-point variations of the fields do not occur in phase, as is already the case in the purely local theory. We expect, and indeed have, complex functions for $\widetilde{\alpha}(\omega, k)$ and $\widetilde{\beta}(\omega, k)$. Thus we could also expect that the above a priori complex measures of disorder in the fields $\widetilde{\boldsymbol{v}}_\infty(\omega, \boldsymbol{r})$ and $\widetilde{b}_\infty(\omega, \boldsymbol{r})$ could take on important *complex values*. They would express complex intertwined inertial and elastic dynamics with in particular more than just a purely geometric content. These new properties would then lead to significant, non-trivial complex variations near resonances, which could potentially be described as complex generalized Veselago-type behavior. Let us for a while consider this.

In any case, such complex functions $\widetilde{\alpha}_\infty(\omega)$ and $\widetilde{\beta}_\infty^{-1}(\omega)$ and their inverse would still have to satisfy the characteristic symmetry relations expressing the reality of physical original fields and stating that they are Hermitian functions:

$$\widetilde{\alpha}_\infty(-\omega) = \widetilde{\alpha}_\infty^*(\omega),\ \widetilde{\beta}_\infty^{-1}(-\omega) = \widetilde{\beta}_\infty^{*-1}(\omega). \tag{93}$$

The real parts $\alpha'_\infty(\omega)$ and $\beta'_\infty(\omega)$ would have to be even functions, the imaginary parts $\alpha''_\infty(\omega)$ and $\beta''_\infty(\omega)$ odd functions of frequency. The simple condition (satisfied at $\epsilon \to 0$) that the propagation is purely undamped physically, would require that these functions are such that their product, $\widetilde{\alpha}_\infty(\omega)\widetilde{\beta}_\infty(\omega)$, which is involved in the expression of the celerity $\widetilde{c}_\infty(\omega)$, $(\rho_0\chi_0\widetilde{\alpha}_\infty\widetilde{\beta}_\infty\widetilde{c}_\infty^2 \equiv 1)$, is positive (recall that we do not consider here the case of band gap). For this to hold, $\widetilde{\alpha}_\infty(\omega)$ and $\widetilde{\beta}_\infty(\omega)$ would have equal and opposite phases. It means equal phases for the ideal-fluid new pseudo-local tortuosity $\widetilde{\alpha}_\infty(\omega)$ and ideal-fluid new pseudo-local inverse compliability $\widetilde{\beta}_\infty^{-1}(\omega)$. Indeed, that this property could hold true is suggested by the form of the mutually akin expressions (92). Note that since the phase of $\langle\widetilde{\boldsymbol{v}}_\infty\rangle$ is the same as that of $\langle\widetilde{b}_\infty\rangle$ (because $\widetilde{k}_\infty = \omega/\widetilde{c}_\infty(\omega)$ is to be found real), and their square is the same double phase quantity, what would happen is a different but same single phase will be found for $\langle\widetilde{\boldsymbol{v}}_\infty^2\rangle$ and $\langle\widetilde{b}_\infty^2\rangle$, as well as for the quadratically defined Umov amplitude field $-\widetilde{H}_\infty$ itself. This would be deduced from the result (92b), first expression, a priori making it possible to write these functions in the form:

$$\widetilde{\alpha}_\infty = \alpha'_\infty(1 + iC_\infty),\ \widetilde{\beta}_\infty = \beta'_\infty(1 - iC_\infty),\ C_\infty = \frac{\alpha''_\infty}{\alpha'_\infty} = -\frac{\beta''_\infty}{\beta'_\infty}. \tag{94}$$

It means that, reactive processes would appear and produce a *complex* characteristic impedance, $\widetilde{Z}_{c\infty}$, defined by, $-H = \widetilde{Z}_{c\infty}V$, for propagation along $+x$, and given by the, then, manifestly complex expression:

$$\widetilde{Z}_{c\infty} = \frac{\rho_0 c_0}{\phi}\sqrt{\frac{\widetilde{\alpha}_\infty}{\widetilde{\beta}_\infty}} = \frac{\rho_0 c_0}{\phi}\sqrt{\frac{\alpha'_\infty}{\beta'_\infty}\cdot\frac{1 + iC_\infty}{1 - iC_\infty}}. \tag{95}$$

This, however, does not occur in the sense that we have $C_\infty = 0$. Indeed, let us now exploit the remaining content (83) of the Umov condition (67) to show this. The macroscopic evaluation has been given in (88) and it remains to make the evaluation from microscopics.

From using (89), the relations $\nabla \cdot \boldsymbol{v}_\infty = -i\omega b_\infty$ and $\nabla \cdot \boldsymbol{v}_\infty^* = i\omega b_\infty^*$, and the previously noted quasi-adiabatic relations, $p_\infty = \chi_0^{-1}[1 - (\gamma - 1)i\epsilon']b_\infty$ and $p_\infty^* = \chi_0^{-1}[1 + (\gamma - 1)i\epsilon']b_\infty^*$, we find:

$$\begin{aligned}
&\big\langle\nabla\cdot(p_\infty\boldsymbol{v}_\infty^* + p_\infty^*\boldsymbol{v}_\infty)\big\rangle = \\
&\qquad\big\langle\boldsymbol{v}_\infty^*\cdot\nabla p_\infty + p_\infty\nabla\cdot\boldsymbol{v}_\infty^* + \boldsymbol{v}_\infty\cdot\nabla p_\infty^* + p_\infty^*\nabla\cdot\boldsymbol{v}_\infty\big\rangle, \\
&= \langle\boldsymbol{v}_\infty^*\cdot i\omega\rho_0(1 + i\epsilon)\boldsymbol{v}_\infty + \chi_0^{-1}[1 - (\gamma - 1)i\epsilon']b_\infty(-i\omega)b_\infty^* + \dots \\
&\qquad + \boldsymbol{v}_\infty\cdot(-i\omega)\rho_0(1 - i\epsilon)\boldsymbol{v}_\infty^* + \chi_0^{-1}[1 + (\gamma - 1)i\epsilon']b_\infty^* i\omega b_\infty\rangle, \\
&= -2\omega\rho_0\epsilon\big\langle\boldsymbol{v}_\infty\cdot\boldsymbol{v}_\infty^*\big\rangle - 2\omega\chi_0^{-1}(\gamma - 1)\epsilon'\big\langle b_\infty b_\infty^*\big\rangle.
\end{aligned} \tag{96}$$

The result is therefore zero, except for the infinitesimal regularization, which we eventually disregard in the limit. Finally by comparison between (88) and (96) we conclude that:

$$\widetilde{\alpha}_\infty(\omega) - \widetilde{\alpha}_\infty^*(\omega) = 0, \quad \beta_\infty^{-1}(\omega) - \widetilde{\beta}_\infty^{*-1}(\omega) = 0\,. \tag{97}$$

The quantities are real, except for the infinitesimal imaginary regularization part. Apart from the possibility of negative-negative values, which will need to be clarified in future work, the disorder measures are expected to be positive and follow the ordering, $\widetilde{\alpha}_\infty(\omega) > \widetilde{\beta}_\infty^{-1}(\omega) > 1$, as the disorder in the vector velocity field is greater than that in the scalar condensation field. The potential presence of resonances that induce very large velocities in small necks can significantly enhance the values of $\widetilde{\alpha}_\infty(\omega)$ compared to the classical, non-divergent local theory value α_∞. To a

lesser extent, $\widetilde{\beta}_\infty^{-1}(\omega)$ may also experience considerable enhancement. However, since this effect is less pronounced, we anticipate a possible significant increase in the product $\widetilde{\alpha}_\infty(\omega)\widetilde{\beta}_\infty(\omega)$ and its square root, resulting in "slow wave" behavior.

It remains now to identify the modified characteristic lengths, evolving from those described by Johnson-Allard, which continue to account for viscous and thermal losses separately. These lengths will be shown to remain real positive quantities, each still linked exclusively to either viscous or thermal effects. However, they now represent the more intricate dynamics encompassing both inertial and elastic interactions, thereby transforming them into frequency-dependent functions. We will see that the new characteristic lengths can now have values significantly modified by the local field imbalances induced by the resonances.

These new lengths must be determined, like the $\widetilde{\alpha}_\infty(\omega)$ and $\widetilde{\beta}_\infty(\omega)$, in function of the same fundamental principal frozen solution "$_{\infty,1}$" of the lossless frozen equations (54)–(58). We will identify them in the present general context by reverting to the original Landau and Lifshitz [15] argument in §79, Absorption of sound, that was later taken over but in the usual local theory context only, by Johnson et al. [11] for viscous losses, and this author [8] Appendix for viscous and thermal losses simultaneously. Allard's different and more simple argument [22] to derive the expression of parameter Λ' is entirely specific to the usual local context and thermal problem and it is not suitable for a generalization. It is already not transposable to obtain Johnson's classical expression of Λ because there, it would miss the effect of a bulk perturbation in ideal flow [45] induced by the presence of a viscous boundary layer. The principle of the general classical argument inspired by Landau and Lifshitz is to express the compatibility of two sound attenuation calculations in the high-frequency limit, one directly macroscopic and the other starting at the microscopic level.

Looking for a plane wave solution varying as $e^{-i\omega t+i\widetilde{k}_1(\omega)x}$ of the macroscopic motion equations simplified in the local form of (51)–(53), (without the source term), we find a dispersion equation:

$$\rho_0\chi_0\widetilde{\alpha}(\omega)\widetilde{\beta}(\omega)\omega^2=\widetilde{k}_1^2(\omega). \tag{98}$$

The indice 1 is here to remind us that this wavenumber is the least-attenuated principal solution to the underlying non-local dispersion equation (50) of the general non-local theory. On a macroscopic scale the intensity will decay like $e^{-2k_1''x}$, with $k_1''=\Im[\widetilde{k}_1(\omega)]$. With HF asymptotics (78) and (79) the attenuation parameter k_1'' is found to be:

$$k_1''=\frac{\omega}{c_0}\sqrt{\widetilde{\alpha}_\infty(\omega)\widetilde{\beta}_\infty(\omega)}\times \left[\frac{1}{\widetilde{\Lambda}_\infty(\omega)}\sqrt{\frac{\nu}{2\omega}}+(\gamma-1)\frac{1}{\widetilde{\Lambda}'_\infty(\omega)}\sqrt{\frac{\nu\prime}{2\omega}}\right]+\dots \tag{99}$$

On the other hand, starting at the microscopic scale, with a classical reasoning given in [15], p. 299, k_1'' can be related to the microscopic fields by writing:

$$k_1''=\frac{|\overline{\dot{E}_{mech}}|}{2\overline{S_0}}, \tag{100}$$

where $\overline{S_0}$ is the time-averaged acoustic energy flux i.e. the intensity of the wave, and $\overline{\dot{E}_{mech}}$ is the time-averaged rate of energy dissipation per unit total volume $V=V_p/\phi$. Indeed, the latter is nothing but $\partial\overline{S_0}/\partial x$, and since the decrease of the intensity occurs according to a law $e^{-2k_1''x}$, one immediately justifies (100). As explained in [15] a simple evaluation of the quantities in (100) is possible when the absorption is small on a wavelength, i.e., k_1'' is a small quantity compared to $k_1'\approx\omega/c_\infty$, i.e., $k_1''c_\infty/\omega<<1$. Here it means that the bracket in (99) is small, i.e., as we have assumed, the actual behavior is a perturbation of the frozen behavior. In this case, see [15] §79, $\overline{S_0}$ can be calculated by ignoring the effects of losses that are already taken into account in the numerator $|\overline{\dot{E}_{mech}}|$, and the latter can be calculated by using the expression for an undamped sound propagation. The mean acoustic energy flux $\overline{S_0}$ is estimated as $c_\infty\overline{E}$ where c_∞ is the principal "frozen" (without losses) speed of sound, $c_\infty=c_0/\sqrt{\widetilde{\alpha}_\infty(\omega)\widetilde{\beta}_\infty(\omega)}$, and $\overline{E}$ is the mean acoustic energy per unit total volume, equal to twice the mean kinetic or potential energy per unit total volume:

$$\begin{aligned}\overline{S_0}&=\frac{c_0}{\sqrt{\widetilde{\alpha}_\infty\widetilde{\beta}_\infty}}2\frac{1}{V}\int_{V_p}\frac{1}{2}\rho_0\overline{\boldsymbol{v}_\infty^2(t,\boldsymbol{r})}dV\\&=\frac{c_0}{\sqrt{\widetilde{\alpha}_\infty\widetilde{\beta}_\infty}}2\frac{1}{V}\int_{V_p}\frac{1}{2}\chi_0\overline{p_\infty^2(t,\boldsymbol{r})}dV.\end{aligned} \tag{101}$$

Inserting the undamped expressions, $\boldsymbol{v}_\infty(t,\boldsymbol{r})=\Re\big[\widetilde{\boldsymbol{v}}_\infty(\omega,\boldsymbol{r})e^{-i\omega t+i\omega x/c_\infty}\big]$, and, $p_\infty(t,\boldsymbol{r})=\Re\big[\widetilde{p}_\infty(\omega,\boldsymbol{r})e^{-i\omega t+i\omega x/c_\infty}\big]$, and performing the time average with $\overline{AB}=\frac{1}{2}\Re[\widetilde{A}\widetilde{B}^*]$ this gives:

$$\begin{aligned}\overline{S_0}&=\frac{c_0}{\sqrt{\widetilde{\alpha}_\infty\widetilde{\beta}_\infty}}\frac{1}{V}\int_{V_p}\frac{1}{2}\rho_0|\widetilde{\boldsymbol{v}}_\infty(\omega,\boldsymbol{r})|^2dV\\&=\frac{c_0}{\sqrt{\widetilde{\alpha}_\infty\widetilde{\beta}_\infty}}\frac{1}{V}\int_{V_p}\frac{1}{2}\chi_0|\widetilde{p}_\infty(\omega,\boldsymbol{r})|^2dV.\end{aligned} \tag{102}$$

The rate of energy dissipation per unit volume $\dot{E}_{mech}$ is [15]:

$$\dot{E}_{mech}=-\frac{\kappa}{T_0}\frac{1}{V}\int(\nabla\tau_1)^2dV+\dots$$

$$-\frac{1}{2}\eta\frac{1}{V}\int\left(\frac{\partial v_{1i}}{\partial x_k}+\frac{\partial v_{1k}}{\partial x_i}-\frac{2}{3}\delta_{ik}\frac{\partial v_{1l}}{\partial x_l}\right)^2dV-\zeta\frac{1}{V}\int(\nabla\cdot\boldsymbol{v}_1)^2dV,$$

(this is the volume integral of the bulk dissipation rate $-\mathcal{D}$, see [4], equation (111)), where the index $_1$ reminds us that our field is made of one principal wave, only, i.e., $\boldsymbol{v}=\widetilde{\boldsymbol{v}}_1(\omega,\boldsymbol{r})e^{-i\omega t+ik_1x}$, etc. After average over a cycle, it reads

$$\overline{\dot{E}_{mech}} = -\frac{\kappa}{T_0}\frac{1}{2}\frac{1}{V}\int |\nabla\widetilde{\tau}_1|^2 dV + \ldots$$
$$-\frac{1}{4}\eta\frac{1}{V}\int\left|\frac{\partial\widetilde{v}_{1i}}{\partial x_k}+\frac{\partial\widetilde{v}_{1k}}{\partial x_i}-\frac{2}{3}\delta_{ik}\frac{\partial\widetilde{v}_{1l}}{\partial x_l}\right|^2 dV - \zeta\frac{1}{2}\frac{1}{V}\int|\nabla\cdot\widetilde{\boldsymbol{v}}_1|^2 dV. \tag{103}$$

We will now evaluate this general expression to first order in the high frequency limit. There are important simplifications we can make in this calculation. The field pattern can be split into three different components: a purely acoustic field, which we can idealize as lossless, (a field that, over a spatial period or averaging volume, will have nearly the pattern of the frozen field, $\widetilde{\boldsymbol{v}}_\infty(\omega,\boldsymbol{r})e^{-i\omega t+ik_{\infty,1}x}$, etc.), and two lossy components induced by this acoustic field and emitted at the pore walls, one composed of the vortical fields (to which no excess temperature is associated) and the other composed of the entropic fields (to which no significant velocity is associated). We refer here to the well-known decomposition in three acoustic, entropic, and vortical fields, see e.g. for a general presentation [4]. All significant losses come from these vortical and entropic fields, directly created by interaction with the pore walls. This analysis immediately tells us that we can discard the third integral term in (103). It is related to the acoustic modes propagating with their intrinsic damping coming in part from the second viscosity ζ; however, these effects are presently higher-order effects which we need not consider. For the evaluation of the remaining first two integrals, we decompose over a representative volume or period the tilde fields, $\widetilde{\boldsymbol{v}}_1 = \widetilde{\boldsymbol{v}}_\infty + \ldots$ and $\widetilde{\tau}_1 = \widetilde{\tau}_\infty + \ldots$, as a superposition of a frozen pattern ∞ to which are added the vortical and entropic motions generated at the pore walls. Assuming that the pore walls appear locally plane at the scale of the viscous and thermal boundary layers of thicknesses $\delta = (2\nu/\omega)$ and $\delta' = (2\nu'/\omega)$, it means, after all is added, taking velocity and excess temperature fields of the following type, near the pore walls:

$$\begin{aligned}\widetilde{\boldsymbol{v}}_1(\omega,\boldsymbol{r}) &= \widetilde{\boldsymbol{v}}_\infty(\omega,\boldsymbol{r}_w)\left[1-e^{ik_v\xi}\right]+\ldots,\ \widetilde{\tau}_1(\omega,\boldsymbol{r})\\ &= \widetilde{\tau}_\infty(\omega,\boldsymbol{r}_w)\left[1-e^{ik_\tau\xi}\right]+\ldots,\end{aligned} \tag{104}$$

where, $k_v = (1+i)/\delta$, is the viscous shear wavenumber, (see equation (66) in [4]), $k_\tau = (1+i)/\delta'$, is the entropic wavenumber, (see equation (57.2) in [4]), $\boldsymbol{r}_w$ denotes a position at S_p, and ξ is a coordinate along the pore-wall normal, ($-\hat{\boldsymbol{n}}\xi = \boldsymbol{r}-\boldsymbol{r}_w$, with $\hat{\boldsymbol{n}}$ the outward normal to the fluid region at $\boldsymbol{r}_w$). Consider, first, the thermal dissipation integral in (103). The above representation of the excess temperature near the pore walls gives the leading order estimate,

$$|\nabla\widetilde{\tau}_1|^2 = \frac{\partial\widetilde{\tau}_1}{\partial\xi}\frac{\partial\widetilde{\tau}_1^*}{\partial\xi}+\ldots = |\widetilde{\tau}_\infty(\omega,\boldsymbol{r}_w)|^2|k_\tau|^2e^{-2k''_\tau\xi}+\ldots$$

Substituted in the integral it yields:

$$\int|\nabla\widetilde{\tau}_1|^2dV = \int|\widetilde{\tau}_\infty|^2|k_\tau|^2e^{-2k''_\tau\xi}d\xi dS_p+\ldots = \int|\widetilde{\tau}_\infty|^2\frac{2}{\delta\prime^2}\frac{\delta\prime}{2}dS_p+\ldots$$

and gives a contribution:

$$-\frac{\kappa}{T_0}\frac{1}{2}\frac{1}{V}\int|\nabla\widetilde{\tau}_1|^2dV = -\frac{\kappa}{T_0}\frac{1}{2}\frac{1}{V}\frac{1}{\delta\prime}\int|\widetilde{\tau}_\infty|^2dS_p+\ldots$$

Consider, then, the viscous dissipation integral. The above representation of the velocity near the pore walls gives a leading order estimate,

$$\begin{aligned}\left|\frac{\partial\widetilde{v}_{1i}}{\partial x_k}+\frac{\partial\widetilde{v}_{1k}}{\partial x_i}-\frac{2}{3}\delta_{ik}\frac{\partial\widetilde{v}_{1l}}{\partial x_l}\right|^2 &= \frac{\partial\widetilde{v}_{1i}}{\partial\xi}\frac{\partial\widetilde{v}^*_{1i}}{\partial\xi}+\ldots\\ &= |\widetilde{\boldsymbol{v}}_\infty(\omega,\boldsymbol{r}_w)|^2|k_v|^2e^{-2k''_v\xi}+\ldots\end{aligned}$$

Substituted in the integral it yields:

$$\begin{aligned}\int\left|\frac{\partial\widetilde{v}_{1i}}{\partial x_k}+\frac{\partial\widetilde{v}_{1k}}{\partial x_i}-\frac{2}{3}\delta_{ik}\frac{\partial\widetilde{v}_{1l}}{\partial x_l}\right|^2dV &= \int|\widetilde{\boldsymbol{v}}_\infty|^2|k_v|^2e^{-2k''_v\xi}d\xi dS_p+\ldots\\ &= \int|\widetilde{\boldsymbol{v}}_\infty|^2\frac{2}{\delta^2}\frac{\delta}{2}dS_p+\ldots,\end{aligned}$$

and gives a contribution:

$$\begin{aligned}&-\frac{1}{4}\eta\frac{1}{V}\int\left|\frac{\partial\widetilde{v}_{1i}}{\partial x_k}+\frac{\partial\widetilde{v}_{1k}}{\partial x_i}-\frac{2}{3}\delta_{ik}\frac{\partial\widetilde{v}_{1l}}{\partial x_l}\right|^2dV\\ &= -\frac{1}{4}\eta\frac{1}{V}\frac{1}{\delta}\int|\widetilde{\boldsymbol{v}}_\infty|^2dS_p+\ldots\end{aligned}$$

With these results for the leading order evaluations of the dissipation integrals, and the expressions (102) of the mean energy flux, a straightforward calculation shows that the equation (100) gives for k''_1:

$$k''_1 = \tfrac{\omega}{c_0}\sqrt{\tilde{\alpha}_\infty(\omega)\tilde{\beta}_\infty(\omega)}\tfrac{1}{4}\times$$
$$\left[\delta\frac{\int_{S_p}|\tilde{\boldsymbol{v}}_\infty(\omega,\boldsymbol{r}_w)|^2dS_p}{\int_{V_p}|\tilde{\boldsymbol{v}}_\infty(\omega,\boldsymbol{r})|^2dV}+(\gamma-1)\delta'\frac{\int_{S_p}|\tilde{\tau}_\infty(\omega,\boldsymbol{r}_w)|^2dS_p}{\int_{V_p}|\tilde{\tau}_\infty(\omega,\boldsymbol{r})|^2dV}\right]+\ldots, \tag{105}$$

(we have used the adiabatic relation between $\widetilde{p}_\infty$ and $\widetilde{\tau}_\infty$ and the general thermodynamic identity (59)). Comparison with the expression (99) obtained directly at the macroscopic level gives the following identification and interpretation of the viscous and thermal characteristic lengths, where we can also put expressions based on the fields $\widetilde{b}_\infty(\omega,\boldsymbol{r})$ or $\widetilde{p}_\infty(\omega,\boldsymbol{r})$ instead of $\widetilde{\tau}_\infty(\omega,\boldsymbol{r})$:

$$\begin{aligned}\frac{2}{\Lambda_\infty(\omega)} &= \frac{\int_{S_p}|\widetilde{\boldsymbol{v}}_\infty(\omega,\boldsymbol{r}_w)|^2dS_p}{\int_{V_p}|\widetilde{\boldsymbol{v}}_\infty(\omega,\boldsymbol{r})|^2dV},\\ \frac{2}{\Lambda'_\infty(\omega)} &= \frac{\int_{S_p}|\widetilde{\tau}_\infty(\omega,\boldsymbol{r}_w)|^2dS_p}{\int_{V_p}|\widetilde{\tau}_\infty(\omega,\boldsymbol{r})|^2dV}.\end{aligned} \tag{106}$$

These are now fully akin expressions which only exchange the frozen velocity and excess temperature (or condensation

or excess pressure) patterns. Previously in conventional local theory assuming divergence-free small scale motion, the same occurred, but the nice affinity was masked by the cancellation of the two up and down squared frozen excess temperature modulus factors that were mere constants in the assumed context.[14] In the classical theory, the relation $\Lambda_\infty < \Lambda'_\infty$ was evident because $2/\Lambda'_\infty$ was the purely geometric specific surface $\int_{S_p} dS/\int_{V_p} dV$ and it always happened that the squared ideal-incompressible-fluid velocities or squared electric-field $\boldsymbol{E}$ were more distributed at pore-surface S_p than in bulk-volume V_p. We anticipate that spatial dispersion and resonance effects may lead to a significant increase in the ideal-fluid tortuosity and an even sharper reduction in the viscous characteristic length. A similar but less pronounced pattern could emerge for other parameters, such as ideal-fluid inverse compliability and thermal characteristic length. These changes could have important acoustic consequences in reflection and transmission problems, such as slow waves and enhanced absorption, which warrant further investigation. The potentially significant decrease in the viscous characteristic length $\Lambda_\infty(\omega)$ from the geometric volume-to-surface ratio $\Lambda\prime_\infty$ is primarily due to the amplification of surface disorder in the squared-velocity field at resonances, which can result in very high velocities at pore walls in narrow necks. Consequently, the surface-to-volume disorder ratio in velocities may become more pronounced. A notable decrease in $\Lambda\prime_\infty(\omega)$ is also expected, though to a lesser extent, as the disorder in condensations is likely to be weaker than in velocities.

6 Solution of reflection-transmission problems

To finish, let us briefly explain how the reflection or reflection-transmission problems sketched in Figure 1 can now be solved in principle from microstructure from the solution of the frozen field problem (54)–(58), for the case of an incident wave whose angular frequency ω lies in the HF range where the asymptotics (78) and (79) applies. Because of the continuity of Umov field the algebra is the same as usual. At the front surface $x = 0$ on the air side, the field is a superposition of incident and reflected waves, with velocity v_x and excess pressure p fields having the form:

$$p(t,x) = \Re\big[A\big(e^{-i\omega t+ik_0x} + R(\omega)e^{-i\omega t-ik_0x}\big)\big],$$

$$v_x(t,x) = \Re\left[\frac{1}{Z_{0c}}A\big(e^{-i\omega t+ik_0x} - R(\omega)e^{-i\omega t-ik_0x}\big)\right], \quad (107)$$

where A is an arbitrary incident amplitude constant, $R(\omega)$ is the reflection coefficient to be determined that will depend on the configuration, k_0 the wavenumber is ω/c_0, Z_{0c} the characteristic impedance is $\rho_0 c_0 = \sqrt{\rho_0/\chi_0}$. Indeed we can neglect the losses and set governing equations in the form,

$$\rho_0\frac{\partial v_x}{\partial t} = -\nabla_x p,\ \chi_0\frac{\partial p}{\partial t} = -\nabla_x v_x, \quad (108)$$

Inside the material, as we set governing macroscopic equations in the form,

$$\rho_0\frac{\widetilde{\alpha}(\omega)}{\phi}\frac{\partial V_x}{\partial t} = \nabla_x H,\ \chi_0\phi\widetilde{\beta}(\omega)\frac{\partial H}{\partial t} = \nabla_x V_x, \quad (109)$$

and the field is a Fabry-Perot superposition of right- and left-going waves formed by multiple reflections, it will write in the form:

$$\begin{aligned} -H(t,x) &= \Re\left[Ce^{-i\omega t+i\tilde{k}x} + De^{-i\omega t-i\tilde{k}x}\right],\\ V_x(t,x) &= \Re\left[\frac{1}{\tilde{Z}_c}Ce^{-i\omega t+i\tilde{k}x} - \frac{1}{\tilde{Z}_c}De^{-i\omega t-i\tilde{k}x}\right], \end{aligned} \quad (110)$$

where C and D are the complex amplitudes associated to the right- and left-going waves and $\tilde{k}$ the wavenumber is $\omega\sqrt{\tilde{\alpha}(\omega)\tilde{\beta}(\omega)}/c_0$, $\tilde{Z}_c$ the characteristic impedance is $\sqrt{\rho_0\tilde{\alpha}(\omega)/(\chi_0\phi\tilde{\beta}(\omega))}$. At the front surface, the continuity of volume flow imposes that, $v_x(t,0) = V_x(t,x)$, which gives a first relation, $\frac{1}{Z_{0c}}A(1-R) = \frac{1}{\tilde{Z}_c}(C-D)$. And as mentioned before the continuity of acoustic energy flux is continuity of Umov stress, $p(t,0) = -H(t,0)$, which gives a second relation, $A(1+R) = C+D$. In the first configuration the condition that the velocity vanishes at the rigid wall, $V_x(t,d) = 0$, gives a third condition, $Ce^{-i\tilde{k}d} - De^{i\tilde{k}d} = 0$, which uniquely determines the reflection coefficient in terms of the thickness d and generalized frozen "parameters" $\alpha_\infty(\omega)/\phi$, $\phi\beta_\infty(\omega)$, $\Lambda_\infty(\omega)$ and $\Lambda'_\infty(\omega)$. In the second configuration, a transmitted wave in the air will emerge at the rear surface $x = d$, that will write in the form:

$$\begin{aligned} p(t,x) &= \Re\big[ATe^{-i\omega t+ik_0(x-d)}\big],\\ v_x(t,x) &= \Re\left[\frac{1}{Z_{0c}}ATe^{-i\omega t+ik_0(x-d)}\right], \end{aligned} \quad (104)$$

by definition of a suitable transmission coefficient T. At $x = d$, the continuity of volume flow, $v_x(t,\ d) = V_x(t,d)$, and the continuity of Umov stress, $p(t,d) = -H(t,d)$, give the two relations, $\frac{1}{Z_{0c}}AT = \frac{1}{Z_c}(Ce^{i\tilde{k}d} - De^{-i\tilde{k}d})$, and $AT = Ce^{i\tilde{k}d} + De^{-i\tilde{k}d}$, which uniquely determine the

[14] Reflecting on an anecdote from the 1990s, I recall my time as a student of Jean-François Allard, right after he introduced the notion of a characteristic thermal length determined by a volume-to-surface ratio [22]. I shared with him my persistent unease regarding the asymmetry between his thermal length concept and Johnson's viscous Lambda. His chagrined response was, "OK, but can you point out the exact error?" It took me thirty years, bolstered by insights from electromagnetic analogies and considerations of spatial dispersion, to finally articulate this "error." This document details the refined reasoning that resolves the asymmetry, employing the Umov-Heaviside-Poynting definition of macroscopic pressure. Through this exploration, a novel and intricate form of compliability has also emerged, serving as the natural counterpart to tortuosity.

reflection and transmission coefficients in terms of the thickness d and generalized frozen "parameters", $\alpha_\infty(\omega)/\phi$, $\phi\beta_\infty(\omega)$, $\Lambda_\infty(\omega)$ and $\Lambda'_\infty(\omega)$, in a way similar as usual in local-theory when we had these replaced by the constants, α_∞/ϕ, ϕ, Λ_∞ and Λ'_∞.

7 Conclusion

The restriction to divergence-free motion on a small scale is by no means a prerequisite for a homogenized, purely macroscopic description of long-wave sound propagation in fluid-saturated porous materials. On the contrary, the most general descriptions of this type, which are inherently non-local but can be transformed into a pseudo-local description within certain limits, require overcoming this condition, which then opens up the possibility of radically new behavior. The present considerations do not come out of context. The need to go beyond conventional divergence-free simplification can be encountered in a very wide variety of scenarios, many of which have recently been analyzed by C. Boutin and other authors, which must be cited here [46–52]. A necessary condition for these scenarios to occur is that markedly different pore sizes (say, differing by one order of magnitude or even more) appear in the Representative Elementary Volume. The very different pore sizes can come from resonators, or just plainly from widely different ordinary components. For example in [52] was considered the case of a bimodal REV made of two single-pore-size materials separately describable in the conventional way, one playing the role of background matrix, the other the role of inclusion. It was shown that when the two different porous components, matrix and inclusion, have very contrasting permeabilities (i.e. pore sizes differing by an order of magnitude or more, the propagation regime in the inclusions being in the range of a very low-frequency Darcy-type diffusive regime), new "co-dynamic" behaviors appear with the so-called pressure-diffusion attenuation mechanism (not a new loss mechanism but a new manifestation of the basic viscous friction loss mechanism, in this context of locally unbalanced diffuse pressure). As a rule, in these works by Boutin and Coll. the dynamical situation considered beyond the case of divergence-free motion at pore scale is coined "co-dynamic" with a number of its characteristics being noted for the different cases. The grid of analysis has been based on the consideration of REV made of juxtaposing and joining separate subregions of markedly different microgeometries, described with different two-scale asymptotic homogenization expansions, and with underlying philosophy of making inherent simplifications in these juxtapositions/junctions and specific resolutions in each case, justified by a physical analysis of order of -magnitude. The present paper is not a place to discuss it; it would perhaps be a difficult task for us to do so, who feel that the employed unconventional two-scale homogenization process with its various re-scalings is not obvious, and that "Der liebe Gott steckt im detail". Our different non-local point of view here, was expressed in a simple case including resonators and a geometry sufficiently simple to admit a long wavelength HF regime where the skin depths can be considered small. Only based on the actual fluid-mechanics governing equations and general non-local considerations, with an electromagnetic analogy suggesting an "Heaviside-Poynting" or "Umov" definition of macroscopic pressure that is rooted in deep thermodynamic reasons [4], it is completely independent of the mentioned works. Its detailed mathematical implementation will pose no problem of principle. It will not need distinguishing any subregions in the REV and matching them, however the question of the concrete solving of the equations will itself be an issue, with in general the necessity to have recourse at numerical techniques.[15] On the general problematics of new "co-dynamic" behaviors set forth by Boutin et al. our point of view exemplified in the present paper will offer we hope a different perspective and provide a more general basis in foregoing studies. For example, our approach will provide the means to appreciate and interpret the considerations made in the recent article [54].

The new effective local high-frequency description that is derived here is susceptible to have applications in noise control problems with structured materials whose complex structures will enable the emergence of new acoustic functions [55]. This is evident as the usual monotonic restrictions on the possible frequency-dependences in the functions $\alpha(\omega)$ and $\beta(\omega)$, (see [8] Appendix and [33] and [1]), explode. It will be important to investigate whether acoustical behaviors analogous to Veselago optical phenomena can occur. Currently, there is in particular a pressing need for the development of thinner and lighter sound absorbing materials. In this paper, we limited ourselves to the consideration of the new high-frequency limits for 1D propagation along a macroscopic symmetry axis and it remains to make definite calculations on example geometries to assess their utility and potential. Beyond that, we would have to consider and clarify a number of more or less endless and considerable generalizations, e.g.: Consider the new full-frequency pseudo-local description within the present simplifications (i.e., the focus on the main least attenuated field); Allow for non-smooth pore walls; Perform an important 3D generalization when symmetry restrictions are removed: by non-local origin one expect arriving at augmented quantities and relations, characteristic of an "equivalent anisotropic solid" instead of an "equivalent fluid" and illustrating even better the electromagnetic analogy; Study the new physical position of the notion of isotropy/anisotropy; Consider situations with macroscopic mean defined by ensemble average instead of volume average and in this context investigate the non-local description independently of the size of wavelengths; In this context, take into account in complete way the non-localities with

[15] Numerical cost can be a challenge. In this context, I would like to point out the recent work [53] that I have recently come across, which proposes an efficient reduced numerical method for perfect fluid simulations. Losses could be incorporated in the high-frequency range using this technique and the formulas provided in the present paper. The Hill-Mandel macroscopic pressure variable of the authors happens to be consistent with our Heaviside-Poynting-Umov variable.

this time, possible intervention of the parts of operators that describe higher order modes; Study the possibility to take into account the end effects at material boundaries ("Drude layers"); Consider the case with frame vibrations allowed beyond the quasi-"en-bloc" simplification; etc. This list of non-exhaustive more or less considerable open questions suggests that a general treatment of rethought problems within the framework of non-local "Maxwell-Umov" theory will be a lengthy task, but the time has come to get down to it. We have started here with the simplest: the redefinition of Johnson-Allard's HF limits, which however already illustrated the fruitfulness of non-local Maxwell-Umov ideas, inspired by the developed electromagnetic-acoustic analogy.

Acknowledgments

I extend my personal thanks and infinite gratitude to Professors Jean-François Allard and Michel Bruneau for the opportunity and support to engage with Jean-François's inspiring work on Biot's theory and the divergence-free approach in the 1990s. This experience was crucial in helping me draw an electromagnetic analogy, which I then developed, under the stern but benevolent tutelary eyes of Maxwell and Umov, into the formulations directly and indirectly accounting for spatial dispersion, as presented in [4, 8] and in this paper. In closing, I would also like to thank my dear friend and colleague, Dr. Navid Nemati, for his invaluable assistance, both personal and scientific, at the start of this work, which greatly contributed to the clarification of ideas. And finally, I would like to express my profound appreciation to Brigitte R. for her enduring support throughout this project.

Conflicts of interest

The author declares that he has no known competing financial interests or personal relationships that could have appeared to influence the work reported in this paper.

Data availability statement

No new data were created or analysed in this study.

References

1. D. Lafarge, N. Nemati, S. Vielpeau: Brownian motion with radioactive decay to calculate the dynamic bulk modulus of gases saturating porous media according to Biot theory. Acta Acustica United with Acustica 7 (2023) 44–73.
2. D. Lafarge: Porous and stratified porous media linear models of propagation, introduction to part 2, and chapter 6, The equivalent fluid model, in: M. Bruneau, C. Potel (Eds.), Materials and acoustics handbook, ISTE, Wiley, London UK, Hoboken USA, 2009, pp. 147–204.
3. D. Lafarge: Porous and stratified porous media linear models of propagation, chapter 7, Biot's model, in: M. Bruneau, C. Potel (Eds.), Materials and acoustics handbook, ISTE, Wiley, London UK, Hoboken USA, 2009, pp. 205–228.
4. D. Lafarge: Acoustic wave propagation in viscothermal fluids – an electromagnetic analogy, in: N. Jimenez, O. Umnova, J. P. Groby (Eds.), Acoustic waves in periodic structures, metamaterials, and porous media, vol. 143, Springer, Springer Nature Switzerland AG, 2021, pp. 205–272.
5. M.A. Biot: The theory of propagation of elastic waves in a fluid-saturated porous solid, I. Low-frequency range, II. Higher frequency range. Journal of the Acoustical Society of America 28 (1956) 168–191.
6. J.-F. Allard, N. Atalla: Propagation of sound in porous media: modelling sound absorbing materials, 2nd edn., Wiley-Blackwell, UK, 2009.
7. L.D. Landau, E. Lifshitz, L. Pitayevski: Electrodynamics of continuous media, Pergamon Press, Oxford, 1984.
8. D. Lafarge: Nonlocal dynamic homogenization of fluid-saturated metamaterials, in: Acoustic waves in periodic structures, metamaterials and porous media, vol. 143, N. Jimenez, O. Umnova, J.P. Groby (Eds.), Springer Nature Switzerland AG, 2021, pp. 273–331.
9. V.M. Agranovich, V.I. Ginzburg: Spatial dispersion in crystal optics and the theory of excitons, Interscience Publishers, London, 1966.
10. P. Belov, R. Marqués, S. Maslovski, I. Nefedov, M. Silveirinha, C. Simovski, S. Tretyakov: Strong spatial dispersion in wire media in the very large wavelength limit. Physical Review B 67 (2003) 113103.
11. D.L. Johnson, J. Koplik, D. Dashen: Theory of dynamic permeability and tortuosity in fluid-saturated porous media. Journal of Fluid Mechanics 176 (1987) 379–402.
12. D. Lafarge, P. Lemarinier, J.-F. Allard, V. Tarnow: Dynamic compressibility of air in porous structures at audible frequencies. Journal of the Acoustical Society of America 102 (1997) 1995.
13. M. Avellaneda, S. Torquato: Rigorous link between fluid permeability, electrical conductivity, and relaxation times for transport in porous media. Physics of Fluids A 3 (1991) 2529.
14. L.D. Landau, E. Lifshitz: Statistical physics, Pergamon Press, London-Paris, 1959.
15. L.D. Landau, E. Lifshitz: Fluid mechanics, Pergamon Press, London, 1987.
16. L.D. Landau, E. Lifshitz: Mechanics, Pergamon Press, London, 1987.
17. H. Goldstein: Classical mechanics, 1st edn., Addison-Wesley, USA, 1950.
18. M.A. Biot, D.G. Willis: The elastic coefficients of the theory of consolidation. Journal of Applied Mechanics 24 (1957) 594–601.
19. D.L. Johnson, T.J. Plona: Recent developments in the acoustic properties of porous media, in: Proceedings of the international school of physics Enrico Fermi, Course XCIII, 17, D. Sette (Ed.), North Holland, Amsterdam, 1986, pp. 255–290.
20. J. Kergomard, D. Lafarge, J. Gilbert: Transients in porous media: asymptotic time-domain Green functions and limits of current frequency-domain models. Acta Acustica united with Acustica 99 (2013) 557–571.
21. R. Roncen, Z.E.A. Fellah, D. Lafarge, E. Piot, F. Simon, E. Ogam, M. Fellah, C. Depollier: Acoustical modeling and bayesian inference for rigid porous media in the low-mid frequency regime. Journal of the Acoustical Society of America 144 (2018) 3084.
22. Y. Champoux, J.-F. Allard: Dynamic tortuosity and bulk modulus in air-saturated porous media. Journal of Applied Physics 70 (1991) 1975–1979.
23. D. Melrose, R. McPhedran: Electromagnetic processes in dispersive media – a treatment based on the dielectric tensor, Cambridge University Press, New York, 1991.
24. D. Lafarge, N. Nemati: Nonlocal maxwellian theory of sound propagation in fluid-saturated rigid-framed porous media. Wave Motion 50 (2013) 1016–1035.

25. B. Brouard, D. Lafarge, J.-F. Allard: A general method of modelling sound propagation in layered media. Journal of Sound and Vibration 183 (1995) 129–142.
26. M. Bruneau, C. Potel (Eds.), Materials and acoustics handbook, John Wiley & Sons, ISTE, London UK, Hoboken USA, 2009.
27. N. Martys, E. Garboczi: Length scales relating the fluid permeability and electrical conductivity in random two-dimensional model porous media. Physical Review B 46 (1992) 6080–6090.
28. H.A. Lorentz:The theory of electrons and its applications to the phenomena of light and radiant heat (a course of lectures delivered in Columbia University, New York, in March and April 1906, Leipzig, B.G. Teubner, 1909).
29. G. Russakoff: A derivation of the macroscopic Maxwell equations. American Journal of Physics 38 (1970) 1188–1195.
30. T. Lévy, E. Sanchez-Palencia: Equations and interface conditions for acoustic phenomena in porous media. Journal of Mathematical Analysis and Applications 61 (1977) 813–834.
31. R. Burridge, J.B. Keller: Poroelastisity equations derived from microstructure. Journal of the Acoustical Society of America 70 (1981) 1140.
32. D. Lafarge: Comments on "rigorous link between fluid permeability, electrical conductivity, and relaxation times for transport in porous media". Physics of Fluids A 5 (1993) 500–502.
33. D. Lafarge: Propagation du son dans les matériaux poreux à structure rigide saturés par un fluide viscothermique, PhD thesis, Université du Maine, 1993, https://cyberdoc.univ-lemans.fr/theses/1993/1993LEMA1009.pdf, in French.
34. D.L. Johnson, J. Koplik, L.M. Schwartz: New pore-size parameter characterizing transport in porous media. Physical Review Letters 57 (1986) 2564.
35. C. Marle: Ecoulements monophasiques en milieux poreux. Revue de l'Institut Français du Pétrole XXII, 10 (1967) 1471–1509, in French.
36. S. Weinberg: Gravitation and cosmology: principle and applications of the general theory of relativity, John Wiley & Sons, New York, 1972.
37. L. Brillouin: Les Tenseurs en Mécanique et en Elasticité, Masson, Paris, 1938.
38. G. Fournet: Electromagnétisme. Traité génie électrique (Techniques de l'ingénieur, D1020, in French), 1993.
39. A.D. Pierce: Acoustics: an introduction to its physical principles and applications, Wiley-Blackwell, Springer Nature Switzerland AG, 1989.
40. N. Nemati, D. Lafarge: Check on a nonlocal Maxwellian theory of sound propagation in fluid-saturated rigid framed porous media. Wave Motion 51 (2014) 716–728.
41. N. Nemati, Y.E. Lee, D. Lafarge, A. Duclos, N. Fang: Nonlocal dynamics of dissipative phononic fluids. Physical Review B 95 (2017) 224304.
42. G. Fournet: Electromagnétisme à partir des Equations Locales, Masson, Paris, 1985. in French.
43. V.G. Veselago: The electrodynamics of substances with simultaneously negative values of ϵ and μ. Soviet Physics Uspekhi 10 (1967) 509–514.
44. V. Langlois: High-frequency permeability of porous media with thin constrictions. I. Wedge-shaped porous media. Physics of Fluids 34 (2022) 077119.
45. A. Cortis, D. Smeulders, J. Guermond, D. Lafarge: Influence of pore roughness on high-frequency permeability. Physics of Fluids 15 (2003) 1766.
46. C. Boutin: Acoustics of porous media with inner resonators. Journal of the Acoustical Society of America 134 (2013) 4717–4729.
47. C. Boutin, F. Becot: Theory and experiments on poro-acoustics with inner resonators. Wave Motion 54 (2015) 76–99.
48. R. Venegas, C. Boutin: Acoustics of permeo-elastic materials. Journal of Fluid Mechanics 828 (2017) 135–174.
49. R. Venegas, C. Boutin, O. Umnova: Acoustics of multiscale sorptive porous materials. Physics of Fluids 29 (2017) 082006.
50. R. Venegas, C. Boutin: Acoustics of permeable heterogeneous materials with local non-equilibrium pressure states. Journal of Sound and Vibration 418 (2018) 221–239.
51. R. Venegas, C. Boutin: Enhancing sound attenuation in permeable heterogeneous materials via diffusion processes. Acta Acustica United with Acustica 104 (2018) 62335.
52. R. Venegas, T.G. Zielinski, G. Nunez, F.-X. Becot: Acoustics of porous composites. Composites Part B 220 (2021) 109006.
53. R. Liupekevicius, J.A.W. van Dommelen, M.G.D. Geers, V. G. Kouznetsova: An efficient multiscale method for sub-wavelength transient analysis of acoustic metamaterials, Philosophical Transactions of the Royal Society A 382 (2024) 20230368.
54. A. Alomar, D. Dragna, M.-A. Galland: Pole identification method to extract the equivalent fluid characteristics of general sound-absorbing materials, Applied Acoustics 174 (2021) 107752.
55. N. Jiménez, O. Umnova, J.P. Groby (Eds.), Acoustic waves in periodic structures, metamaterials, and porous media – from fundamentals to industrial applications (Topic in Applied Physics, vol. 143), Springer, 2021.
56. W. Heisenberg: The physical principles of the quantum theory, S. Hirzel Verlag, University of Chicago Press, Dover Publications, USA, 1930.
57. A.E. Scheidegger: Physics of flow through porous media, University of Toronto' Press, Canada, 1974.

Cite this article as: Lafarge D. 2024. Acoustic waves in gas-filled structured porous media: Asymptotic tortuosity/compliability and characteristic-lengths reevaluated to incorporate the influence of spatial dispersion. Acta Acustica, **8**, 41. https://doi.org/10.1051/aacus/2024019.

Appendix A

Biot-Allard's theory

In this appendix we show how Biot-Allard's macroscopic linear theory, in either its frozen ($\omega \to \infty$) or relaxed ($\omega \to 0$) limit, can be conceptualized as a semi-phenomenological continuum field theory of the type described in [56] §9. This is justified by the assumed underlying incompressibility. In addition, we discuss the extension to the harmonic arbitrary regime using the same simplifying hypothesis, and, along the way, the necessary additional extension when this simplification is abandoned for the fluid, so that the tortuosity and compliability operators $\hat{\alpha}$ and $\hat{\beta}$ correspondingly turn out to be non-local. In this view we take as the continuum field variables $\psi_\alpha(x,y,z,t)$ of [56] §9, the mean displacements $U_i^a(x,y,z,t) = \langle u_i^a \rangle_a(x,y,z,t)$ of the solid and fluid phases, where $(a = s, f)$ $(i = 1, 2, 3)$. Indeed, within Biot-Allard's theory framework, both solid and fluid phases permeate each other, creating their own interconnected clusters. The average (macroscopic) motions of both solid and fluid parts are followed separately. The mean displacements are the integrals of microscopic displacements within a Representative Elementary Volume (REV) for solid and fluid, respectively, normalised by the volumes of the solid and fluid: the fluid mean $\langle . \rangle_f = \frac{1}{V_f} \int_{V_f} .dV$ was denoted $\langle . \rangle_p$ in the text, the solid mean is $\langle . \rangle_s = \frac{1}{V_s} \int_{V_s} .dV$. The V_f and V_s represent the fluid and solid part in the REV V, respectively. Volumes are denoted by abuse of language with same letter as used for corresponding domains. It is envisioned that the dimension of the REV is small compared to the relevant wavelength. Assume that the macroscopic linear wave theory in the frozen/relaxed limit is derived from a Hamiltonian variational principle (without/with dissipation function). The Lagrange $L = T - V$ and dissipation D density functions of this principle can a priori include the continuum variables ψ_α (the $U_j^s = \langle u_j^s \rangle_s$ and $U_k^f = \langle u_k^f \rangle_f$) as well as their first derivatives $\frac{\partial \psi_\alpha}{\partial x_i}$ with respect to the spatial coordinates $\frac{\partial U_j^s}{\partial x_i}$ and $\frac{\partial U_k^f}{\partial x_i}$ and their first derivatives $\frac{\partial \psi_\alpha}{\partial t}$ with respect to time $\frac{\partial U_j^s}{\partial t}$ and $\frac{\partial U_k^f}{\partial t}$. This is because we seek equations of the type of wave-equations. The density functions L and D are scalar quadratic functions formed with these continuum variables and the unit tensor δ_{ij} (the only rotationally invariant true tensor), with no explicit dependence on time and space. This is because we assume linearity of the equations of motion, homogeneity in time and space, and isotropy for simplicity.

First of all, let us assume that there are no losses (a completely frozen scenario that may be relevant to consider in a theoretical limit $\omega \to \infty$ that allows to neglect viscoelastic and viscothermal losses while still having large wavelengths). The principle of Hamiltonian variation is

$$\int L\left(\psi_\alpha, \frac{\partial \psi_\alpha}{\partial x_i}, \dot{\psi}_\alpha\right) dVdt = \text{Extremum}, \tag{A.1}$$

from which the Euler-Lagrange equations of motion are derived (in the following, summations on repeated indices are automatically implied)

$$\frac{\partial}{\partial x_k} \frac{\partial L}{\partial(\partial \psi_\alpha / \partial x_k)} + \frac{\partial}{\partial t} \frac{\partial L}{\partial \dot{\psi}_\alpha} - \frac{\partial L}{\partial \psi_\alpha} = 0. \tag{A.2}$$

In ordinary elasticity theory, where there is only one displacement field, the dependence of the Lagrangian on the ψ_α in (A.1), and thus the last term in (A.2), can be suppressed. This is due to the fact that the uniform displacement of the medium has no energy cost. Similarly here, there is no energy cost associated with uniform macroscopic displacement of either the fluid or the solid components. Therefore, here also, the dependence on ψ_α in (A.1) and the last term in (A.2) can be discarded. Also similar to elasticity theory, is the fact that potential energy comes from phase deformations and kinetic energy comes from velocities. This puts us in a scenario where densities can be sought in the following form:

$$L\left(\frac{\partial U_i^s}{\partial x_k}, \frac{\partial U_i^f}{\partial x_k}, \dot{U}_i^s, \dot{U}_i^f\right) = T\left(\dot{U}_i^s, \dot{U}_i^f\right) - V\left(\frac{\partial U_i^s}{\partial x_k}, \frac{\partial U_i^f}{\partial x_k}\right). \tag{A.3}$$

For the kinetic energy density, the possible independent quadratic scalars formed with $\dot{U}_i^s$, $\dot{U}_j^f$ and δ_{ij} are three: $\dot{U}_i^s \dot{U}_j^s \delta_{ij}$, $\dot{U}_i^f \dot{U}_j^f \delta_{ij}$, $\dot{U}_i^s \dot{U}_j^f \delta_{ij}$, which gives the representation

$$T = \frac{1}{2}\rho_{11} \dot{U}_i^s \dot{U}_i^s + \frac{1}{2}\rho_{22} \dot{U}_i^f \dot{U}_i^f + \rho_{12} \dot{U}_i^s \dot{U}_i^f, \tag{A.4}$$

where ρ_{11}, ρ_{22}, ρ_{12} are scalar constants of the medium to be identified later. They can only depend on the solid and fluid densities and the microgeometry. Concerning the potential energy, it should be noted that it depends on the variables only through their symmetric combinations, since it is the latter that define the linear component of the strains. In other words, we can reexpress the function $V\left(\partial U_i^s/\partial x_k, \partial U_i^f/\partial x_k\right)$ in the form of a function $V\left(U_{ik}^s, U_{ik}^f\right)$, where $U_{ik}^a \equiv \left(\partial U_i^a/\partial x_k + \partial U_k^a/\partial x_i\right)/2$, $(a = s,f)$. In addition, we impose the condition that the macroscopic shear deformations of the fluid do not involve any energy cost. This flexibility is due to the inherent properties of the fluid, which allow it to move freely with respect to the solid without experiencing any restoring force, and thus also to withstand shear between the two, without any restoring force arising. It follows that the dependence on U_{ik}^f, is instead a dependence on the trace $U_{ii}^f = U_{ij}^f \delta_{ij}$ only: $V = V\left(U_{ik}^s, U_{ll}^f\right)$. The possible independent quadratic scalars made of U_{ij}^s, U_{ll}^f and δ_{ij} are four: e^2, ϵ^2, $e\epsilon$ and $U_{ij}^s U_{ij}^s$, where $e \equiv U_{ii}^s$ and $\epsilon \equiv U_{ii}^f$, giving the representation

$$V = \frac{1}{2}Ae^2 + \frac{1}{2}B\epsilon^2 + CU_{ij}^s U_{ij}^s + De\epsilon, \tag{A.5}$$

where A, B, C and D are scalar constants of the medium to be identified later. They can only depend on the fluid and solid elastic constants and the microgeometry. In the following, we replace these constants by the following symbols in order to adhere to the notations used in Biot's theory:

$$A \leftrightarrow P - 2N,\ B \leftrightarrow R,\ C \leftrightarrow N,\ D \leftrightarrow Q. \tag{A.6}$$

Later we will explore the interpretation of the constants ρ_{11}, ρ_{22}, ρ_{12}, P, Q, R, and N to ensure that T and V can properly represent kinetic and potential energy densities. For now, let us present the equations of motion. Write the Euler-Lagrange equations explicitly and evaluate the derivatives with formulas such as $\frac{\partial \dot{U}_j^b}{\partial \dot{U}_i^a} = \delta_{ij}\delta_{ab}$, $\frac{\partial U_{lm}^b}{\partial \frac{\partial U_l^a}{\partial x_k}} = \frac{1}{2}(\delta_{km}\delta_{il} + \delta_{kl}\delta_{lm})\delta_{ab}$. We get the following Biot equations:

$$\frac{\partial \pi_i^s}{\partial t} = \frac{\partial \sigma_{ik}^s}{\partial x_k},\ \frac{\partial \pi_i^f}{\partial t} = \frac{\partial \sigma_{ik}^f}{\partial x_k}, \tag{A.7}$$

where the σ_{ik}^s given by

$$\sigma^s_{ik} = -\frac{\partial L}{\partial U^s_{i,k}} = [(P-2N)e + Q\epsilon]\delta_{ik} + 2NU^s_{ik}, \tag{A.8}$$

are interpreted as macroscopic contact stresses exerted by the solid on the solid phase per unit total cross-surface of the material; the σ^f_{ik} given by

$$\sigma^f_{ik} = -\frac{\partial L}{\partial U^f_{i,k}} = [R\epsilon + Qe]\delta_{ik}, \tag{A.9}$$

are interpreted as the complementary macroscopic contact stresses exerted by the fluid on the fluid phase per unit total cross-surface of the material; the momentum π^s_i

$$\pi^s_i = \frac{\partial L}{\partial \dot{U}^s_i} = \rho_{11}\dot{U}^s_i + \rho_{12}\dot{U}^f_i, \tag{A.10}$$

is interpreted as the special part of solid-fluid overall momentum per unit total volume, created by the differential solid macroscopic contact stresses exerted on the solid part; and the momentum π^f_i

$$\pi^f_i = \frac{\partial L}{\partial \dot{U}^f_i} = \rho_{22}\dot{U}^f_i + \rho_{12}\dot{U}^s_i, \tag{A.11}$$

is interpreted as the complementary special part of solid-fluid overall momentum per unit total volume, created by the differential fluid macroscopic contact stresses exerted on the fluid part. In explicit form the above Biot's equations are:

$$\rho_{11}\ddot{\boldsymbol{U}}^s + \rho_{12}\ddot{\boldsymbol{U}}^f = P\nabla e + Q\nabla\epsilon - N\nabla\times\nabla\times\boldsymbol{U}^s, \tag{A.12}$$

$$\rho_{22}\ddot{\boldsymbol{U}}^f + \rho_{12}\ddot{\boldsymbol{U}}^s = Q\nabla e + R\nabla\epsilon. \tag{A.13}$$

Before proceeding with the interpretation of intervening macroscopic constants in these equations, let us be very clear about the meaning we give to the macroscopic stresses $\sigma^{a=s,f}_{ik}$. Let us imagine that we cut a small macroscopically oriented area $dS\hat{\boldsymbol{n}}$ of the material, of normal direction $\hat{\boldsymbol{n}}$. It consists of a fluid part of the area $dS\phi$ and a solid part of the area $dS(1-\phi)$. Let M^+ and M^- denote the particles directly in contact on either side of this surface at a given point M on $dS\hat{\boldsymbol{n}}$, with $\hat{\boldsymbol{n}}$ pointing from $-$ to $+$. The forces $\sigma^{s,f}_{ik}n_k dS$ are macroscopically relevant mean expressions of contact forces exerted through this surface, resp., by solid particles $+$ on solid particles $-$ or by fluid particles $+$ on fluid particles $-$. In the conventional interpretation of Biot's theory, the relevant mean expressions are derived by calculating the algebraic sum of the microscopic forces and normalizing them *per unit total surface*. It is important to note that our goal is to interpret the density L as the difference between kinetic energy and potential energy *per unit total volume* V of the material. Consequently, the fluid's macroscopic contact force is represented by $-\phi P^f n_i dS$, leading us to conclude that

$$\sigma^f_{ik} = -\phi P^f \delta_{ik}. \tag{A.14}$$

Here, $P^f = \langle p^f\rangle_f$ represents the macroscopic excess pressure in the fluid, which is the mean more simply denoted $P = \langle p\rangle_p$ in the main text (indice p for pore space). In the extension of Biot's theory presented in this paper, it is important to consider our reassessment of the concept of mean or macroscopic stresses in the fluid. For the sake of simplicity in the following discussions, we will adhere to the classic Biot-Allard scenario where p^f equals P^f plus a fluctuating correction term δp^f, the amplitude of which is significantly smaller than that of P^f, even though both gradients ∇P^f and $\nabla\delta p^f$ are of the same order, as detailed in [8] Appendix and re-explained here in the text after equation (1). It is important to highlight that this scenario shifts within the extension. When questioning fluid incompressibility while still accepting solid incompressibility, our usual understanding of the macroscopic solid stresses σ^s_{ik} remains unchallenged. However, the conception of fluid macroscopic mean stress needs to be modified to align with the Umov definition discussed in the text:

$$\sigma^f_{ik} = \phi H^f \delta_{ik},\ \langle p^f \dot{\boldsymbol{u}}^f\rangle_p = -H^f\langle \dot{\boldsymbol{u}}^f\rangle_p. \tag{A.15}$$

The Biot-Willis arguments outlined below, for the sake of simplicity, apply to the straightforward Biot-Allard case, but retain their significance within the broader context of the extended interpretation that incorporates the revised Umov perspective on fluid stresses. In the initial Biot-Willis framework, the fluid pressure p_f is designated as p_e – representing an externally applied pressure – accompanied by a deviatoric response pressure δp_f of negligible magnitude, which is distributed at the pore level. However, in the expanded approach where Umov definitions are essential, this p_f is articulated as $-H_e+\delta p_f$, where $-H_e$ symbolizes the homogeneous Umov component (thereby reinterpreting previous analyses by substituting $-H_e$ for p_e), and δp_f reflects a varying complementary component at the pore scale; though significant, it does not affect the overall outcomes. In essence, the discussions that fit within the conventional Biot-Allard framework continue to be applicable in the extended scenario, with adaptations limited to the non-local definitions discussed in the manuscript, of tortuosity and compliance metrics operators, $\hat{\alpha}$ and $\hat{\beta}$.

With these considerations in mind, we can now start with the interpretation of constants ρ_{11}, ρ_{22} and ρ_{12} by analyzing the fluid and solid motions in a representative volume V. For later use we recall that the dimensions of the volume are sufficiently small (and the microgeometry sufficiently simple) to consider that the fluid motion is quasi-divergence-free and the solid motion is quasi-"en-bloc" motion. Let us write the equation of motion for the fluid mass contained in the volume of fluid $V^f = V\phi$ contained inside a representative sphere bounded by a closed surface S. This surface is the union of surfaces $S^f = \phi S$ and surfaces $S^s = (1-\phi)S$, which are the intersections of S with the fluid and the solid, respectively. The fluid itself contained in V forms a volume V_p bounded by the outer boundary, called S^f, and the inner surfaces S_p where the fluid interfaces with the solid pore walls (V_p and S_p to conform with notations in the text for the pore space filled by the fluid and the pore wall, fluid-solid interface). In the case of a unit volume, V=1, Newton's fundamental law of mechanics $\boldsymbol{F} = m\boldsymbol{a}$ holds for the motion of the fluid mass in question (we denote ρ_0 the fluid ambient density):

$$\rho_0\phi\ddot{U}^f_i = \frac{\partial\sigma^f_{ik}}{\partial x_k} + R_i, \tag{A.16}$$

where the two force terms are the resultant of the stresses applied to the fluid at S^f and at the pore wall surface S_p, respectively. The writing of the first force results from the consideration of the unit volume and the definition of σ^f_{ik} as stresses per unit of total material surface. Internal pressures at the pore walls, due to the relative accelerations of fluid and solid, give rise to an additional inertial reaction force $\boldsymbol{R}$ exerted by the solid on the fluid. Correspondingly, when considering the motion of the solid mass within the same volume of material (we denote ρ_s the solid ambient density), an equal and opposite reaction force is exerted by the fluid on the solid, coming from the same opposite actions exterted at the pore walls:

$$\rho_s(1-\phi)\ddot{U}^s_i = \frac{\partial\sigma^s_{ik}}{\partial x_k} - R_i. \tag{A.17}$$

It comes in addition to the resultant of the stresses carried by the solid and applied directly to it at the surface S^s. Now let us find the expression for $\boldsymbol{R}$. To simplify the analysis, we will first assume that the solid is quite heavy and not very deformable, so that only the fluid responds to acoustic motion. In this case, there is no need to consider the first Biot equation (A.12). It is sufficient to focus on the second equation (A.13), which remains well-conditioned. The two terms $\rho_{12}\ddot{\boldsymbol{U}}^s$ and $Q\nabla e$ vanish: the coefficients ρ_{12} and Q are coupling coefficients which as such remain finite (this is easily checked a posteriori on their expressions), whereas the quantities $\ddot{\boldsymbol{U}}^s$ and ∇e tend to zero in the considered limit. Therefore, this second Biot equation (A.13) writes

$$\frac{\partial}{\partial t}\left(\rho_{22}\dot{U}_i^f\right) = \frac{\partial}{\partial x_k}(R\epsilon\delta_{ik}). \tag{A.18}$$

By using (A.9) we see that

$$R\epsilon\delta_{ik} = \sigma_{ik}^f. \tag{A.19}$$

Hence, subtracting (A.18) from (A.16) allows us to eliminate the term $\partial\sigma_{ik}^f/\partial x_k$, resulting in:

$$R_i = (\rho_0\phi - \rho_{22})\ddot{U}_i^f. \tag{A.20}$$

We see that this force is opposite and proportional to the fluid momentum rate of change, according to a relationship

$$R_i = -(\alpha_\infty - 1)\phi\rho_0\frac{\partial}{\partial t}\dot{U}_i^f, \tag{A.21}$$

with

$$\alpha_\infty \equiv \frac{\rho_{22}}{\phi\rho_0}. \tag{A.22}$$

To identify the constant α_∞ greater than 1 (the reactive force opposing the fluid acceleration), we simply need to recognize that the macroscopic equation (A.18) which also expresses as

$$\frac{\rho_{22}}{\phi}\frac{\partial}{\partial t}\dot{U}_i^f = -\frac{\partial}{\partial x_i}P^f, \tag{A.23}$$

(according to (A.19) and (A.15)) is only intended to show how, at the microscopic level, the motion of the fluid obeys a simplified version of the equations describing ideal fluid motion, which takes into account the quasi-incompressibility of the fluid. Normally, the ideal fluid equations would be, with χ_0 the fluid compressibility, $\dot{u}_i^f$ the fluid microscopic velocity components, p^f the fluid pressure:

$$\rho_0\frac{\partial\dot{u}_i^f}{\partial t} = -\nabla_i p^f, \quad \text{in } V_p, \tag{A.24}$$

$$\chi_0\frac{\partial p^f}{\partial t} = -\nabla\cdot\dot{\boldsymbol{u}}^f, \quad V_p, \tag{A.25}$$

with boundary conditions ($\hat{\boldsymbol{n}}$ normal to S_p)

$$\dot{\boldsymbol{u}}^f\cdot\hat{\boldsymbol{n}} = 0, \quad \text{on } S_p. \tag{A.26}$$

The key here is to examine geometries that are simple enough for the fluid to move within the pore network in a REV without undergoing differential local compression or dilatation, to a first approximation (note that for this reason we do not need to add infinitesimal dissipation to the above problem to make it definite, since the geometry is assumed to be simple enough not to lead to resonance). In such geometries, this comes from the supposed long wavelengths compared to the REV dimensions. For this reason, we consider it justified to replace the exact equations (A.24)–(A.26) (which by themselves would not lead to (A.23) with ρ_{22} a constant) by the following model[16] equations (equations of the incompressible ideal fluid):

$$\rho_0\frac{\partial\dot{u}_i^f}{\partial t} = -\nabla_i p^f, \quad \text{in } V_p, \tag{A.27}$$

$$\nabla\cdot\dot{\boldsymbol{u}}^f = 0, \quad \text{in } V_p, \tag{A.28}$$

with,

$$\dot{\boldsymbol{u}}^f\cdot\hat{\boldsymbol{n}} = 0, \quad \text{on } S_p. \tag{A.29}$$

The variable p^f is no longer strictly speaking a pressure (there is no pressure concept in an incompressible fluid), but an abstract field defined by the value of the macroscopic pressure gradient ∇P^f and the microgeometry. These model equations are expected to yield the (almost) correct form of the velocity profile at the microscopic level, due to the large wavelengths, based on the implicit restrictions on allowed microgeometries. Taking the mean of (A.27) gives

$$\rho_0\frac{\partial\langle\dot{u}_i^f\rangle_p}{\partial t} = -\langle\nabla_i p^f\rangle_p, \tag{A.30}$$

and the comparison of this equation with (A.23) implies:

$$\left[\alpha_\infty \equiv \frac{\rho_{22}}{\phi\rho_0}\right]\langle\nabla p^f\rangle_p = \nabla\langle p^f\rangle_p. \tag{A.31}$$

This equation, joined with the model equations (A.27)–(A.29), is a definition that determines in unique manner the value of the coefficient $\alpha_\infty>1$, that is termed the (ideal-fluid) tortuosity coefficient. By using the spatial averaging theorem (84) we can re-express $\frac{1}{\alpha_\infty} = 1-\lambda_\infty$ with λ_∞ defined by

$$\frac{1}{V_p}\int_{S_p} p^f\hat{\boldsymbol{n}}dS = \lambda_\infty\nabla P^f. \tag{A.32}$$

The surface integral is the reaction force exerted by the fluid on the solid, resulting from a pore scale distribution of pressures. Note that since the material is assumed to be homogeneous, a constant in p^f does not contribute by symmetry. Furthermore, a purely linear variation such as that corresponding to macroscopic variations of $\boldsymbol{x}\cdot\nabla P^f$ does not contribute either (see e.g. [8] (7.23)). Thus, in the notations used in (17)–(20), where p^f is written $p'_\infty + P^f$, only the fluctuating stationary (or periodic) part p'_∞ of the pressure contributes to the integral. The coefficient $0<\lambda_\infty<1$ is interpreted as the hydrodynamic drag coefficient. If the solid is set in motion from rest with a final velocity of $\boldsymbol{U}^s$, the fluid is partially entrained and assumes a final velocity of $\lambda_\infty\boldsymbol{U}^f$. It can be proven that the definition (A.31) of α_∞ is the same as:

$$\alpha_\infty = \frac{\langle(\dot{\boldsymbol{u}}^f)^2\rangle_p}{\langle\dot{\boldsymbol{u}}^f\rangle_p^2}. \tag{A.33}$$

Here, to obtain it physically, we may content ourselves to remember that in the present scenario the kinetic energy per unit total volume only comes from the fluid. It is given by (A.4) i.e. $T = \rho_{22}(\dot{\boldsymbol{U}}^f)^2/2 = \rho_{22}\langle\dot{\boldsymbol{u}}^f\rangle_p^2/2$, and, from microscopics, we know that it is also given by $T = \phi\langle\rho_0(\dot{\boldsymbol{u}}^f)^2/2\rangle_p$ (ϕ is the volume of fluid in a unit total volume), hence the result. In this representation,

[16] It is precisely through this transition to presumed justified model equations for incompressible fluid, and by a similar transition for the solid, that the aforementioned restrictions on microgeometries are implicitly introduced, making the Lagrangian approach with first order derivatives possible.

the meaning of α_∞ as a measure of disorder in the fluid velocity pattern is clear, and it is immediately seen that in any complex geometry where the velocity field cannot be a uniform field, the condition $\alpha_\infty > 1$ necessarily holds. We wish to mention for future reference that α_∞ is the inertial coefficient in the following macroscopic form of Newton's law:

$$\rho_0 \alpha_\infty \frac{\partial \langle \dot{\boldsymbol{u}}^f \rangle_p}{\partial t} = -\nabla \langle p^f \rangle_p. \tag{A.34}$$

Finally, before leaving the current motionless solid scenario, it is worth mentioning also for future reference that we have the following option to define the incompressible ideal-fluid pattern $\dot{\boldsymbol{u}}^f$. It is the only solution to the following problem:

$$\nabla \cdot \dot{\boldsymbol{u}}^f = 0, \quad \text{(incompressibility) in } V_p, \tag{A.35}$$

$$\nabla \times \dot{\boldsymbol{u}}^f = \boldsymbol{0}, \quad \text{(ideal} - \text{fluid) in } V_p, \tag{A.36}$$

$$\hat{\boldsymbol{n}} \cdot \dot{\boldsymbol{u}}^f = 0, \quad \text{(ideal} - \text{fluid) on } S_p, \tag{A.37}$$

$$\langle \dot{\boldsymbol{u}}^f \rangle_p = \frac{1}{V_p} \int_{V_p} \dot{\boldsymbol{u}}^f dV = \dot{\boldsymbol{U}}^f,$$

$$\text{(removal of amplitude/direction ambiguity)}. \tag{A.38}$$

Let us now relax the simplification made above (immobile solid) and come to the general case where the acoustic disturbance affects both the solid and the fluid. The wavelength scales are still assumed to be large compared to REV dimensions. By generalizing the logic that previously brought us to recognize fluid motion as incompressible by virtue of this condition, we now accept that solid motion is, in fact, locally uniform motion. Again, this is an implicit restriction on the type of microgeometry allowed. The assumption means that, locally, the shape and dimensions of the volumes V^s and V^f occupied by the solid and the fluid, and of the interface S_p, are practically unchanged. In fact, as for the local small acoustic amplitudes uniform compression-dilatation of solid and pore space dimensions, there is no point in considering them because we are making a linear theory. The only new element compared to previous considerations is that now the solid particles in V^s and at S_p advance "en-bloc" with velocity $\dot{\boldsymbol{u}}^s = \dot{\boldsymbol{U}}^s$. For the fluid, we write $\dot{\boldsymbol{u}}^f = \dot{\boldsymbol{U}}^s + \dot{\mathbf{w}}$, where $\dot{\mathbf{w}}$ is the relative velocity of the fluid with respect to the solid. In the moving frame of reference animated by the velocity of the solid, velocities $\dot{\mathbf{w}}$ play the role of previous $\dot{\boldsymbol{u}}^f$ velocities. What we have seen above shows us that the field $\dot{\mathbf{w}}$ verifies the equations of problem (A.35–A.38), where we replace $\dot{\boldsymbol{u}}^f$ by $\dot{\mathbf{w}}$ and $\dot{\boldsymbol{U}}^f$ by $\langle \dot{\mathbf{w}} \rangle_p = \frac{1}{V_p} \int_{V_p} \dot{\mathbf{w}} dV = \dot{\boldsymbol{U}}^f - \dot{\boldsymbol{U}}^s$. Applying relation (A.21) in the inertial coincident moving frame of reference driven by the instantaneous velocity of the solid, we thus have the following expression for the reaction force (exerted by the solid on the fluid):

$$\boldsymbol{R} = -(\alpha_\infty - 1)\phi\rho_0 \frac{\partial}{\partial t} \langle \dot{\mathbf{w}} \rangle_p = -(\alpha_\infty - 1)\phi\rho_0 \frac{\partial}{\partial t} \left(\dot{\boldsymbol{U}}^f - \dot{\boldsymbol{U}}^s \right), \tag{A.39}$$

where $\alpha_\infty = \langle \mathbf{w}^2 \rangle_p / \langle \mathbf{w} \rangle_p^2$ is exactly the same tortuosity factor as defined above since $\mathbf{w}$ is the same *pattern* as the previous $\dot{\boldsymbol{u}}^f$. Carrying this expression into relations (A.16) and (A.17) gives:

$$\rho_0 \phi \ddot{U}_i^f = \frac{\partial \sigma_{ik}^f}{\partial x_k} - (\alpha_\infty - 1)\phi\rho_0 \left(\ddot{U}_i^f - \ddot{U}_i^s \right), \tag{A.40}$$

$$\rho_s (1 - \phi) \ddot{U}_i^s = \frac{\partial \sigma_{ik}^s}{\partial x_k} + (\alpha_\infty - 1)\phi\rho_0 \left(\ddot{U}_i^f - \ddot{U}_i^s \right). \tag{A.41}$$

Comparison of (A.40) and (A.41) with equations (A.7), (A.11), (A.10) then gives the following relationships:

$$\rho_{11} = \rho_s (1 - \phi) + \rho_0 \phi (\alpha_\infty - 1), \tag{A.42}$$

$$\rho_{22} = \phi \rho_0 \alpha_\infty, \tag{A.43}$$

$$\rho_{12} = -\phi \rho_0 (\alpha_\infty - 1), \tag{A.44}$$

which fully determine macroscopic effective Biot densities ρ_{ij} based on solid and fluid densities, and porosity and tortuosity parameters linked to the microgeometry of the medium. Let us now turn to the identification/interpretation of elastic parameters P, Q, R and N, in the same completely frozen scenario (no losses). Identifying the elastic parameter N is easy: it is the shear modulus of the solid skeleton; the fluid (which does not exert elastic restoring forces in shear) does not contribute to its value. The identification of the parameters P, Q and R, which depend on the two phases, is more delicate. This is done in two steps, using the following two (jacketed and unjacketed) "thought experiments" inspired by those (quasi-static) of Biot and Willis [18]. Let us start with the jacketed experiment. Let us consider a REV – thus a volume of small dimension compared to wavelengths – that we imagine is encased by an impermeable membrane, which is easily extendable and retractable, but also strongly attached to the solid and capable of transmitting to it, through the attachments, the external variable stresses that are exerted. We also assume that the membrane is not closed but terminates in a capillary that connects the air inside the volume in question to a reservoir of fixed pressure P_0, representing the ambient pressure. In this way, it is assumed that the fluid escapes and enters the volume by passing through the capillary, keeping the internal fluid pressure constantly at zero mean overpressure. The membrane or diaphragm is subjected to a uniform and harmonic overpressure $p_e = \tilde{p}_e e^{-i\omega t}$, i.e. isotropic stresses $-p_e \delta_{ij}$ are applied to it. Note that the membrane is not strictly necessary to consider. We can envision ourselves being able to directly manipulate the solid using numerous small pistons that cling only to the solid while allowing the fluid to move freely. In response, the solid is assumed to undergo a certain isotropic uniform and harmonic macroscopic compression-dilatation:

$$U_{ij}^s = \frac{e}{3} \delta_{ij}. \tag{A.45}$$

Because the volume is small compared to wavelengths of interest there is no difficulty in imagining uniform harmonic compression-dilatation everywhere synchronous with no lag. Since the presence of the capillary is intended to allow the equilibration of the internal air pressure with P_0, so that no excess pressure appears in the air, we have

$$\sigma_{ij}^f = (Qe + R\epsilon)\delta_{ij} = 0 \Rightarrow Qe = -R\epsilon, \tag{A.46}$$

and since the above stresses on the diaphragm are integrally transferred to the solid via the attachments, we can also write

$$\sigma_{ij}^s = -p_e \delta_{ij} = [(P - 2N)e + Q\epsilon]\delta_{ij} + 2N U_{ij}^s. \tag{A.47}$$

Combining the three relations we find

$$\sigma_{ij}^s = -p_e \delta_{ij} = \left[P - \frac{4}{3} N - \frac{Q^2}{R} \right] e \delta_{ij}. \tag{A.48}$$

Note that, as we have used in (A.47) Biot's relation (A.8) we have implicitly assumed the absence of significant differential solid motions at pore scale, what we have termed the solid quasi-"en-bloc" motion. Here, this characteristic is assumed automatically satisfied by the very fact of considering a small volume the size of a REV. Also in (A.46) obtained by setting $\sigma_{ij}^f = 0$ in (A.9), we are making a replacement consistent with the vision of a fluid divergence-free motion, which also can be justified in same manner. In the generalization that will have to consider the $\hat{\alpha}$ and $\hat{\beta}$ as coming from underlying non-local quantities, the same structure of equations will make sense to describe corresponding motions occurring in the material, but with appropriate changes in interpretation. The externally applied excess pressure p_e will represent an applied macroscopic $-H_e$ stress field, while we will have to interpret (A.46) as the vanishing of the macroscopic excess pressure, meant in the sense of the Umov-averaged pressure in the fluid H^f only, not p^f itself. Now notice that the quantity $-p_e/e$ can, by definition, be called the compression modulus K_b of the solid skeleton at constant pressure in the fluid, or else the compression modulus K_b of the solid skeleton in vacuum. In the generalization this meaning will be allowed to be kept in relation with the understanding of the vanishing of the overpressure in the fluid, as a vanishing in the Umov sense only, $-H^f = 0$. This bulk modulus is in principle directly measurable and we thus have obtained a first relation on constants P, Q, R, and N:

$$K_b = P - \frac{4}{3}N - \frac{Q^2}{R}. \tag{A.49}$$

In the imagined frozen scenario, there are no losses at all and K_b would be a positive quantity. Turning now our attention to the unjacketed experiment, the same REV sample is no longer enveloped by a diaphragm. It is directly subjected to the action of the external uniform harmonic overstresses $-p_e\delta_{ij} = \tilde{p}_e e^{-i\omega t}\delta_{ij}$. Macroscopically these externally applied stresses will be divided into fluid and solid stresses proper, applied on corresponding phases per unit of total surface

$$\sigma_{ij}^f = -\phi p_e \delta_{ij},\ \sigma_{ij}^s = -(1-\phi)p_e\delta_{ij}, \tag{A.50}$$

whereas microscopically, the fluid and solid stresses are simply the applied $-p_e\delta_{ij}$. In response at macroscopic level certain isotropic uniform and harmonic compression-dilatation arise:

$$U_{ij}^f = \frac{\epsilon}{3}\delta_{ij},\ U_{ij}^s = \frac{e}{3}\delta_{ij}, \tag{A.51}$$

and there follows that (with same type of calculation as before, for the solid)

$$-p_e\phi = (Qe + R\epsilon),\ -p_e(1-\phi) = \left(P - \frac{4}{3}N\right)e + Q\epsilon. \tag{A.52}$$

At microscopic level because the stresses are simply $-p_e\delta_{ij}$ there is also uniform and different compression-dilatation for the solid and fluid. By the way in this experiment the ϵ and e represent indifferently the divergence of macroscopic/microscopic displacements. There follows that the quantity $-p_e/e$ has the interpretation of the bulk modulus K_s of the solid itself, of which the skeleton is made. Thus from the two relations (A.52) we get $K_s\phi = \left(Q + R\frac{\epsilon}{e}\right)$ and $K_s(1-\phi) = P - \frac{4}{3}N + Q\frac{\epsilon}{e}$ and by eliminating ϵ/e

$$K_s(1-\phi) = P - \frac{4}{3}N + Q\frac{K_s\phi - Q}{R}. \tag{A.53}$$

Similarly, since there is isotropic uniform microscopic expansion-compression of the fluid, the quantity $-p_e/\epsilon$ has the interpretation of the bulk modulus K_f of the fluid itself, which is here the adiabatic bulk modulus K_a because of the frozen scenario where losses are neglected. From the two relations (A.52) we get $K_f\phi = Q\frac{e}{\epsilon} + R$ and $K_f(1-\phi) = \left(P - \frac{4}{3}N\right)\frac{e}{\epsilon} + Q$ and by eliminating e/ϵ

$$K_f(1-\phi) = \left(P - \frac{4}{3}N\right)\frac{K_f\phi - R}{Q} + Q. \tag{A.54}$$

The algebraic combination of the relations (A.49), (A.53) and (A.54) determine the following P, Q and R:

$$P = \frac{(1-\phi)\left(1-\phi-\frac{K_b}{K_s}\right)K_s + \phi\frac{K_s}{K_f}K_b}{1-\phi-\frac{K_b}{K_s}+\phi\frac{K_s}{K_f}} + \frac{4}{3}N. \tag{A.55}$$

$$Q = \frac{\phi\left(1-\phi-\frac{K_b}{K_s}\right)K_s}{1-\phi-\frac{K_b}{K_s}+\phi\frac{K_s}{K_f}}. \tag{A.56}$$

$$R = \frac{\phi^2 K_s}{1-\phi-\frac{K_b}{K_s}+\phi\frac{K_s}{K_f}}. \tag{A.57}$$

These equations determine the effective elastic constants P, Q and R based on the moduli N (skeletal shear modulus), K_b (skeletal bulk modulus), K_s (solid bulk modulus), $K_f = K_a$ (fluid adiabatic bulk modulus) and the porosity parameter ϕ related to the microgeometry of the medium.

We will now introduce losses in the opposite, low-frequency, relaxed limit, where we will reconsider in an appropriate manner the derivations and statements above. As known and discussed in Landau and Lifshitz [14], within the Lagrangian formalism, which assumes the dependence of the equations of motion on the generalized coordinates and their first-order-in-time derivatives, the presence of losses can be usefully considered when the macroscopic state of affairs is still fixed by the considered macroscopic variables and their first-order-in-time variations. Within a Lagrangian approach, losses can be considered in a special quasi-static limit where a dissipation function determined by first-order-in-time derivatives exists. Here it corresponds to the relaxed scenario that may be relevant to consider in a theoretical limit $\omega \to 0$, which allows to introduce a viscous dissipation determined only by macroscopic velocities. From a microscopic perspective, fluid undergoes shear as it flows adjacent to solid surfaces. This shear results from the necessity for the fluid velocity to change rapidly over pore-scale distances – transitioning from a value corresponding to the solid velocity at the pore wall, as dictated by the no-slip boundary condition, to a distinct bulk velocity determined by the microgeometry of the system and the overall amplitude of the fluid-solid motion. From a macroscopic perspective, the underlying viscous friction processes inevitably associated with this fluid shear are expressed by a dissipation function $D\left(\dot{U}_i^s, \dot{U}_i^f\right)$ determined by the $\mathbf{w}$ field of relative velocities $\dot{\boldsymbol{U}}^f - \dot{\boldsymbol{U}}^s$. As a quadratic scalar constructed with $\mathbf{w}$ and δ_{ij} we have no choice but to write it as follows

$$D = \frac{1}{2}b\left(\dot{\boldsymbol{U}}^f - \dot{\boldsymbol{U}}^s\right)^2, \tag{A.58}$$

where the interpretation of coefficient b is to be made. The previous considerations leading to the expressions (A.4) and (A.5) for the kinetic energy and the potential energy still hold, but the interpretation of the coefficients is to be resumed in the

present different, relaxed instead of frozen context. The presence of the dissipation function expresses by the appearance of the dissipative forces $-\partial D/\partial \dot{U}_i^s$ and $-\partial D/\partial \dot{U}_i^f$ in (A.7)

$$\frac{\partial \pi_i^s}{\partial t} = \frac{\partial \sigma_{ik}^s}{\partial x_k} - \frac{\partial D}{\partial \dot{U}_i^s}, \quad \frac{\partial \pi_i^f}{\partial t} = \frac{\partial \sigma_{ik}^f}{\partial x_k} - \frac{\partial D}{\partial \dot{U}_i^f}, \tag{A.59}$$

with the quantities σ_{ik}^s, σ_{ik}^f, π_i^s and π_i^f, which are formally still given by the same equations as before (A.8)–(A.11), but now changed in meaning and values, reflecting the new interpretations and values of the coefficients to be made now. Before proceeding we explicitly write the new Biot equations (A.59)

$$\rho_{11}\ddot{\boldsymbol{U}}^s + \rho_{12}\ddot{\boldsymbol{U}}^f = P\nabla e + Q\nabla\epsilon - N\nabla\times\nabla\times\boldsymbol{U}^s + b\big(\dot{\boldsymbol{U}}^f - \dot{\boldsymbol{U}}^s\big), \tag{A.60}$$

$$\rho_{22}\ddot{\boldsymbol{U}}^f + \rho_{12}\ddot{\boldsymbol{U}}^s = Q\nabla e + R\nabla\epsilon - b\big(\dot{\boldsymbol{U}}^f - \dot{\boldsymbol{U}}^s\big). \tag{A.61}$$

Let us start with the interpretation of parameter b. As before, to simplify the analysis, the solid is made quite heavy and not very deformable, so that only the fluid responds to acoustic motion. Only (A.61) is well-conditioned and it writes $\rho_{22}\ddot{\boldsymbol{U}}^f = R\nabla\epsilon - b\dot{\boldsymbol{U}}^f$. Since we are considering a limit $\omega\to 0$, the second-order time-derivative term must be negligible compared to the first-order one, and since $R\epsilon = -P^f\phi$ where P^f is macroscopic excess pressure in fluid

$$b\,\dot{\boldsymbol{U}}^f = -\phi\nabla P^f. \tag{A.62}$$

Now obviously in this limit, fluid motion must be that given by Darcy's law [57]:

$$\phi\,\dot{\boldsymbol{U}}^f = -\frac{k_0}{\eta}\nabla P^f, \tag{A.63}$$

where k_0 is Darcy's permeability, and there follows the identification of parameter b:

$$b = \frac{\eta\phi^2}{k_0}. \tag{A.64}$$

In this limit, the fluid flow at the pore scale does not obey the frozen model equations (A.27)–(A.29) but instead obeys the following relaxed viscous model equations

$$0 = \eta\Delta\dot{u}_i^f - \nabla_i p^f, \quad \text{in } V_p, \tag{A.65}$$

$$\nabla\cdot\dot{\boldsymbol{u}}^f = 0, \quad \text{in } V_p, \tag{A.66}$$

with,

$$\dot{\boldsymbol{u}}^f = \boldsymbol{0}, \quad \text{on } S_p. \tag{A.67}$$

The excess "pressure" $p^f = \big(P^f = Cste + \boldsymbol{r}\cdot\nabla P^f\big) + \delta p^f$ decomposes into the macroscopic excess pressure P^f, that is fixed up to a constant by the macroscopic pressure gradient, and a fluctuating response δp^f ($\langle\delta p^f\rangle_p$=0) fixed as $\dot{\boldsymbol{u}}^f$ by the solution of the problem. In (A.27)–(A.29) the same kind of decomposition of p^f applies, with obviously a different solution for $\dot{\boldsymbol{u}}^f$ and the fluctuating δp^f. With present relaxed $\dot{\boldsymbol{u}}^f$ the Darcy permeability is given by [8] Appendix

$$\frac{\phi}{k_0} = \frac{\langle -\dot{\boldsymbol{u}}^f\cdot\Delta\dot{\boldsymbol{u}}^f\rangle_p}{\langle\dot{\boldsymbol{u}}^f\rangle_p^2}, \tag{A.68}$$

while the following set

$$\alpha_0 = \frac{\langle(\dot{\boldsymbol{u}}^f)^2\rangle_p}{\langle\dot{\boldsymbol{u}}^f\rangle_p^2}, \tag{A.69}$$

now takes on an increased value compared to the one (α_∞) it had in the frozen case. This is because the viscous effects introduce additional perturbations to the microscopic fluid pattern as a result of the need for the velocities at the pore walls to go to zero. To make the interpretation of previous parameters ρ_{11}, ρ_{12} and ρ_{22} in the present relaxed limit and show that they are given by the equations (A.42)–(A.44) where α_0 is substituted for α_∞:

$$\rho_{11} = \rho_s(1-\phi) + \rho_0\phi(\alpha_0 - 1), \tag{A.70}$$

$$\rho_{22} = \phi\rho_0\alpha_0, \tag{A.71}$$

$$\rho_{12} = -\phi\rho_0(\alpha_0 - 1), \tag{A.72}$$

we resume our previous reasonings adding the contributions of friction forces between solid and fluid. At the pore walls the reaction forces exterted are not only inertial, directed along the normal, but also viscous, directed along a pore tangent, resulting in the new macroscopic expression $\boldsymbol{R} = -(\alpha_0-1)\phi\rho_0\frac{\partial}{\partial t}\big(\dot{\boldsymbol{U}}^f - \dot{\boldsymbol{U}}^s\big) - b\big(\dot{\boldsymbol{U}}^f - \dot{\boldsymbol{U}}^s\big)$. By following the logic previously established we arrive at the expressions presented in Equations (A.70)–(A.72). These equations give the macroscopic effective relaxed Biot densities ρ_{ij} based on solid and fluid densities, and porosity and static tortuosity parameters linked to the microgeometry of the medium. For the identification/interpretation of the elastic parameters P, Q, R, and N, we have to resume our previous considerations in present context of very low frequencies and presence of loss terms in the underlying microscopic equations. There are no changes in the discussion except that the values of elastic constants are seen to correspond to a quasi-static limit. For the fluid bulk modulus, K_f, the consideration of very low frequencies instead of very high, means that the thermal exchanges between solid and fluid have time to fully occur, so that the excess temperature in fluid is fixed to zero by these exchanges. (The solid is assumed thermally inert and to remain at constant ambient temperature). Therefore, K_f instead of taking the adiabatic value K_a, takes on the isothermal value K_0=K_a/γ. Finally, in arbitrary harmonic regime and as explained in Landau and Lifshitz [14] the Lagrangian method is not applicable. Nevertheless, in the frozen and relaxed limit we only used it as a quick derivation short-cut. We did not need it and the real point was the introduction of incompressibility simplifications. It should now be clear that, in arbitrary harmonic regime and without needing any Lagrangian derivation, generalized results can be directly obtained in same manner as before by continuing to assume the validity of the incompressibility for solid and fluid, in such a way that the Biot equations become

$$\tilde{\rho}_{11}\ddot{\boldsymbol{U}}^s + \tilde{\rho}_{12}\ddot{\boldsymbol{U}}^f = \tilde{P}\nabla e + \tilde{Q}\nabla\epsilon - \tilde{N}\nabla\times\nabla\times\boldsymbol{U}^s, \tag{A.73}$$

$$\tilde{\rho}_{22}\ddot{\boldsymbol{U}}^f + \tilde{\rho}_{12}\ddot{\boldsymbol{U}}^s = \tilde{Q}\nabla e + \tilde{R}\nabla\epsilon, \tag{A.74}$$

with this time the following interpretations of macroscopic coefficients

$$\tilde{\rho}_{11} = \rho_s(1-\phi) + \rho_0\phi(\tilde{\alpha} - 1), \tag{A.75}$$

$$\tilde{\rho}_{22} = \phi\rho_0\tilde{\alpha}, \tag{A.76}$$

$$\tilde{\rho}_{12} = -\phi\rho_0(\tilde{\alpha} - 1), \tag{A.77}$$

$$N:\ \text{Skeletal Shear Modulus}, \tag{A.78}$$

$$\tilde{P} = \frac{(1-\phi)\left(1-\phi-\frac{K_b}{K_s}\right)K_s + \phi\frac{K_s}{K_f}K_b}{1-\phi-\frac{K_b}{K_s}+\phi\frac{K_s}{K_f}} + \frac{4}{3}N, \tag{A.79}$$

$$\tilde{Q} = \frac{\phi\left(1-\phi-\frac{K_b}{K_s}\right)K_s}{1-\phi-\frac{K_b}{K_s}+\phi\frac{K_s}{K_f}}, \tag{A.80}$$

$$\tilde{R} = \frac{\phi^2 K_s}{1-\phi-\frac{K_b}{K_s}+\phi\frac{K_s}{K_f}}, \tag{A.81}$$

$$\tilde{K}_f = K_a/\tilde{\beta}(\omega), \tag{A.82}$$

where $\tilde{\alpha}(\omega)$ and $\tilde{\beta}(\omega)$ are the dynamic divergence-free classical response functions, termed dynamic tortuosity and dynamic compressibility, whose definitions have been re-discussed and made in [1], and again in present Section 2. To grasp the emergence of $\tilde{\alpha} = \tilde{\alpha}(\omega)$ in (A.75)–(A.77), consider that in the harmonic regime, under the scenario of an immobile solid with divergence-free modeling of the fluid's small-scale motion, a macroscopic Newton's law analogous to Equation (A.34) is applicable

$$\rho_0\tilde{\alpha}(\omega)\frac{\partial\langle\dot{\boldsymbol{u}}^f\rangle_p}{\partial t} = -\nabla\langle p^f\rangle_p, \tag{A.83}$$

where $\tilde{\alpha}(\omega)$ is the dynamic tortuosity function in question. For an explanation of what is $\tilde{\beta}(\omega)$, that satisfies in the same scenario,

$$\frac{1}{K_a}\tilde{\beta}(\omega)\frac{\partial\langle p^f\rangle_p}{\partial t} = -\nabla\cdot\langle\dot{\boldsymbol{u}}^f\rangle_p, \tag{A.84}$$

and how it is modeled from the incompressibility assumption, we also refer to [1] and present Section 2. Finally, in these expressions and to account for viscoelastic losses, additional frequency-dependencies generally arise in the elastic coefficients, mainly $N \sim \tilde{N}$ and $K_b \sim \tilde{K}_b$, making them complex quantities with generally small, feebly frequency-dependent, loss angle e.g. $\tilde{N} = N(1+i\epsilon)$. In the case where the geometry is sufficiently complex for the fluid to experience local compression-dilatation, the notion of $-H^f$ field must be substitued to the above mean pressures $\langle p^f\rangle_p$ and the understanding of the $\hat{\alpha}$ and $\hat{\beta}$ must be extended in the non-local operators discussed in the text. In this case, room is opened for fundamentally new behaviors incorporating effects of spatial dispersion.

Appendix B

Proof of equation (47), complex representation of real Umov condition

As analyzed at the microscopic level, the forced solution $V = \tilde{V}e^{-i\omega t+ikx} = V^{\mathfrak{R}} + iV^{\mathfrak{I}}$, etc., is a mixture in its real and imaginary parts, $V^{\mathfrak{R}}$, $V^{\mathfrak{I}}$, etc., (resp. associated to $f_x^{\mathfrak{R}}$ and $f_x^{\mathfrak{I}}$ in the abstract total $-ik\mathcal{P} = f_x^{\mathfrak{R}} + if_x^{\mathfrak{I}} = \tilde{f}e^{-i\omega t+ikx}$ with $\tilde{f}$ real), of scaled $'$ and $''$ real amplitudes appearing in quadrature in the tilde amplitudes, $\tilde{V} = \left[\tilde{V}' + i\tilde{V}''\right]\tilde{f}$, etc. In same manner as before, there will be the relations, $V^{\mathfrak{R}} = \left[\tilde{V}'cos(kx-\omega t) - \tilde{V}''sin(kx-\omega t)\right]\tilde{f}$, etc., and $V^{\mathfrak{I}} = \left[\tilde{V}'sin(kx-\omega t) + \tilde{V}''cos(kx-\omega t)\right]\tilde{f}$, etc. Let us now check the equation (47). In more detail, it states: $\left(H^{\mathfrak{R}} + iH^{\mathfrak{I}}\right)\langle v_x^{\mathfrak{R}} + iv_x^{\mathfrak{I}}\rangle = -\langle\left(p^{\mathfrak{R}} + ip^{\mathfrak{I}}\right)\left(v_x^{\mathfrak{R}} + iv_x^{\mathfrak{I}}\right)\rangle$, which we refer by †. The real part of † poses no problem, owing to the obviously licit: $H^{\mathfrak{R}}\langle v_x^{\mathfrak{R}}\rangle = -\langle p^{\mathfrak{R}}v_x^{\mathfrak{R}}\rangle$, and, $H^{\mathfrak{I}}\langle v_x^{\mathfrak{I}}\rangle = -\langle p^{\mathfrak{I}}v_x^{\mathfrak{I}}\rangle$, (these are written on the real fields, as is the original (38)). Now note for immediate subsequent use, that, in one or the other of the two last equalities, if we represent the $\mathfrak{R}$ and $\mathfrak{I}$ amplitudes in terms of their scaled $'$ and $''$ components, then extract the cos and sin factors and their products from the $\langle\cdot\rangle$, (long-wavelengths), and identify the resulting terms in *cos cos*, *sin sin*, and *cos sin*, we find that the amplitudes $'$ and $''$ verify the following equalities: $\{\tilde{H}'\langle\tilde{v}_x'\rangle = -\langle\tilde{p}'\tilde{v}_x'\rangle$, $\tilde{H}''\langle\tilde{v}_x''\rangle = -\langle\tilde{p}''\tilde{v}_x''\rangle$, and, $-\tilde{H}'\langle\tilde{v}_x''\rangle - \tilde{H}''\langle\langle\tilde{v}_x'\rangle = \langle\tilde{p}'\tilde{v}_x''\rangle + \langle\tilde{p}''\langle\tilde{v}_x'\rangle\}$. With this in mind it is now easy to see that the imaginary part of † poses no problem either. It states that, $H^{\mathfrak{R}}\langle v_x^{\mathfrak{I}}\rangle + H^{\mathfrak{I}}\langle v_x^{\mathfrak{R}}\rangle = -\langle p^{\mathfrak{R}}v_x^{\mathfrak{I}}\rangle - \langle p^{\mathfrak{I}}v_x^{\mathfrak{R}}\rangle$. This is also verified: if we substitue the $\mathfrak{R}$ and $\mathfrak{I}$ amplitudes in terms of the $'$ and $''$ and then identify the terms *cos cos*, *sin sin*, and *cos sin*, we find the equalities previously stated in $\{\}$.